CORRELATION AND REGISTRATION OF ERTS MULTISPECTRAL IMAGERY

CR 134294

L. O. Bonrud

P. J. Henrikson

CONTROL DATA CORPORATION
MINNEAPOLIS, MINNESOTA

April, 1974

Contract NAS9-13114

EARTH OBSERVATION DIVISION
LYNDON B. JOHNSON SPACE FLIGHT CENTER
HOUSTON, TEXAS

CONTROL DATA
CORPORATION

NOTICE

When Government drawings, specifications, or other data are used for any purpose other than in connection with a definitely related Government procurement operation, the United States Government thereby incurs no responsibility nor any obligation whatsoever; and the fact that the government may have formulated, furnished, or in any way supplied the said drawings, specifications, or other data, is not to be regarded by implication or otherwise as in any manner licensing the holder or any other person or corporation, or conveying any rights or permission to manufacture, use, or sell any patented invention that may in any way be related thereto.

CORRELATION AND REGISTRATION OF ERTS MULTISPECTRAL IMAGERY

L. O. Bonrud

P. J. Henrikson

FOREWORD

This report was prepared by Control Data Corporation, Minneapolis, Minnesota 55440, for the National Aeronautics and Space Administration (NASA), Earth Observation Division (EOD), located at the Johnson Space Center. The work described herein was performed in partial fulfillment of contract number NAS9-13114 and constitutes a part of a continuing program at EOD to further the application of remote sensing in the management of our natural resources.

As a part of this work effort Control Data performed digital image registration techniques on four sets of multispectral scanner (MSS) imagery and delivered registered data tapes for NASA use and evaluation. Major emphasis in regard to techniques, studies, and analyses was put on automatic processing methods. It is hoped that these investigations will in some measure assist NASA in a practical solution of its data base management objectives.

The early phases of this work were performed by the Electro-Optics Department of the Research Division of Control Data. In July, 1973, this department became the Digital Image Systems Division, and R. L. Lillestrand was accordingly promoted to the position of general manager of the new division.

The Control Data Project Engineer, L. O. Bonrud, was responsible for the overall technical direction of the project. P. J. Henrikson, assisted by T. Mercier, was responsible for software development, processing, and analysis. Image reproduction was performed by P. A. Mazorol and J. C. Garley, and graphics and publications services were provided by F. M. Dailey, D. M. Olson, and A. A. Yost.

This program was funded under the above named contract during the period July 1972 through August 1973. Special recognition is given to

R. Bizzell and K. Hancock, each of whom served as NASA technical monitors on this program, as well as to R. Hill, Chief of the Photogrammetry and Cartography Section, Mapping Sciences Branch at NASA JSC, for his program support.

This technical report was submitted on behalf of Control Data by L. O. Bonrud on May 15, 1974. The report has been reviewed and is approved.

ABSTRACT

Examples of automatic digital processing demonstrate feasibility of registering one ERTS Multispectral Scanner (MSS) image with another obtained on a subsequent orbit. Additionally, automatic matching, correlation, and registration of MSS imagery with aerial photography (multisensor correlation) is demonstrated. Excellent correlation is obtained with patch sizes exceeding 16 pixels square.

Qualities which lead to effective control point selection are distinctive features, good contrast, and constant feature characteristics. The size of the features should ideally be of such a size that correlation patch sizes in the range of 15 to 100 pixels square can be used. This allows sufficient detail to minimize noise problems associated with resolution limits of the imagery, and yet holds spatial distortions to negligible proportions across the width of a patch.

Results of the study indicate that more than 300 degrees of freedom are required, typically, to register two standard ERTS-1 MSS frames covering 100 by 100 nautical miles to an accuracy of 0.6 pixel mean radial displacement error. Global polynomial solutions are unsatisfactory, except over relatively small areas, e.g. 20 to 30 nautical miles square. A very acceptable approach is piecewise fitting, as with quadrilateral submatrices; however, interpolation can be very important dependent upon the application.

A Control Data automatic strip processing technique (TRAK) easily demonstrates 600 to 1200 degrees of freedom over a quarter frame of ERTS imagery (and is not limited to this). Registration accuracies in the range of 0.3 to 0.5 pixel mean radial error were confirmed by independent error analysis. Accuracies in the range of 0.5 to 1.4 pixel mean radial error were demonstrated by semi-automatic registration over small geographic areas.

TABLE OF CONTENTS

TABLE OF CONTENTS (Continued)

LIST OF ILLUSTRATIONS

LIST OF ILLUSTRATIONS (Continued)

LIST OF ILLUSTRATIONS (Continued)

LIST OF ILLUSTRATIONS (Continued)

LIST OF TABLES

1. INTRODUCTION

Remote sensing of the earth's surface with electromagnetic radiation has shown great promise for the future management of our natural resources. This technology provides opportunities for detecting new resources and natural phenomena, as well as measuring and evaluating the extent of resources in such areas as agriculture, forestry, geology, hydrology, meteorology, and oceanography.

The Earth Resources Technology Satellite (ERTS) program has demonstrated that excellent imagery can be obtained from multispectral scanners in space. Moreover this data is produced in very large quantities.

To a large extent the successful utilization of such data will depend upon transforming this data into a known ground coordinate system or registering one image with another. It is desirable then, that these processes be as automatic as possible in order that the work load can be performed efficiently and economically.

This report includes the final results and recommendations concerning correlation and registration of ERTS-1 MSS imagery. In general this report attempts to show the applicability of several geometric registration techniques between separate images of identical or overlapping geographic areas which were produced at different times, under different illumination conditions, and in certain cases by different sensors.

1.1 OBJECTIVES

The motivation for this study is to provide a means of rectifying any set of remotely sensed imagery of a given region to a standard coordinate mapping system. With the latter process accomplished it will then be possible to store and access all such imagery by their standard grid coordinates. The resultant ability to compare and analyze data applying to a common geographic locus will

greatly facilitate such further analysis and classification as may be required by the Johnson Space Center ERTS program.

Basically the process of registration of any two separate images depicting a common area is to choose one image of the pair as a reference and then to transform the other so that it will superimpose as closely as possible upon the chosen reference. In the simplest case, if the two images were taken under identical conditions, a simple translation, rotation of coordinates, and scale change would suffice to produce exact registration. Generally this case does not prevail and because of variations in sensors, viewing angle, field of view, optical system, and the like a simple linear transformation will not result in exact registry. In such cases a more complicated transformation must be applied.

The ultimate goal to be achieved is the eventual fully automatic processing of ERTS imagery. To this end it is necessary to investigate both automatic and semi-automatic techniques of image registration. In general the methods are completely dependent on being able to generate an interpolative spatial transformation based upon sets of corresponding control points in both members of image pairs. In one case these control points are found manually and in the other they are located automatically by the computer. In both cases the actual fitting process is carried out fully automatically by the computer.

The immediate goal of this current study then is to show how specific methods of image registration developed by Control Data can be applied to typical examples of ERTS imagery. The results of this fitting process, with special regard to accuracy of registration, will then establish a means of judging the applicability to the overall ERTS image processing problem. Finally, based on these results Control Data will make recommendations concerning the possibility of implementing the appropriate registration algorithms on special purpose hardware.

1.2 DESCRIPTION OF IMAGERY

The image data used in this study is from the ERTS-1 multispectral scanner,

and in two cases the ERTS data is augmented with a photomosaic constructed from aerial photographs to provide a ground reference.

The multispectral scanner repetitively scans a swath transverse to the satellite track on the surface of the earth using a moving mirror, and the motion of the satellite over the ground defines the other image coordinate. The light reflected from each swath is divided into four optical paths. In each path the light passes through an optical filter defining a given spectral band and is then focused upon a detector associated only with that band. The signal from each channel is sampled, digitized and telemetered to ground receiving stations using pulse code modulation techniques. The nominal spatial resolution of each resolution element is approximately 75 meters square. The four spectral bands are designated as Bands 4, 5, 6 and 7 which cover the respective intervals 0.5 to 0.6 micrometers, 0.6 to 0.7 micrometers, 0.7 to 0.8 micrometers, and 0.8 to 1.1 micrometers.

Four sets of imagery (Table 1.1) corresponding to four separate geographic areas within the continental United States were supplied to Control Data by the Johnson Space Center (JSC). The designations for these four sites used in this

TABLE 1.1. MULTISPECTRAL SCANNER IMAGERY, ERTS-1 SATELLITE

NAME	NUMBER	DATE
Hill County, Montana	1015-17342-MB-1	August 7, 1972
Trinity Bay, Texas	1036-16192-MB-1-3Y 1072-16190-MB-1-3A 1126-16195-MB-1-3Z	August 28, 1972 October 3, 1972 November 26, 1972
Snook Site (Somerville Reservoir), Texas	A07348 A05948	August 30, 1972 November 28, 1972
Imperial Valley, California	1106-17504-M4 1124-17504-M4	November 6, 1972 November 24, 1972

report are Hill County, Trinity Bay, Snook Site and Imperial Valley, which will be more precisely defined in the following sections. Additionally, uncontrolled photomosaics were supplied for Hill County, Montana and Imperial County, California.

1.2.1 Hill County

The Hill County study is based upon a quarter frame of ERTS-1 MSS imagery collected over a region containing Hill County, Montana on August 7, 1972. All four bands were used in the study. Associated with this set of satellite images is an uncontrolled photomosaic covering the same area and constructed from aerial photographs. The photomosaic was digitized by Control Data to provide an equivalent ground element which was about one-third of the size of an ERTS element.

1.2.2 Trinity Bay

The Trinity Bay imagery is that part of MSS imagery covering the upper Trinity Bay region in the Galveston-Houston, Texas area. There are three sets of imagery (all four bands) taken on three separate dates: August 28, 1972, October 3, 1972 and November 26, 1972.

1.2.3 Snook Site

Snook Site is a local area just north of the Sommerville Reservoir in Texas. Two quarter frames of MSS imagery (25 by 100 nautical miles) including the Snook Site near one end and Columbus, Texas near the other end were used for this study. The data was acquired on separate passes of the satellite and separated 90 days in time (August 30, 1972 and November 28, 1972).

1.2.4 Imperial Valley

The final set of images is for a region of checkerboard agricultural land in the Imperial Valley, California. Again the data is in the form of 25 by 100 nautical mile strips of MSS images taken on two different dates: November 6, 1972

and November 24, 1972. An uncontrolled photomosaic of Imperial County, California was used to simulate registry to map coordinates.

1.3 SCOPE OF EFFORT

The work effort of this project consisted of digital processing of bulk MSS data described in Section 1.2 and studies concerning techniques of image registration and error analysis.

Digital processing included reformatting of data for use at Control Data, contrast enhancement, removal of noise from the image data, registration of imagery, and generation of 9-track tapes in MSDS format for delivery to the Johnson Space Center. Error analysis constitutes another aspect of digital processing which was used to evaluate the final results.

The requirements for registration were to provide image-to-image registration of bulk MSS data in two cases and image-to-ground registration in the other two cases. The method, whether semi-automatic or automatic, was not specified. Expediency in returning registered data for use by the Johnson Space Center was the prime consideration. Nevertheless, fully automatic registration processing was demonstrated in three of the four cases.

Correlation studies investigated the applicability of automatic correlation of MSS data and aerial photography. These studies included the effect of correlation patch size, spectral band, image contrast, size and shape of image features, control point selection, and enhancement and resolution differences.

Specific processing tasks are described in the following paragraphs.

1.3.1 Hill County

MSS image data from one pass over Hill County, Montana was first registered to an uncontrolled photomosaic of Hill County with semi-automatic processing.

A quadratic fit was made by computer on the basis of 21 control points which were measured manually.

The transformed MSS data from the semi-automatic processing run was then registered with the photomosaic data using Control Data's automatic strip (TRAK) processing technique.

These two techniques simulate registration of MSS imagery to ground coordinates. Moreover, the automatic technique demonstrated multi-sensor correlation. It is the Hill County data which was used for the comprehensive studies of correlation which are discussed in this report.

1.3.2 Trinity Bay

Since a very large fraction of the image area is water, which cannot be correlated, and for the sake of expediency, semi-automatic processing was used to register three sets of MSS data with one another.* Testing of 50 control points showed that a linear transformation should be satisfactory. Therefore, a linear bi-variant polynomial transformation with six independent coefficients was computed on the basis of these 50 control points.

Error analysis of the results was performed with an automatic correlation method (WECK) and with a polynomial error analysis using polynomials ranging from 3 to 12 degrees of freedom.

1.3.3 Snook Site

Choosing one of two quarter frames (25 by 100 nautical miles) of MSS imagery as the reference, the second image was registered with the reference

*Based upon the success of strip (TRAK) processing on the other examples described in this report, it is anticipated that this method will work for the land mass surrounding Trinity Bay, also. Furthermore, a procedure has been developed which allows TRAK to conform with assigned control point coordinates.

using a fully automatic strip (TRAK) processing method.

Again error analysis was performed with correlation (WECK) and polynomial analysis routines.

1.3.4 Imperial Valley

The processing of this final image set utilizes a combination of the techniques discussed before. Quarter frames of MSS imagery were first registered between satellite passes using the completely automatic strip correlation program TRAK which was mentioned previously. Then part of this data was registered semi-automatically to an uncontrolled photomosaic of Imperial County. For this latter step a linear bi-variant polynomial transformation with six degrees of freedom was computed on the basis of 16 control points which was measured manually.

Error analysis was performed with correlation (WECK) and polynomial analysis routines.

1.4 SUMMARY OF RESULTS

The main objective of this work was to investigate to what extent automatic digital processing might be effective in registering ERTS MSS imagery, and in the three cases where such techniques were employed in this work the results were successful. Two examples of automatic registration of MSS data obtained on different passes and one example of automatic registration of MSS data to a mosaic of aerial photographs demonstrate that registration accuracies in the range of 0.3 to 0.8 pixel mean radial displacement error are possible.

These results are summarized in the following paragraphs together with considerations of correlation patch size, spectral qualities, control point selection and enhancement and resolution differences.

1.4.1 Semi-Automatic Versus Automatic Registration

In the context of this discussion semi-automatic and automatic processing are distinguished on the basis of how the matching points are found in two images which are to be registered. In the semi-automatic process all matching point coordinates are determined manually by an operator. In the automatic process only a sufficient number of control points are determined manually to initiate the process (and minimize the search area for initial lock-on) or to provide adequate ground control information to match a specific ground coordinate system. The majority of matching locations are determined by automatic matching and correlation processes. The relative merits of these two general approaches will be decided, then, upon the complexity of spatial transformation that is required, the process performance, work load, and economic considerations.

The results of this study indicate that more than 300 degrees of freedom are required, typically, to register two standard ERTS-1 frames covering 100 by 100 nautical miles to an accuracy of about 0.6 pixel mean radial displacement error. By way of example, if global polynomials are used to effect the spatial transformation this complexity requires second order bi-variant polynomials (12 degrees of freedom) over an area of 20 by 20 nautical miles. A linear solution (6 degrees of freedom) is satisfactory over an area of about 14 by 14 nautical miles.

From the foregoing it follows that more than 150 match points must generally be determined to match ERTS-1 MSS imagery to a ground coordinate system or to match two frames of MSS data obtained on different passes. Thus, semi-automatic processing requires a considerable amount of tedious and time consuming work by an operator to obtain the required match points.

By contrast the Control Data automatic strip processing technique (TRAK) has been demonstrated to yield excellent results with the equivalent of 600 to 1200 degrees of freedom over a quarter frame of ERTS imagery, and the process is by no means limited to this range of capability. The strip process technique is accordingly capable of more than 4800 degrees of freedom over a full frame of ERTS

imagery. It is worth noting at this point that the strip process computes a new, updated warp (spatial transformation) for each line of imagery. The spatial response rate is controlled by a selectable damping distance parameter.

Global polynomial solutions are unsatisfactory, except over relatively small areas, say 20 or 30 nautical miles square. A maximum of about 40 degrees of freedom is practical with global polynomials. At higher orders the polynomials deviate considerably between fit points. A very acceptable approach is piecewise fitting, as with quadrilateral submatrices formed from 4 adjacent match points. These techniques are applicable to either semi-automatic or automatic registration processes.

The accuracy of registration was analyzed with the aid of an automatic correlation technique (WECK) for both semi-automatic and automatic registration processes. Where care was exercised in obtaining accurate control points, semi-automatic registration of MSS imagery to a photomosaic image (Imperial County) resulted in a mean radial displacement error of 0.5 pixel over an area less than 20 nautical miles square. MSS data obtained from three different passes over a 90 day time-span was registered in this manner with a resultant 0.7 pixel mean radial error (Trinity Bay). With a less precise measurement procedure MSS data was registered to a photomosaic of Hill County to an accuracy of 1.4 pixel.

Using the automatic strip (TRAK) process quarter frames of MSS imagery acquired at different times were registered to 0.28 pixel (Snook Site) and 0.58 pixel (Imperial County) mean radial error. The transformed data obtained from the Hill County run described above was further improved in the TRAK run to 0.4 pixel mean radial error.

These results are encouraging in two respects. First, it is possible to register two MSS images having temporal changes with an automatic matching and correlation procedure. Second, it is possible to correlate ground control areas in a photomosaic with MSS imagery.

Semi-automatic processing has the advantage of less computer time and the disadvantage of greater clock time. Pre-processing enhancement is also desirable to aid the operator in feature recognition. Automatic processing has the advantages of less clock time, greater volume, and no need for pre-processing (though pre-processing may be desirable for other reasons). Automatic processing has the disadvantage of more computing time, but it may have the further advantage of greater accuracy under given work load conditions, particularly where there is a lack of sharp feature detail.

1.4.2 Image Correlation

Cross correlation of ERTS-1 MSS data and a photomosaic of Hill County provides the following observations concerning the effects of patch size, spectral region of the sensor, and image features.

Excellent correlation is obtained with patch sizes exceeding 16 pixels square in the MSS data matrix. It is observed that recognizable features are normally evident within a 16 by 16 pixel window. However, a correlation window 4 pixels square seldom includes recognizable features. Therefore, such a small patch creates problems with secondary maxima and minima in the correlation surface.

For the Hill County example band 5 MSS data was most similar to the photomosaic as judged by visual appearance, joint gray-scale distribution diagrams, and cross correlation. The mean correlation value for 21 control points varied from a minimum of 0.556 for band 4 data to a maximum of 0.615 for band 5 data (Table 2.2-1). The mean coordinate locations of maximum correlation between each of the image bands and the photomosaic did not differ by more than 0.2 pixel for the 21 control points (in terms of MSS data matrix). Likewise, band 5 data was judged to be most reliable for matching Trinity Bay, Snook Site, and Imperial Valley data.

Qualities which lead to effective control point selection are distinctive features, good contrast, and constant feature characteristics. The size of the

features should ideally be of such a size that correlation patch sizes in the range of 15 to 100 pixels square can be used. This allows sufficient detail to minimize noise problems associated with resolution limits of the imagery, and yet holds spatial distortions to negligible proportions across the width of a patch. This latter condition is important lest distortions have a significant effect upon the location of maximum correlation for the entire patch.

Either man-made or natural features can be used as control points, provided they are not subject to significant change. One of the greatest problems here, of course, is seasonal variation. A solution to this problem is maintaining control point reference images that are typical of several seasons.

A number of examples are analyzed to show the effect of various image patterns upon the correlation function. It is demonstrated that automatic correlation is effective even under conditions of low contrast features.

Experimental results demonstrate that two images can be effectively matched and correlated even though resolution is significantly different in the two images. A mathematical analysis is offered to support this observation. Therefore, there is no need to equalize resolutions prior to correlation. Nor is the use of a gradient function advantageous in area correlation.

2. DISCUSSION OF RESULTS

2.1 ERTS REGISTRATION REQUIREMENTS

2.1.1 Techniques and Objectives

In designing an image processing system there are two basic questions to be answered: What will work and what will work best. The second question is in many ways more difficult to answer than the first because it requires definition of user objectives and user enviroment. Given these, trade-off studies can be performed to establish preferred techniques and to optimize parameters. The question of which techniques are best for ERTS image registration depends on the particular registration requirements and on user objectives, particularly processing volume, time constraints and accuracy requirements.

This section is concerned with the basic question: What will work? Only digital techniques will be considered here. Under this classification is, of course, a relatively wide spectrum of techniques which can be differentiated on the basis of operator intervention or interaction required. At the two ends of the spectrum are what will be termed "semi-automatic" and "fully-automatic" techniques. In both cases the computer performs a spatial warp "automatically." The difference between methods lies in the means for acquiring data on which to base the spatial warp.

In the registration process two images are to be brought into accurate alignment. This may be accomplished by spatially transforming or "warping" either or both images. For purposes of this discussion it will be assumed that one image will be the reference or independent image. Only the second image, which will be referred to as the collateral or dependent image, will be spatially transformed to bring the two images into registration. Note incidently that the reference "image" need not be an actual image; it may be a map or nothing more than a set of control points.

The spatial warp applied by the computer to the dependent image is based on a mathematical fit to matching points on the reference and dependent images. For semi-automatic methods these control points are selected through some sort of operator intervention. The operator can match points visually on an interactive display, from photographic prints, etc. Point coordinates can be entered interactively or manually in a batch processing mode. Also the computer may be used to improve accuracy through automatic correlation techniques from manually matched points.

In "fully-automatic" image registration the computer finds its own control points through automatic correlation.

This section presents an investigation of both techniques for ERTS registration requirements. Two registration requirements are considered:

- ERTS image-to-image or temporal registration.
- Registration of ERTS imagery to ground control.

A third registration requirement, registration of ERTS imagery to underflight data, was not investigated because underflight data was unavailable.

Requirements for image-to-image registration are different from those for image-to-ground registration. Therefore, different techniques may be required. The objectives of this investigation are twofold: to establish registration requirements and to compare semi- and fully-automatic registration techniques based on samples of typical ERTS data. In the former case the emphasis is on establishing spatial warp complexity for the above registration requirements. In the latter case the emphasis is on comparative registration accuracy.

The most difficult task in image registration is sampling the coordinate transformation between a given image and a reference. These samples in the form of coordinates of corresponding features on the reference and dependent images form the basis for the spatial warp.

For semi-automatic registration samples are provided manually. The automatic phase in which the dependent image is spatially warped into registration with the reference tends to be straightforward. A mathematical fit to the samples forms the basis for a point-by-point spatial warp of the dependent image. The mathematical fit can be of a number of forms, depending on the properties of the spatial distortion present. Given no priori knowledge of the form of this spatial distortion, a least squares polynomial fit provides a reasonable fit and is widely used [1,2,3]. Locations predicted by the fit will generally lie between pixels on the dependent image. Therefore some sort of interpolation, either nearest-neighbor or multi-point, must be used in conjunction with the fit. Generally the former is sufficient, but is again subject to the application and properties of the imagery.

As for nearly any data processing application, the most important performance parameters for image registration are speed, accuracy and storage requirements. Storage requirements are tied to spatial warp complexity, particularly linear terms, e.g. scale change and rotation. Speed and accuracy are also tied to spatial warp complexity and to measurement accuracy in the samples provided.

If measurement accuracy is poor, either computer aid must be enlisted to improve accuracy through automatic correlation or more samples must be provided than would otherwise be required. In the former case the computer actually matches control points, with the operator greatly reducing computer search time by basically telling it where to look. In the latter case registration error is reduced through least squares techniques. In either case the spatial complexity of the warp is an important factor. Accuracy in automatic correlation is directly related to spatial warp complexity. Also, the complexity of the mathematical fit and hence the number of samples required is directly related to warp complexity.

Processing speed is also directly related to spatial warp complexity. For example, the simpler the spatial warp, the simpler the techniques required for registration. In particular for linear transformations, the spatial warp can be implemented with a table-look-up method to yield substantial savings in processing time [3].

Registration accuracy and warp complexity are therefore the two most important considerations for semi-automatic registration. We would therefore like to establish warp accuracy as a function of warp complexity, and on the basis of this analysis recommend production processing procedures for ERTS imagery.

On the other hand, feasibility of fully-automatic registration techniques for ERTS imagery need to be proven. Automatic techniques are not only affected by spatial warp complexity but also by the relative properties of reference and dependent images. In this connection it is important to distinguish between the two ERTS registration requirements under consideration, namely image-to-image and image-to-ground registration. In the following subsections the objectives in terms of automatic registration are twofold.

- To establish feasibility of automatic registration for both ERTS image registration requirements
- To compare registration accuracy of automatic techniques with semi-automatic techniques.

Automatic registration for image-to-ground registration is the harder of the two ERTS registration requirements. Consequently, automatic registration studies for this problem, presented in Section 2.2 are more basic than ERTS image-to-image registration studies performed in Sections 2.4 and 2.5. In Section 2.2 we are trying to establish that a sufficient base exists for automatic registration. For image-to-image registration it is assumed that this base already exists.

Control Data has gained extensive experience in automatic image-to-image registration through its pioneering research and development in Side Looking Radar (SLR) change detection [4-11]. An operational system that includes a high-speed automatic registration capability has been built by Control Data for the U.S. Air Force [9]. This system is based on a unique method of pipeline processing known as strip processing. Additionally, Control Data has also developed these techniques to perform cancellation, registration, and change detection with aerial photography [12].

Strip processing was employed in this work to investigate the feasibility of image-to-ground correlation and image-to-image correlation.

It is implemented in the form of a software simulator, Program TRAK. Program TRAK, also known as the "strip processor," is an experimental FORTRAN/COMPASS program designed for the CDC 6600 and Cyber series computers. It must be emphasized that this is not a production processing program for ERTS imagery. Rather it has been used with the intention of establishing feasibility and processing requirements for ERTS imagery.

The fact that Program TRAK is a hardware simulator has operational significance. Successful TRAK processing of ERTS imagery implies that special purpose hardware can be designed for production processing of ERTS imagery. Such hardware can automatically process imagery one to two orders of magnitude faster than general purpose computers at JSC, while at the same time freeing the latter for image research application.

In summary both semi-automatic and "fully" automatic registration techniques are employed in the following investigations. Four sets of ERTS imagery (Hill County, Trinity Bay, Snook Site, and Imperial Valley) were processed. Registration requirements, processing methods, and studies performed for each image set are summarized in Table 2-1. These investigations have the following objectives:

TABLE 2.1. SUMMARY OF ERTS REGISTRATION INVESTIGATIONS

TEST SITE	REGISTRATION REQUIREMENTS	INVESTIGATIONS PERFORMED
Hill County	Image-to-ground	1. Polynomial Error Analysis for Semi-Automatic Registration 2. Automatic Correlation/Registration Feasibility Study
Trinity Bay	Image-to-Image	1. Polynomial Error Analysis for Semi-Automatic Registration 2. WECK Error Analysis for Semi-Automatic Registration
Snook Site	Image-to-Image	1. Polynomial Error Analysis for Automatic Registration 2. WECK Error Analysis for Automatic Registration
Imperial Valley	Image-to-Image and Image-to-Ground	1. Polynomial Error Analysis for Automatic Image-to-Image Registration 2. WECK Error Analysis for Automatic Image-to-Image Registration 3. Polynomial Error Analysis for Semi-Automatic Image-to-Ground Registration

- To establish feasibility of automatic registration techniques for both ERTS image-to-image and image-to-ground registration.
- To establish automatic registration requirements, i.e. algorithm modifications and parameter settings, for ERTS image-to-image registration.
- To establish spatial warp complexity requirements for both image-to-image and image-to-ground registration.
- To establish accuracy of both semi- and fully-automatic registration techniques.

2.1.2 Error Analysis

Aside from establishing feasibility of automatic registration techniques, the two most important objectives of this investigation are to establish warp complexity requirements for both ERTS registration requirements and to establish accuracy specifications for both semi- and fully-automatic

processing. Accordingly, it is important that qualitative and quantitative procedures be developed for assessing registration accuracy.

Three good methods of qualitatively assessing warp accuracy are color superposition, gradient superposition, and change detection. The latter two are used in this report to visually demonstrate the results of registration processing.

In gradient superposition the gradient of the reference image is superimposed on the collateral image following registration processing. The gradient operator emphasizes edges. Hence by thresholding the gradient of the reference and superimposing it on the dependent image, one can assess registration accuracy by assessing the degree to which edges or boundaries are in alignment on the two images.

Change detection also provides a means of assessing registration accuracy. Spatial misregistration between reference and dependent images will result in black and white change pairs or "ghosting" in the difference image. This assumes, of course, that the two images are in registration radiometrically, i.e. density values for corresponding features on the two images have the same distributions. If not, some sort of photoequalization is necessary for change detection to yield meaningful results.

Both of these methods provide only qualitative visual results. Quantitative evaluation requires statistical evaluation of processing results. Quantitative evaluation of registration accuracy for real data is generally difficult because of difficulty in establishing an absolute reference. In laboratory simulations, of course, establishing an absolute reference is straightforward. Program TRAK has been tested extensively in this manner, and registration accuracy was found to be on the order of one-fourth pixel mean radial error [7.9]. But the question of interest is not how techniques perform in the laboratory, but how they perform on real data, i.e. "in the field."

Two types of statistical studies will be performed to evaluate spatial registration accuracy: polynomial error analysis and WECK analysis. In both cases, analysis is based on samples representing matching features on the reference and dependent images. In areas where there are no matching features, either because of temporal change or because there are simply no prominent features, neither method can provide a measure of warp accuracy.

Polynomial error analysis assumes that spatial distortion between reference and dependent images can be modelled by a polynomial, i.e.

$$x' = \sum_{i=0}^{N} \sum_{j=0}^{N-i} a_{ij} x^i y^j$$

$$y' = \sum_{i=0}^{N} \sum_{j=0}^{N-i} b_{ij} x^i y^j \qquad (2.1\text{-}1)$$

where $(x,y),(x'y')$ are coordinates of some point on the reference and dependent image, respectively, N is the order of the polynomial, and the coefficients $\{a_{ij},b_{ij}\}$ are determined by a least squares fit to some set of control points. These control points can result from either manually matching features or from automatic correlation. In either case, polynomial error analysis can be used to compile error statistics as a function of the order of the warp. These statistics can then be used both to assess warp accuracy and to establish warp complexity.

An important consideration in polynomial error analysis is degree of over-determination. Residual error at fit points will <u>always</u> decrease as the complexity, i.e. the number of unknowns or "degrees of freedom," is increased for a least squares polynomial fit. In the limiting case where the number of measurements equals the number of unknowns, the residual error at each fit point is identically zero. For this reason, one should, if at all possible, divide the set of control points into a set of fit points and a control set of "check" points.

The reason for employing check points is to measure fit error at points other than those employed in the fit. As fit complexity is increased, the fit begins to respond to "measurement noise" at the fit points. The result is increased error at points other than fit points. Within the set of fit points, fit error tends to be greatest at points farthest from the fit points, hence, a reasonable choice of check points is as shown in Figure 2.1-1.

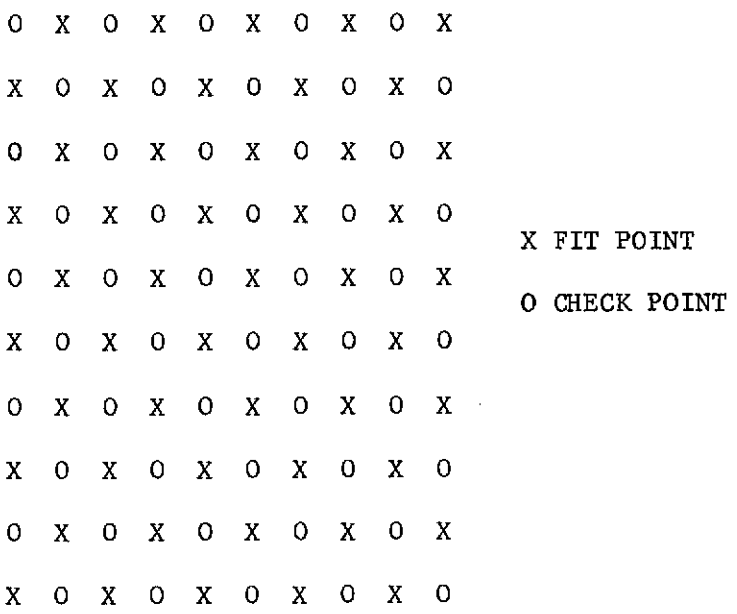

Figure 2.1-1. Typical Pattern of Fit and Check Points for Polynomial Warp Error Analysis

Separating the set of control points into sets of fit and check points is worthwhile only if there are enough control points to provide a reasonable degree of overdetermination. That is, only if the set of fit points represents considerably more measurements than there are degrees of freedom in the highest order fit of interest. A good rule of thumb is that the number of measurements should be at least twice the number of unknowns.

The second error analysis method makes no assumptions about the form of the spatial warp. This method is based on an automatic correlation technique which is analogous to that used in visual evaluation of the gradient superposition image. Reference and spatially warped dependent images are compared on a subregion basis to locate matching features. Given a matching feature, a hill-climbing technique is used to find the maximum correlation between images with an interpolation technique used to increase precision to a fraction of a pixel. The distance that a correlation maximum is displaced from the null condition is a direct measure of registration error for the feature in question.

This method which has been implemented in Program WECK (Warp Error Check) has proved to be quite accurate in controlled tests. The program automatically locates matching features and measures displacements, then accumulates statistics over all points. A test on the correlation coefficient is used to establish which features are similar enough to be considered "common" features. Points with low correlation are rejected.

Semi-automatic registration for this study was performed with Program SAW (Semi-Automatic Warp). This program is a research (as opposed to production) program with extensive warp error analysis capabilities. Control points or "samples" were selected using two techniques. The first technique, applied to image-to-ground registration for Hill County, is purposely crude to simulate point matching with an interactive display. Points were matched from photographic prints of the photomosaic map and different bands of the ERTS MSS data with contrast enhancement. These prints were made from photographs taken from Control Data's Dicomed Model 36 display.

Measurements were made visually subject to a grid with a 25-pixel spacing. Measurement accuracy is approximately 2 to 3 pixels for this method.

The second method for matching points, employed for Trinity Bay and for image-to-ground registration for Imperial Valley, is much more accurate. Points are matched from transparencies plotted on an OPTRONICS P1500 Film writer, and coordinates are measured with a Bendix Datagrid Digitizer. Accuracy is limited by a combination of image scale, 0.003 inch operator tolerance in directing the cursor, and sharpness of image features.

Since the method is so straightforward, semi-automatic registration can almost always be made to work. However, in any high-volume production processing enviroment, manual intervention in the selection of control points creates a severe bottleneck. In a production mode automatic registration is therefore nearly mandatory from a time standpoint alone. Additionally, automatic processing is potentially more accurate because its measurement accuracy in matching control points is higher and because the number of control points that can be sampled automatically is much larger.

2.2 HILL COUNTY

The registration requirement for Hill County is ERTS image-to-ground registration, where ground control is provided by an uncontrolled photomosaic. The following discussion describes how ERTS-1 MSS data was registered to a photomosaic image with a semi-automatic process and how registration accuracy was subsequently improved with a fully automatic correlation and registration process.

Correlation studies are discussed in some depth to assess the feasibility of automatic registration to ground control. Principal topics are:

- Data Preparation
- Semi-Automatic Registration Processing
- Automatic Multi-Sensor Correlation Studies
- Correlation Patch Size
- Spectral Considerations
- Control Point Selection
- Enhancement and Resolution Differences
- Automatic Multi-Sensor Registration

2.2.1 Data Preparation

Data preparation includes reformatting of MSS bulk data, cosmetic removal of noise, and digitization of an uncontrolled photomosaic.

MSS data was obtained in MSDS format with 8-bit encoding, 800 BPI on 9-track tape. The data was reformatted to produce separate files for each of the four bands with 6-bit encoding, 556 BPI on 7-track tape.

Since the MSS data is noisy it is desirable that the data be processed to detect and remove this noise. The chosen method is automatic and consists of replacing any bad data in a given line with the average of good data in the preceeding and following lines (Figures 2.2-1 through 2.2-4).

One noise problem occurs because of faulty recording or transmission to produce an interruption of the image data along scan lines. This deficiency is evident in the light and dark scan line streaks (Bands 4, 6 and 7, particularly). Close inspection of the data reveals that these streaks are not always continuous. In such instances only "bad" sections are replaced to avoid degeneration of "good" data. This problem was very effectively corrected to improve the appearance of the imagery.

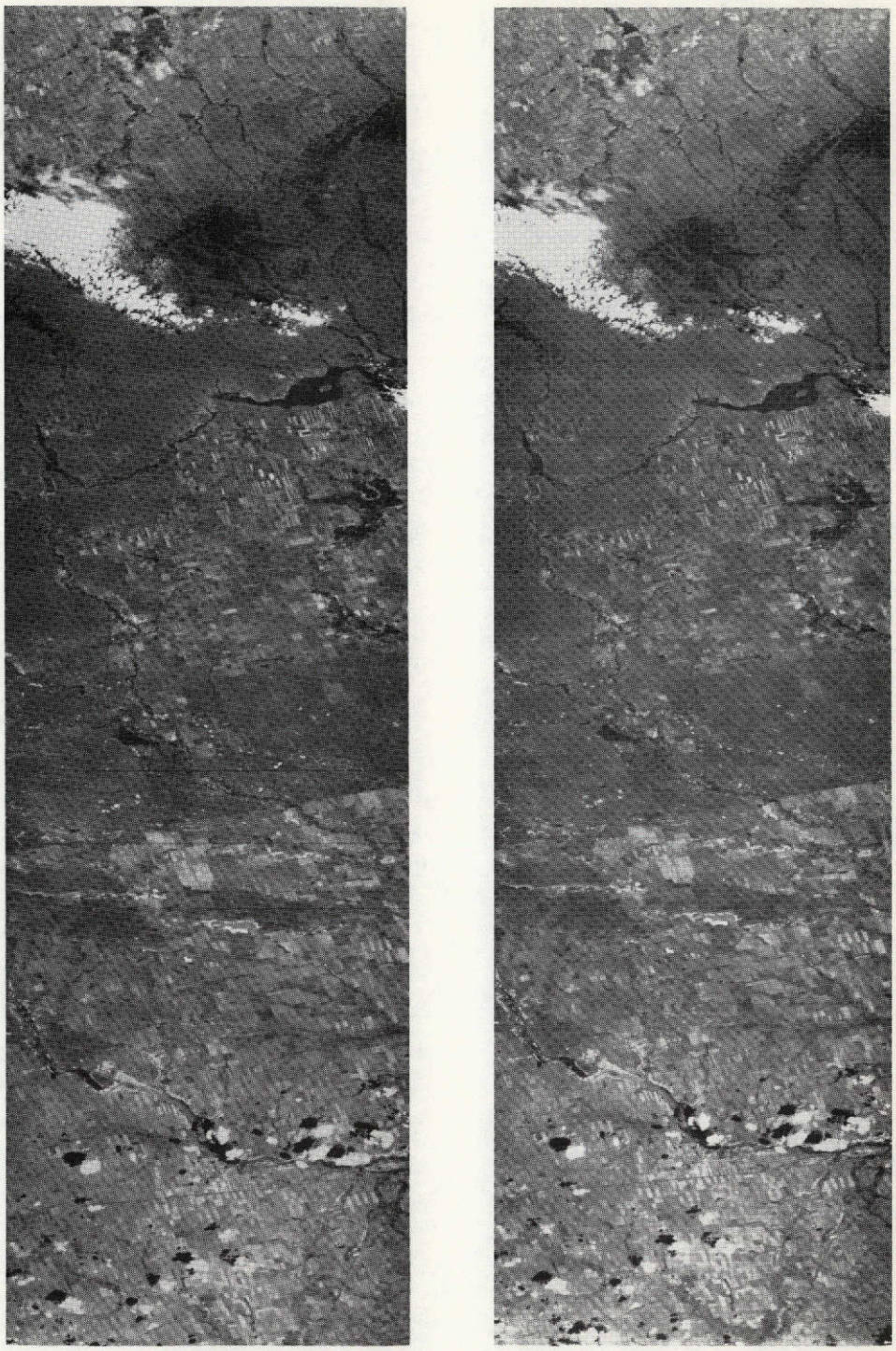

a) Bulk Data

b) Noise Removed

Figure 2.2-1. Noise Reduction in ERTS Imagery
ERTS-1 MSS, Band 4, Hill County, Montana

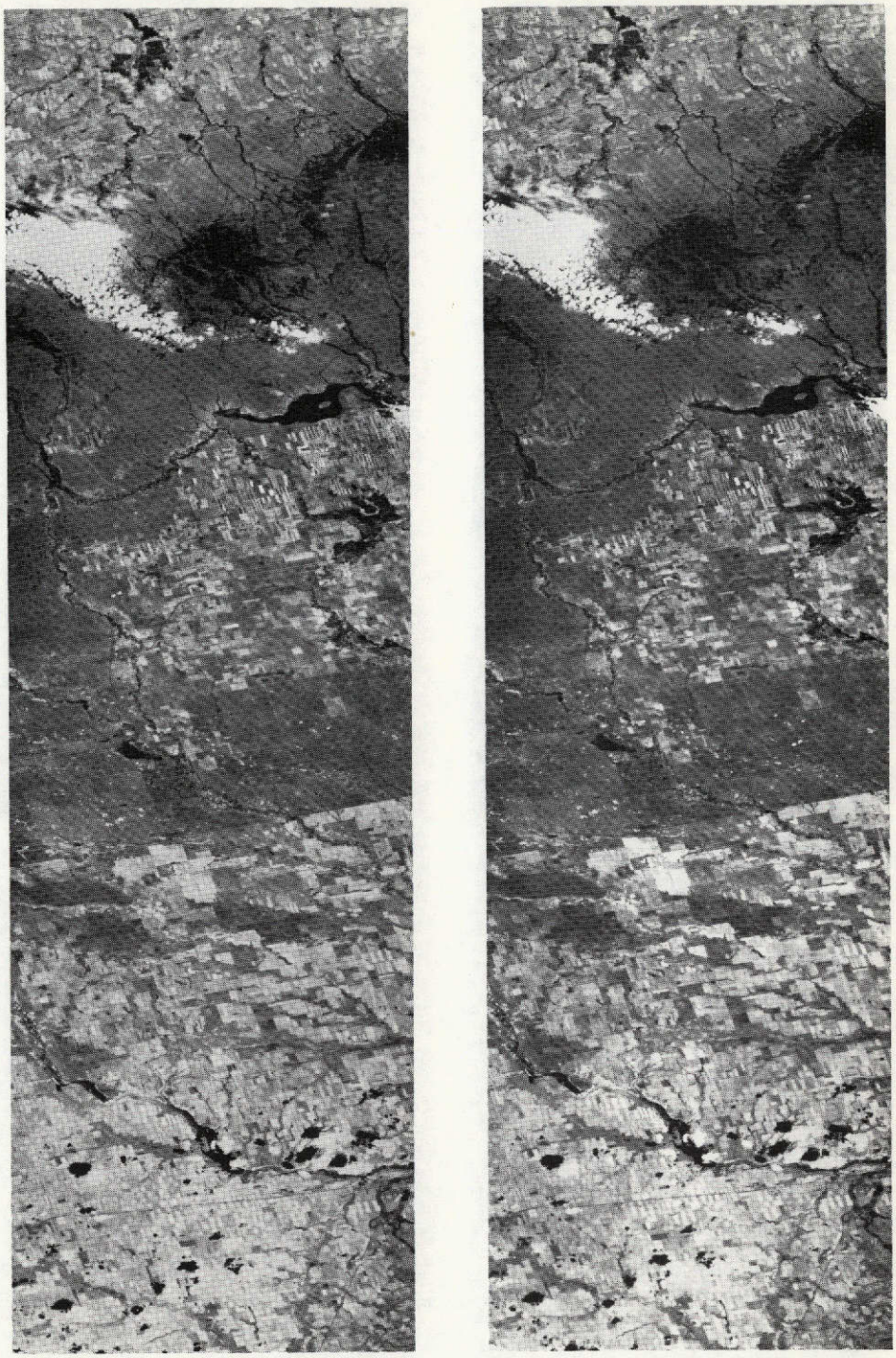

a) Bulk Data

b) Noise Removed

Figure 2.2-2. Noise Reduction in ERTS Imagery
ERTS-1 MSS, Band 5, Hill County, Montana

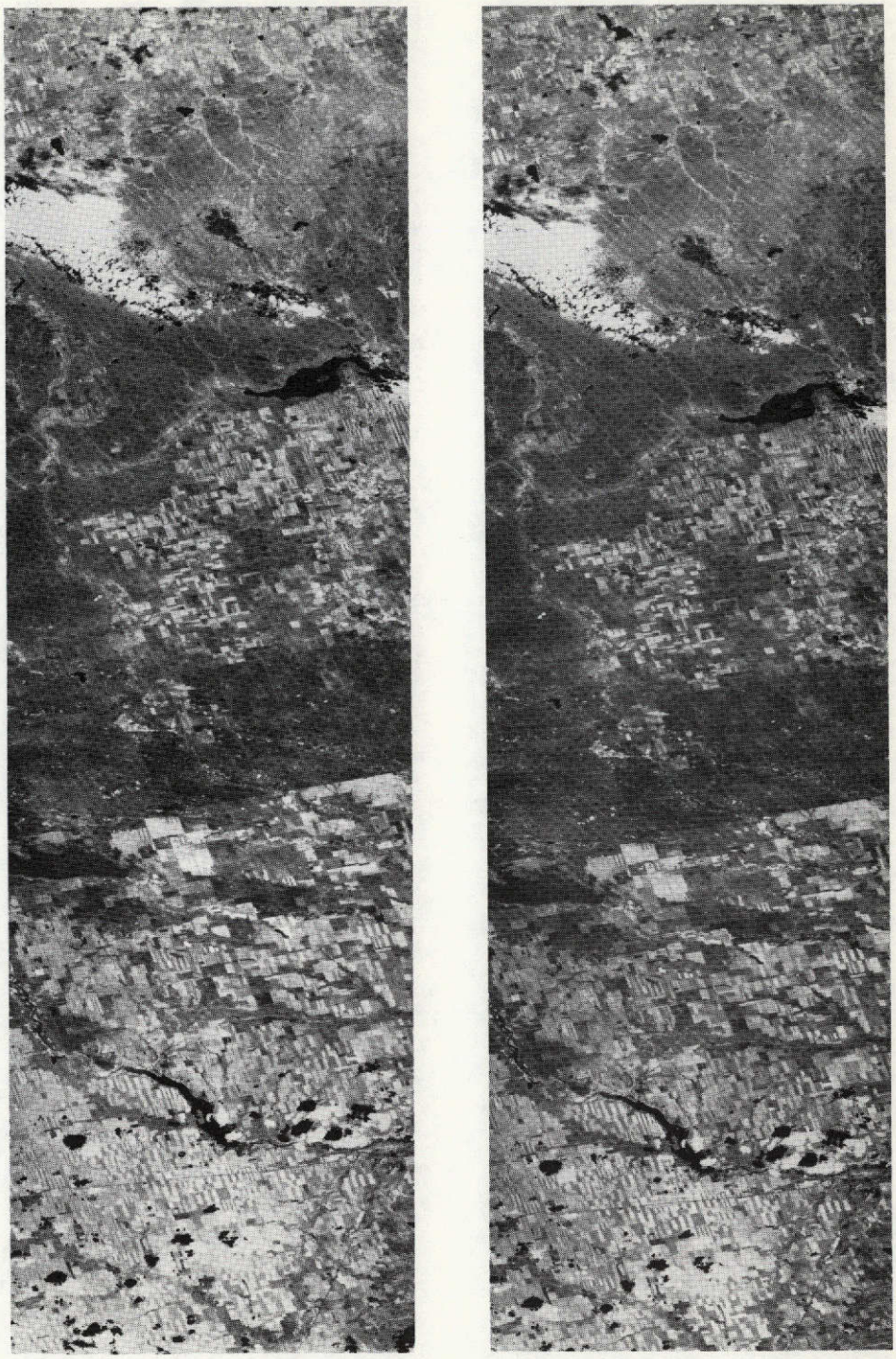

a) Bulk Data

b) Noise Removed

Figure 2.2-3. Noise Reduction in ERTS Imagery
ERTS-1 MSS, Band 6, Hill County, Montana

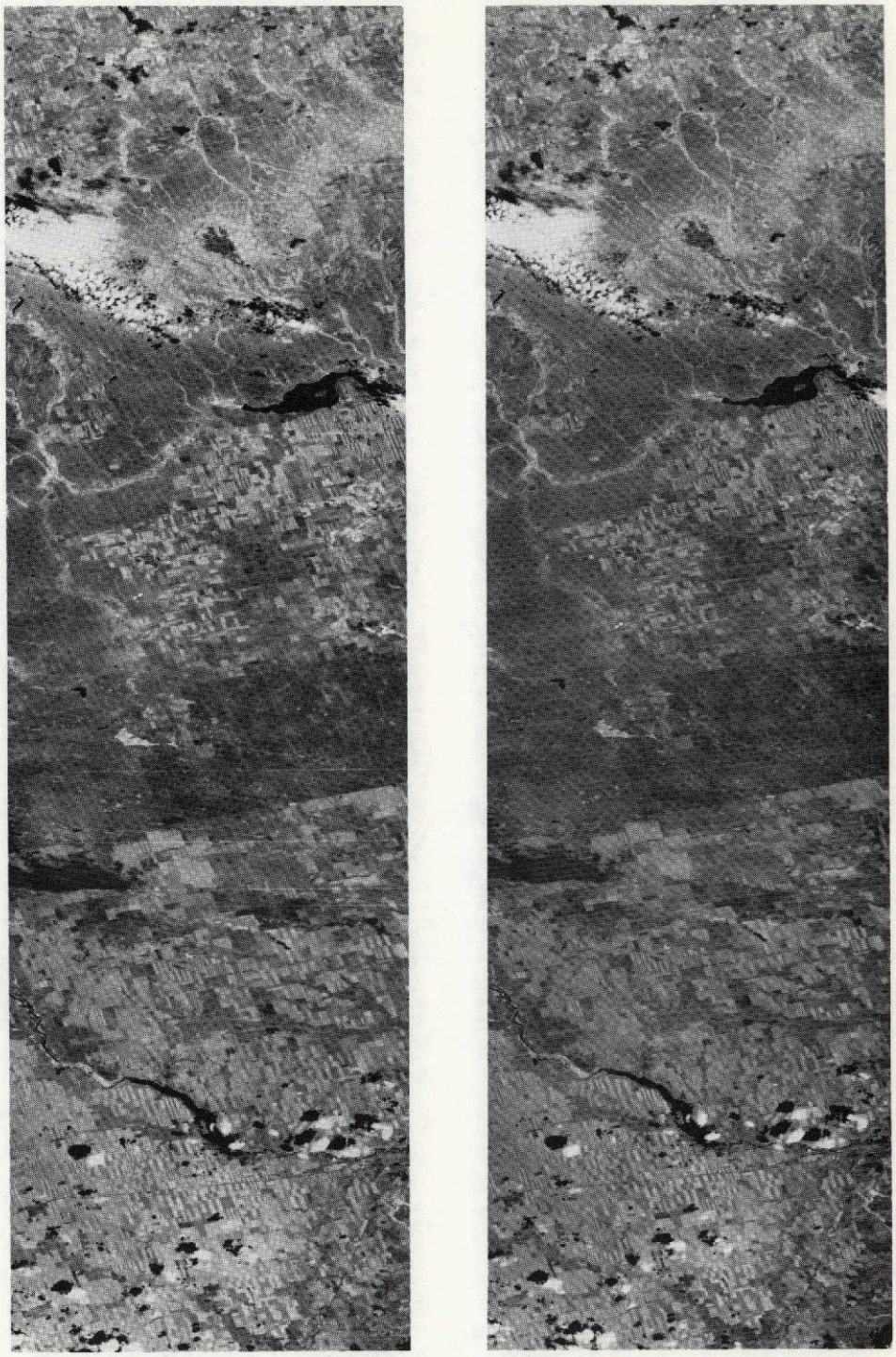

a) Bulk Data

b) Noise Removed

Figure 2.2-4. Noise Reduction in ERTS Imagery
ERTS-1 MSS, Band 7, Hill County, Montana

Another data collection problem is associated with the data format grouping of six lines at a time. This is particularly evident in Band 6 (Figure 2.2-3a) as a striated scan pattern with periodicity over six scan lines. The cosmetic correction technique is moderately successful here, but somewhat finer discrimination is required than that which was applied to this image.

An uncontrolled photomosaic of Hill County was digitized in order that studies of correlation between the ERTS data and photomosaic data could be conducted. It is desirable that the encoding of the photomosaic be done at somewhat higher resolution than the ERTS imagery. Thus, the photomosaic was encoded to 64 gray levels in a matrix of 867 pixels by 1010 lines.

In terms of ground scale one pixel in the digitized photomosaic corresponds to 80 feet. Scale of the bulk ERTS data is approximately:

$$s_x = \frac{100 \text{ nm } (6076 \text{ ft./nm})}{2340 \text{ lines}} = 260 \text{ ft./line}$$

$$s_y = \frac{25 \text{ nm } (6076 \text{ ft./nm})}{700 \text{ pixels}} = 217 \text{ ft./pixel} \qquad (2.2\text{-}1)$$

Therefore the spatial transformation required to register the ERTS MSS data to the digitized photomosaic represents a digital enlargement by a factor of approximately 3.2 in x and 2.7 in y.

Semi-automatic registration of the MSS data to the photomosaic in preparation for correlation and automatic registration studies is described in the following paragraphs.

2.2.2 Semi-Automatic Registration

ERTS MSS imagery was registered semi-automatically to ground control points over Hill County. That is, the spatial warp was performed automatically but it was based on manually matched control points. Each of the four bands of ERTS data were registered to the photomosaic with a quadratic warp based upon the 21 control points shown in Figure 2.2-5.

Figure 2.2-5. Selection of Control Points on Photomosaic Hill County, Montana

To improve visual recognition of features the contrast of ERTS imagery was enhanced digitally. Also, to maintain maximum fidelity in reproduction both images were digitally enlarged to a matrix of 1734 by 2020 pixels. Grid spacing for the MSS imagery was 25 pixels, so measurement error was approximately 2 to 3 pixels RMS in either x or y.

Of paramount importance in registering an ERTS image to ground control points are answers to two questions. How complicated is the spatial warp and how accurately can the MSS image be registered to ground control? Consider the accuracy question first. On the basis of measurement error alone mean radial registration error should be approximately

$$\bar{r}_M = \frac{\sqrt{2}}{\sqrt{N}} \sigma_M \qquad (2.2\text{-}2)$$

where $\bar{r}_M$ is the mean radial error, N is the number of control points and σ_M is the RMS measurement error in either x or y. For measurement error estimates given above mean radial registration error should lie between 0.62 and 0.93 pixels. The measured value for a quadratic fit to 21 control points is 1.36 pixels (ERTS image scale).

Possible reasons for this discrepancy between estimated and measured errors are:

- Estimated measurement errors are low.
- Spatial warp is not exactly quadratic.

Results of a spatial warp error analysis performed in [13]indicate that a quadratic or even a linear fit is an adequate approximation to the spatial warp between the photomosaic and ERTS imagery over a relatively small area such as Hill County. The higher than predicted mean radial error may result either from random local variations or from higher-order systematic variations not accounted for in the quadratic model. Error analysis results indicate that the former is more likely, but there are really not enough control points to be conclusive.

In answer to the warp complexity question, then, it appears that the spatial warp in ERTS imagery relative to ground control for Hill County is predominately linear. The ERTS data is skewed roughly 12^{o} relative to ground coordinates and its scale is different in x and y directions (Table 3-1 in [13]). At least six degrees of freedom (linear warp) are required to accurately model the spatial warp. The increase in accuracy for 12 degrees of freedom (quadratic warp) is insignificant (Table 3-2 in [13]).

2.2.3 Automatic Multi-Sensor Correlation Studies

The foundation of automatic image registration is the correlation process. The first step in establishing feasibility for automatic image-to-ground registration is therefore to verify that automatic correlation can provide accurate control points for this application. That is, it must be established that the computer can recognize the same feature on the photomosaic reference and ERTS MSS image without ambiguity.

The correlation process is performed on a subregion basis; for this study square subregions are employed. Performance is therefore related to subregion size in addition to other considerations. These include:

- Spatial distortion effects on correlation
- Temporal change
- Different sensor resolution
- Different sensor spectral response.

The effect of spatial distortion is discussed by Henrikson, Glish, and Hoyt [5]. Basically spatial distortion between images means that subregions on reference and dependent images will not be in complete alignment during correlation. The consequence is lower accuracy in matching control points and more "false locks." Effects of spatial distortion may be compensated for by "shaping" data prior to correlation. This is done for rotation and down-track scale variations with Control Data's current automatic strip processing technique.

For this investigation spatial distortion effects were minimized by performing correlation studies after semi-automatic registration of ERTS MSS imagery to the photomosaic reference. The remaining effects are those of temporal change, different sensor resolution between ERTS and the digitized photomosaic, and different sensor spectral response.

In establishing feasibility for automatic ERTS image-to-ground registration, these problems demand an answer to the basic question:

- Can automatic correlation techniques recognize enough common features accurately enough to form the basis for a spatial warp of acceptable accuracy?

This question of course implies a number of additional questions, namely:

- What correlation patch size should be employed?
- Which MSS spectral band or combination of bands yields the best results when correlated with the photomosaic reference?
- Which features are generally best for correlation?
- What effect if any does difference in resolution have?
- Is any preprocessing necessary to improve correlation results?

Automatic multisensor correlation and registration is obviously a very difficult problem. Therefore the temptation in designing a feasibility study is to make it too elaborate.

The approach taken here is to make the automatic correlation feasibility study as simple and direct as possible. Basically the test for feasibility is to see if automatic techniques can correctly identify and match to at least the same accuracy the 21 control points upon which the semi-automatic warp was based. In the course of this test answers to the above questions will be sought.

For these studies correlation was performed over an NxN square subregion surrounding each control point. If the ERTS and photomosaic images are in perfect registration, the maximum of the cross correlation surface for each control point is at zero shift in x and y. Since registration is not perfect

the correlation maximum is shifted. Error analysis discloses a residual fit error having a mean radial value of 1.36 pixels on the ERTS scale, which translates to a value between 3.7 and 4.4 pixels on the digital photomosaic scale. Some of this error is, of course, a result of measurement error in the sampling processes. Accordingly, it is to be observed in the following multisensor correlation studies that the peak of the cross correlation surface is displaced radially from the null position by about 4 pixels on the average.

For a given control point an NxN patch surrounding the point on the photomosaic is correlated with a window of the same size on a selected band of the spatially warped ERTS MSS imagery. The window is moved about on the ERTS imagery according to the pattern shown in Figure 2.2-6.

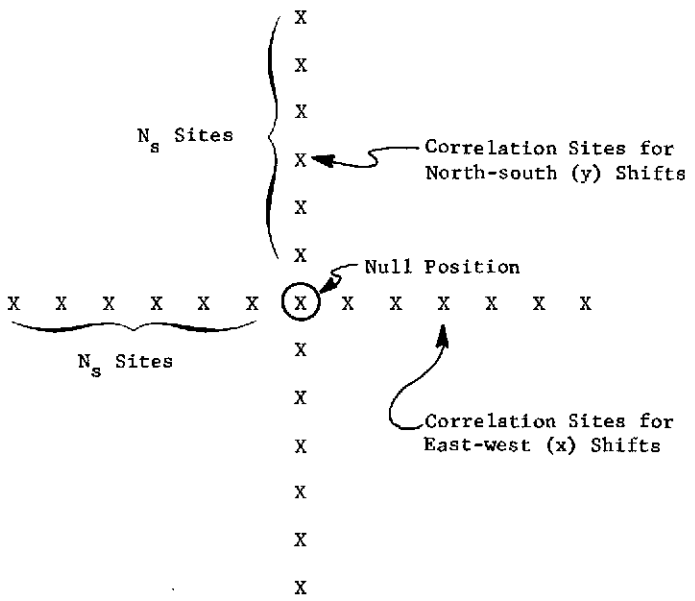

Figure 2.2-6. Correlation Sites for Multi-Sensor Correlation Study Hill County Photomosaic and ERTS-1 MSS Image

Shifts are made only along the x (east-west) and y (north-south) axis about the null position. A total of $2N_s+1$ evaluations of the correlation coefficient are made along each axis.

Generally this pattern will not include the maximum of the cross-correlation surface but the position of the maximum can be estimated with acceptable accuracy from positions of the maxima for x and y shifts. This also means that absolute maximum correlation will be somewhat higher than local maxima for x and y shifts. The peak value given in Table 2.2-1 is the larger of these local maxima.

TABLE 2.2-1. SUMMARY OF AUTOMATIC MSS TO PHOTOMOSAIC CORRELATION STUDY FOR HILL COUNTY

CONTROL POINT	PEAK CORRELATION VALUES				PREDICTED DISPLACEMENT OF PEAK FROM NULL POSITION							
					BAND 4		BAND 5		BAND 6		BAND 7	
	BAND 4	BAND 5	BAND 6	BAND 7	Δ x	Δ y	Δ x	Δ y	Δ x	Δ y	Δ x	Δ y
1	.487	.689	.617	.573	-3	-2	-3	-1	-3	0	-3	-1
2	.336	.324	.217	.126	0	-2	0	-2	1	-3	-12	-13
3	.596	.700	.714	.698	4	-4	4	-3	4	-3	5	-3
4	.766	.777	.733	.638	6	-4	6	-5	6	-4	6	-4
5	.607	.658	.686	.647	3	-5	2	-4	2	-5	2	-4
6	.602	.638	.648	.638	0	-1	-1	-1	1	-1	2	-1
7	.455	.508	.597	.601	3	2	3	2	3	1	3	1
8	.594	.656	.662	.637	2	-3	2	-3	2	-3	2	-4
9	.560	.642	.656	.615	2	0	1	-1	2	-1	2	-1
10	.609	.677	.696	.709	1	-2	2	-3	2	-4	2	-5
11	.569	.542	.580	.568	-2	-3	-2	-3	-2	-3	-3	-3
12	.636	.689	.710	.702	4	-4	4	-4	3	-3	3	-3
13	.403	.512	.488	.442	4	2	4	0	5	1	5	-1
14	.610	.696	.707	.699	-1	-6	-1	-6	-1	-6	-1	-6
15	.569	.619	.522	.423	2	-3	3	-3	4	-4	4	-6
16	.337	.368	.602	.639	0	-4	0	-5	-1	-5	-2	-6
17	.627	.770	.649	.578	2	-2	1	-2	1	-3	1	-3
18	.510	.539	.476	.459	-1	-4	-2	-5	-3	-5	-3	-4
19	.633	.692	.684	.649	2	4	1	-4	2	-3	2	-4
20	.541	.604	.594	.556	3	-1	2	-2	2	-2	2	-2
21	.630	.621	.512	.424	-6	-4	-4	-4	-4	-4	-4	-4
Mean	.556	.615	.607	.595*	1.19	-2.19	1.05	-2.81	1.24	-2.86	1.25	-3.20*
Mean Radial Displacement					4.09		4.04		4.26		4.62*	

*Excluding Control Point 2

Note that the mean radial displacement of the correlation peak, except for Band 7, falls within the range predicted above. Note also that peak correlation values (for each-west and north-south shifts only) are on the average about 0.6, a reasonably high correlation coefficient. Graphs of the correlation coefficient as a function of x and y shifts are included in the following discussion of correlation patch size.

2.2.4 Correlation Patch Size

The question of what patch size to use in correlation is a fundamental one. Generally the patch size must be just large enough to "capture" enough strong features common to both images to allow an unambiguous match. If the correlation patch is made too large it may include areas in which correlation between the two images is low and the correlation coefficient will decrease accordingly. Also, of course, larger patches require more computation time. Computation time is at least proportional to N^2.

On the other hand, if the correlation patch is taken too small, it may not include enough area to uniquely define the feature of interest. There are also noise problems associated with "small sample statistics." Random local differences between images over the feature of interest can make the correlation surface uneven and can lead to prominant secondary maxima. This is not acceptable for automatic registration. Prominent secondary maxima can lead to false matches, and an uneven correlation surface means problems for hill climbing algorithms which locate the correlation peak.

A good rule of thumb is that the patch size be taken the same as that needed to visually match features uniquely on the two images. Consider control points 3 and 17, for example. Computer line printer gray-scale dumps for these two control points on the photomosaic are presented in Figure 2.2-7 for patch sizes of N=11, 51 and 81. For each control point the three patches relate to the same feature but are not precisely centered at the same point. Also each plot represents the negative of the image in Figure 2.2-5 with contrast enhance-

ment. The line printer gray-scale has 21 levels; to completely cover this range the minimum density over a patch is assigned to the first level, the maximum density is assigned the twenty-first and all intermediate levels are scaled linearly, i.e.

$$P_{out} = \frac{20(P_{in} - P_{min})}{P_{max} - P_{min}} + 1 \qquad (2.2\text{-}3)$$

where P_{min} = minimum density over patch

P_{max} = maximum density over patch

P_{in} = density at a point

P_{out} = line printer gray-level corresponding to P_{in}

Obviously the 11 by 11 patch is too small to uniquely identify either feature. The 51 by 51 patch seems to be large enough to include enough of the feature so that it can be readily recognized and the 81 by 81 patch begins to bring in additional features. For example, at control point 3 roads become apparent in addition to the dam and reservoir. At control point 17 additional fields enter the picture.

In the case of multi-sensor correlation, more features are not necessarily a good thing, as these additional features are not necessarily the same for the two sensors. For example, compare the included features at control point 3 when N=51 and N=81. In the N=51 case one can generally recognize the reservoir and dam in all four ERTS spectral bands (Figure 2.2-11), but the area surrounding the reservoir does not have the same appearance in the aerial photomosaic and ERTS MSS images (Figures 2.2-7 and 2.2-8, respectively).

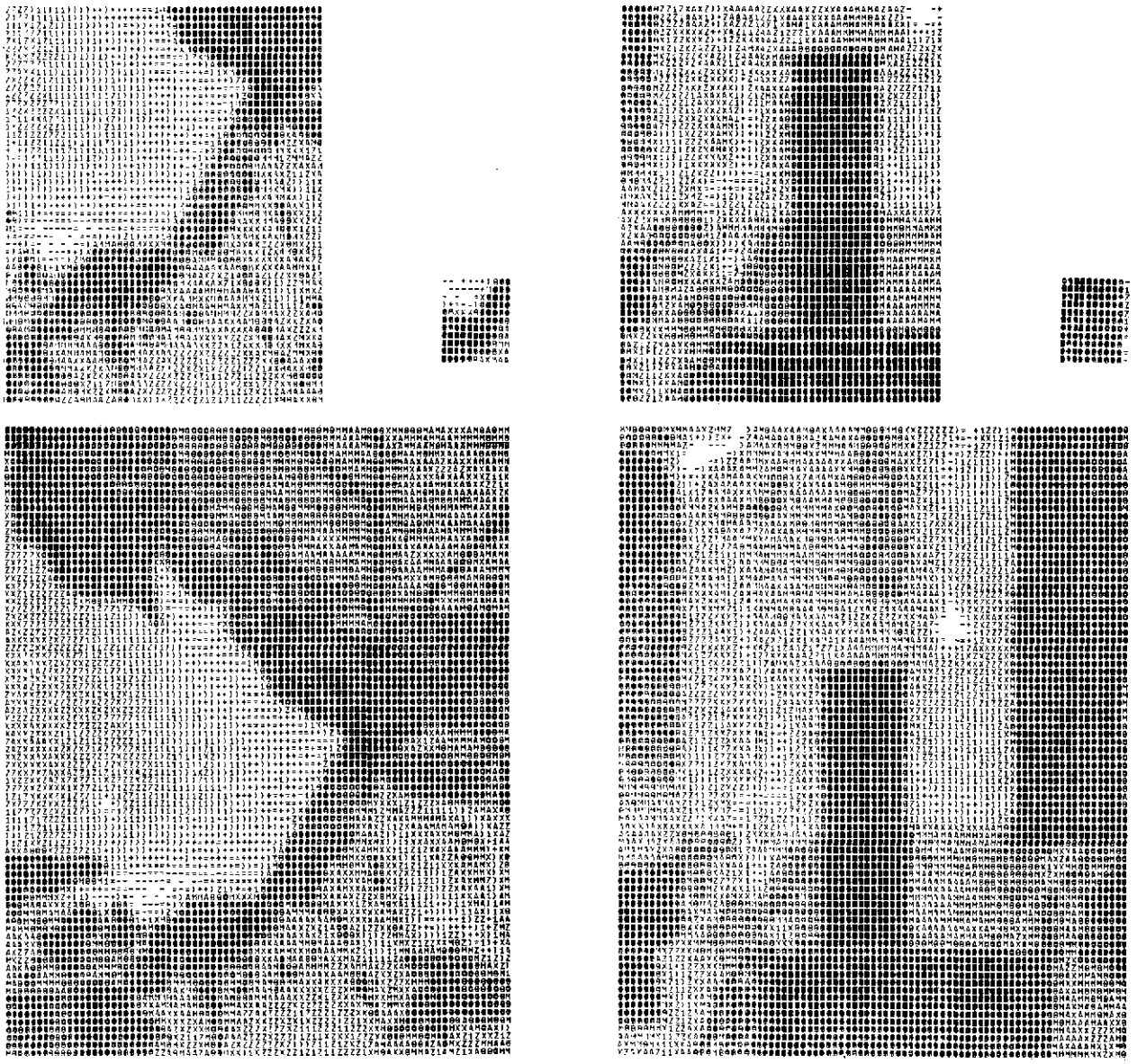

D2150

Control Point 3

Control Point 17

Figure 2.2-7. Hill County Photomosaic Correlation Correlation Patch Size 11 by 11, 51 by 51 and 81 by 81 pixels.

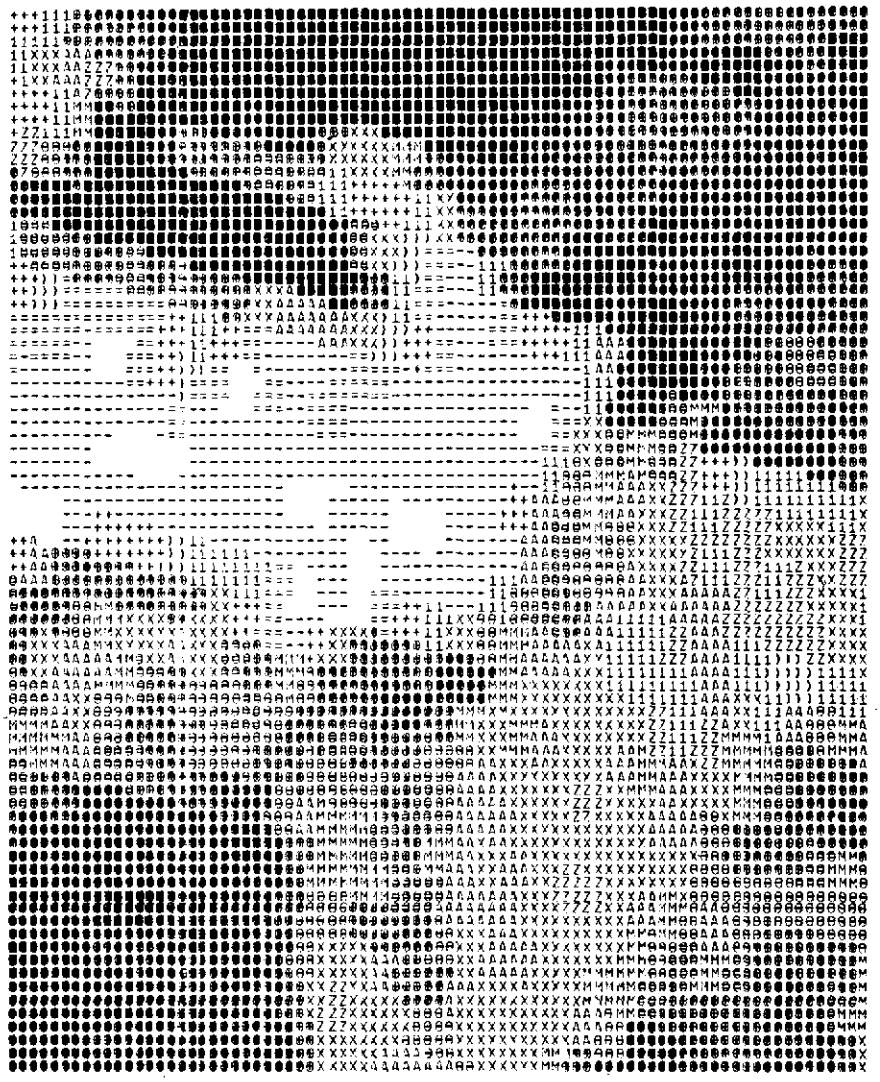

D1800

Figure 2.2-8. ERTS Band 5 for Control Point 3, 81 by 81 Patch

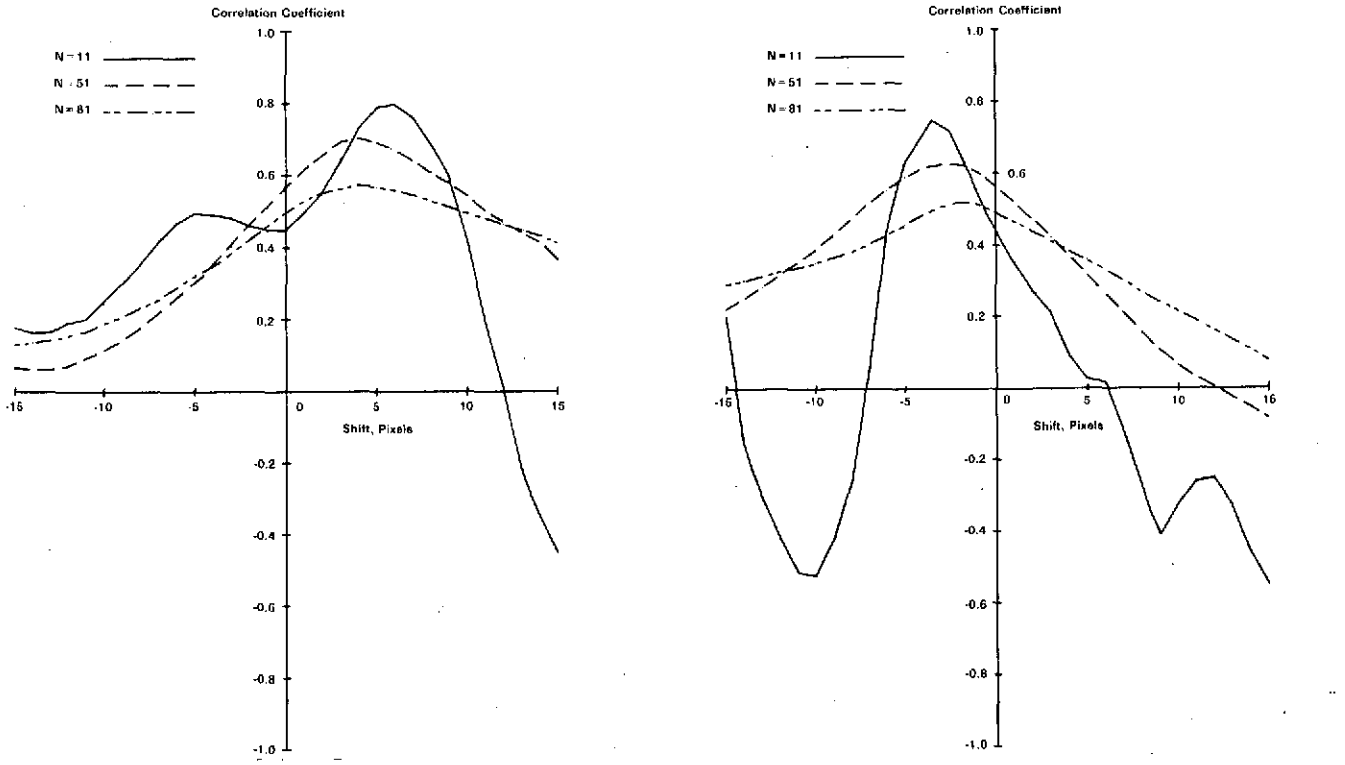

(a) East-West Shifts (b) North-South Shifts

Figure 2.2-9. Cross Correlation, Control Point 3

Effects of patch size on the cross correlation surface can be seen in Figures 2.2-9 and 2.2-10. These figures present cross sectional plots of the cross correlation surface between the photomosaic and ERTS Band 5. Plots are presented for east-west and north-south shifts with patch sizes defined by N = 11, 51 and 81. Note that the correlation surface is generally more uneven for the N = 11 case with pronounced secondary maxima. Moreover, the location of the correlation peak is not necessarily the same for N = 11 as for N = 15 or N = 81.

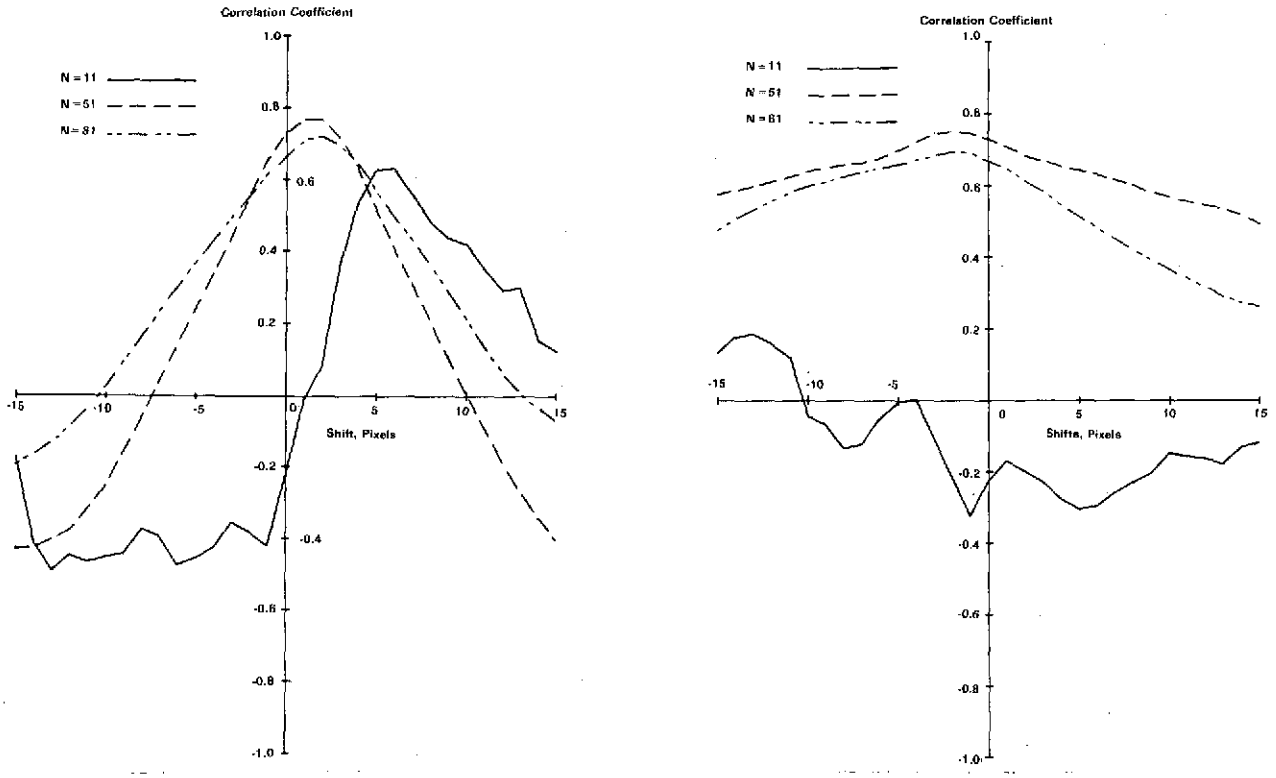

(a) East-West Shifts (b) North-South Shifts

Figure 2.2-10. Cross Correlation, Control Point 17

On the other hand for N = 51 and 81 the correlation surface tends to be smoother with a single well-defined peak. Location of the peak is approximately the same for N = 51 and N = 81. Note however that the peak value tends to be somewhat lower for the N = 81 case. This is a reflection of the face that the area is enough larger to include features that are unrelated on the two images.

In conclusion N = 11 represents too small a patch and N = 81 too large a patch. N = 51 appears to represent a reasonable compromise, although this value could probably be lowered somewhat with further research. Furthermore there is really no reason to hold patch size constant. It may be adjusted empirically to fit the size of a given feature.

In terms of ground scale and ERTS MSS resolution a 51 by 51 pixel patch represents an area of approximately

$$S = [(51 \text{ pixels}) \times (80 \text{ ft./pixel})]^2 = (4080 \text{ ft.})^2 \simeq 0.6 \text{ miles}^2 \qquad (2.2\text{-}4)$$

or on the order of 16 x 19 pixels in the ERTS MSS scale.

2.2.5 Spectral Considerations

The various imagery features are emphasized differently by each spectral band of detected radiation. Hence, best correlation can be anticipated when similar spectral sensitivities are used for two different sensors.

The correlation studies with the Hill County data show that on the average Band 5 imagery is most nearly similar to the photomosaic, followed by Bands 6, 7 and 4 in that order.

At control point 3 ERTS Bands 5 and 6 (Figure 2.2-11) are most similar to the photomosaic (Figure 2.2-7), although the feature can be recognized for all four bands. However, at control point 17 only Band 5 (Figure 2.2-12) is distinctly similar to the photomosaic (Figure 2.2-7).

Note that in the former case where visual recognition is high for Bands 5, 6 and 7 the measured peak correlation values are uniformly high, while for Band 4 recognition is not so definite and the peak correlation is correspondingly lower (Table 2.2-1). On the other hand at control point 17, for which Band 5 is obviously the most nearly similar to the photomosaic, the peak correlation coefficient is much higher for that band than for any other. The joint probability distribution of gray-scale values affords another means of assessing similarity between images (Figures 2.2-13 and 2.2-14). In these charts the vertical axis represents density for the photomosaic, and the

BAND 4

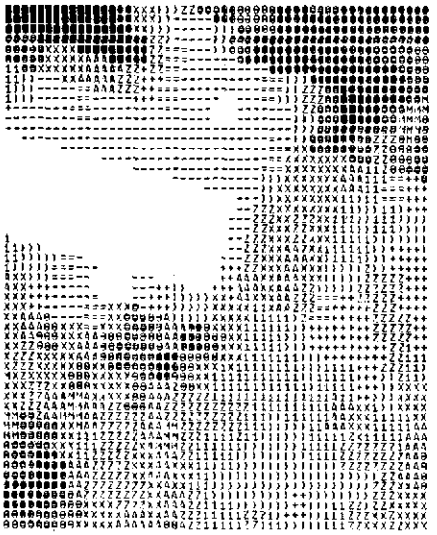

BAND 5

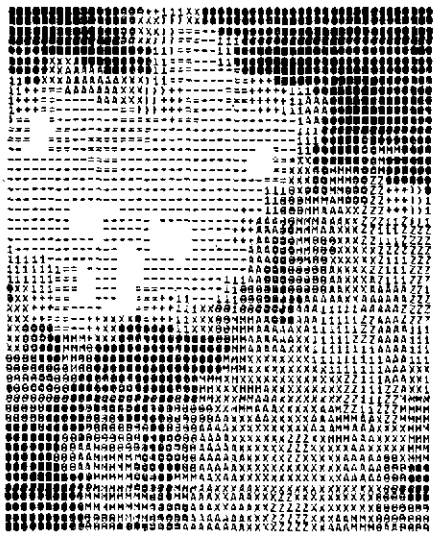

BAND 6

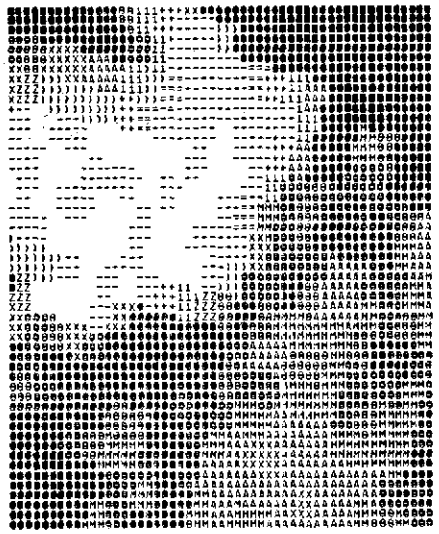

BAND 7

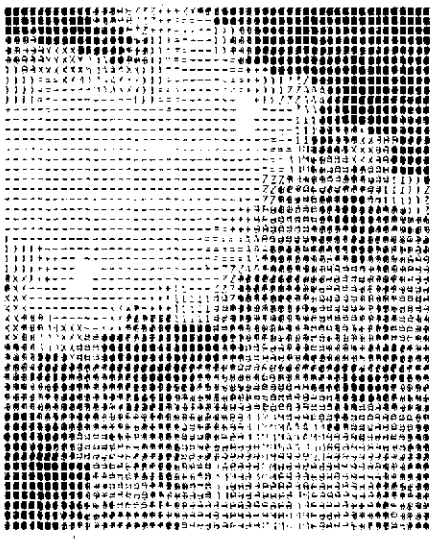

D1799

Figure 2.2-11. Computer Line Printer Gray Scale Dump for Hill County Control Point 3, ERTS MSS.

BAND 4

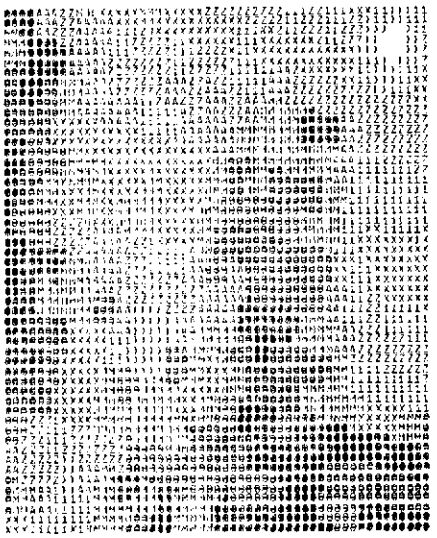

BAND 5

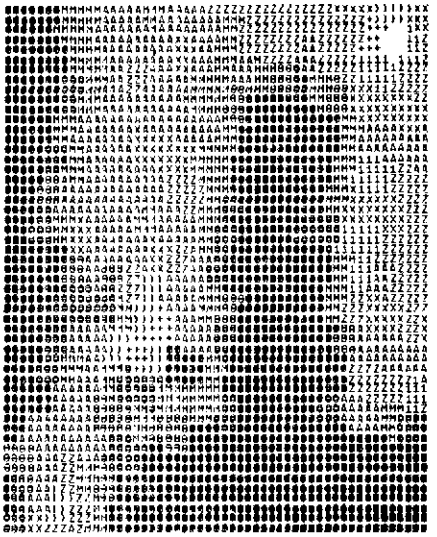

BAND 6

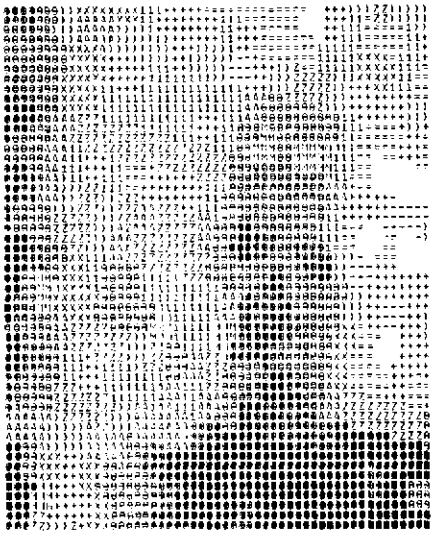

BAND 7

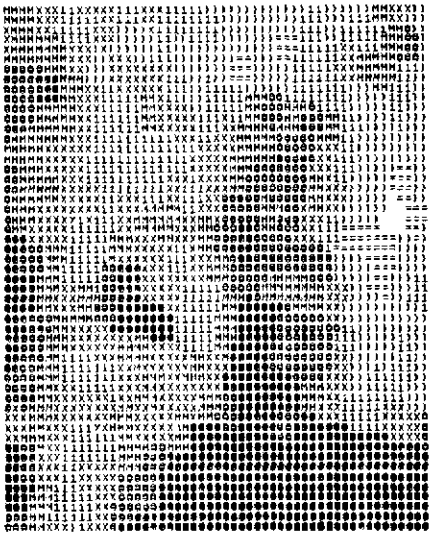

D1800

Figure 2.2-12. Computer Line Printer Gray Scale Dump for Hill County, Control Point 17, ERTS MSS.

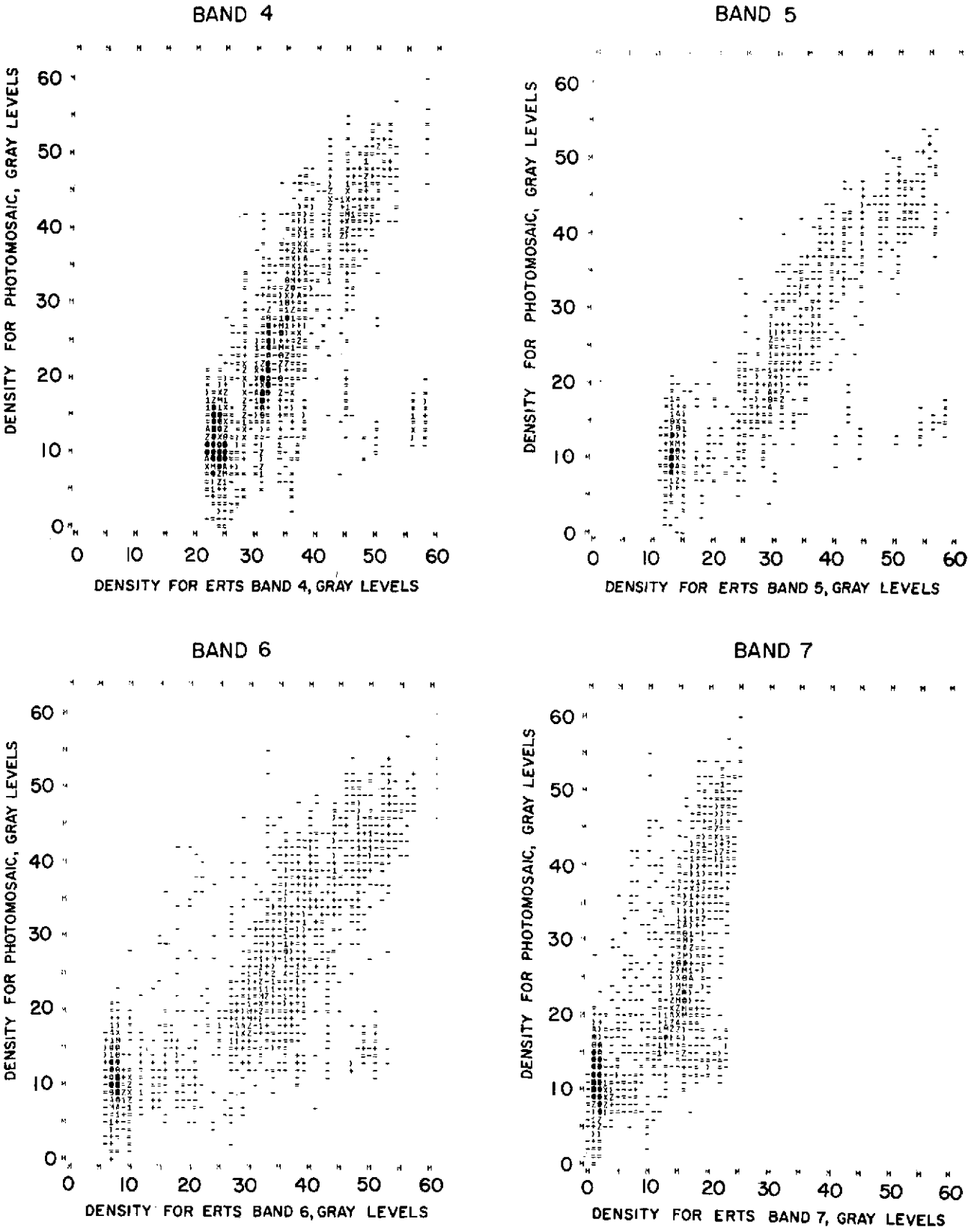

Figure 2.2-13. Joint Distributions for Hill County Control Point 3

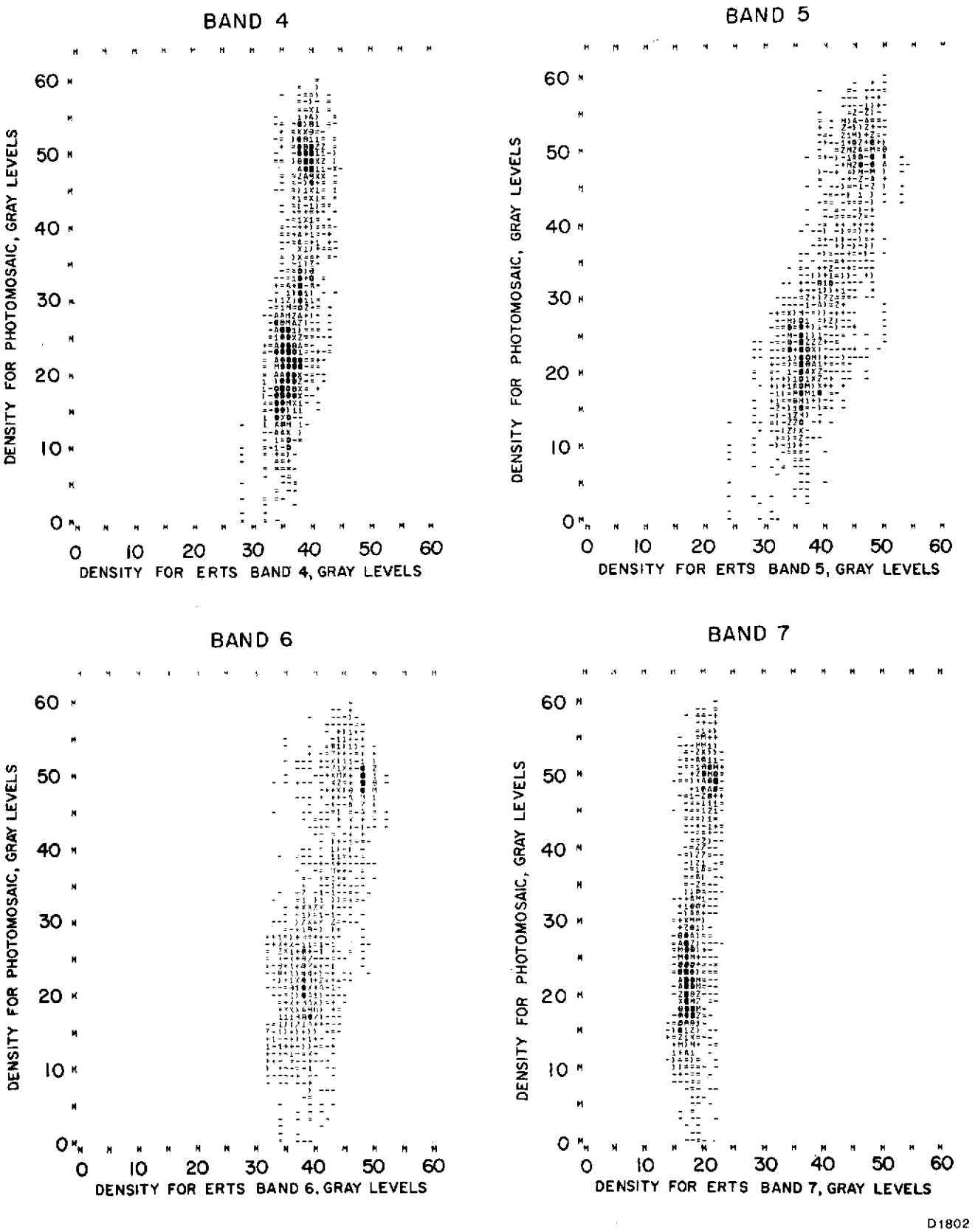

Figure 2.2-14. Joint Distributions for Hill County Control Point 17

horizontal axis represents density for the appropriate band of ERTS. Frequency is displayed in gray scale form with the same contrast enhancement algorithm that was used above. These results were obtained by positioning patch matrices of 51 by 51 pixels to yield peak correlations.

In interpreting joint distributions of this type one should look for distinct patterns in the shape of the distribution. If there is no geometrical organization the two processes under consideration are unrelated. On the other hand if the two processes are identical, all entries in the joint distribution would lie along a line of slope 45^{o} passing through the origin. If the two processes have some degree of similarity but are not identical, a definite trend in the data should be in evidence. However, there will be some spread about the trend curve.

For control point 3 there is obviously a considerable degree of similarity between the photomosaic and each band of ERTS. One means of comparing this degree of similarity is of course the correlation coefficient. Other important parameters are slope of the regression line, standard deviation perpendicular to the regression line, mean density for both processes and standard deviation for both processes. These parameters are summarized in Table 2.2-2 for both control points.

For control point 3 Bands 5 and 6 are most nearly similar to the photomosaic. The correlation coefficient is high and the regression line is within a few degrees of 45^{o}. Note also that contrast on the ERTS image is reasonably good. For Band 4 both contrast and correlation coefficient are much lower. Also slope of the regression line is 60^{o}. For Band 7 correlation is nearly as high as for Bands 5 and 6, but contrast is about half as much. This is because Bands 5 and 6 are on a seven bit scale (which has been truncated at six bits) and Band 7 is on a six bit scale. The slope of the regression line must also be adjusted by a factor of two to be equivalent to that for Bands 5 and 6.

TABLE 2.2-2. SUMMARY OF STATISTICAL PARAMETERS FOR JOINT DISTRIBUTIONS AT PEAK CORRELATION BASED ON A 51 x 51 PATCH

PARAMETER	CONTROL POINT 3				CONTROL POINT 17			
	BAND 4	BAND 5	BAND 6	BAND 7	BAND 4	BAND 5	BAND 6	BAND 7
ρ	0.695	0.782	0.790	0.760	0.663	0.880	0.710	0.622
p_{min}	0	0	0	0	0	0	0	0
$\bar{p}$	23.7	23.7	23.7	23.7	31.1	31.1	31.1	31.1
p_{max}	60	60	60	60	60	60	60	60
σ_p	12.6	12.6	12.6	12.6	14.0	14.0	14.0	14.0
q_{min}	22	11	6	0	28	24	32	14
$\bar{q}$	33.7	30.5	29.4	12.2	37.4	40.0	40.8	18.6
q_{max}	63	63	61	25	45	54	52	23
σ_q	8.7	13.2	14.9	7.4	2.6	5.4	4.6	1.9
θ	60^o	44^o	39^o	63^o	83^o	72^o	76^o	85^o
$\sigma_\perp$	5.5	6.02	6.23	4.4	2.0	3.1	3.1	1.5

ρ = correlation coefficient (peak value)

p_{min} = minimum density for photomosaic, gray levels

$\bar{p}$ = mean density for photomosaic, gray levels

p_{max} = maximum density for photomosaic, gray levels

σ_p = density standard deviation (contrast) for photomosaic, gray level

q_{min} = minimum density for ERTS, gray levels

$\bar{q}$ = mean density for ERTS, gray levels

q_{max} = maximum density for ERTS, gray levels

σ_q = density standard deviation (contrast) for ERTS, gray levels

θ = slope of regression line, degrees

$\sigma_\perp$ = standard deviation perpendicular to regression line, gray levels

In summary, based on the statistical parameters of Table 2.2-2 Bands 5 and 6 are most nearly similar to the photomosaic, and Band 7 is only slightly less so. Band 4 however is significantly less similar and has much lower contrast.

For control point 17 Band 5 is clearly the most nearly similar to the photomosaic, Band 6 represents an intermediate case, and Bands 4 and 7 are clearly inferior. Note the very low contrast in this case.

In conclusion, for best results Bands 5 or 6 should be used for correlation with the photomosaic. In any case, high correlation peak values are preferred for error reduction in the hill-climbing algorithms. Even if the other bands are used here, however, nearly equivalent results are expected since the peak correlation value is at nearly the same location in each case.

2.2.6 Control Point Selection

The above results provide a clue for the next question, namely how does one select features to be control points? From the above results it appears that both man made features (fields) and natural features (rivers) can be used. An obvious first requirement is that the feature be subject to very little long term temporal change, since a considerable time lapse is to be expected between dates at which imagery is collected for the reference data base and from ERTS. The two year lapse for this Hill County case can probably be considered typical. Clearly automatic techniques will not work in cases with pronounced short term temporal, e.g. seasonal, changes.

In addition, features selected for control points must have reasonably high contrast on the ERTS imagery, the features must be large enough to cover a reasonable area and have variation in both x and y. If contrast is low the feature can be lost in "noise," i.e. nonrepeatability between the reference and ERTS images.

Generally, but not always, low contrast means lower correlation peaks

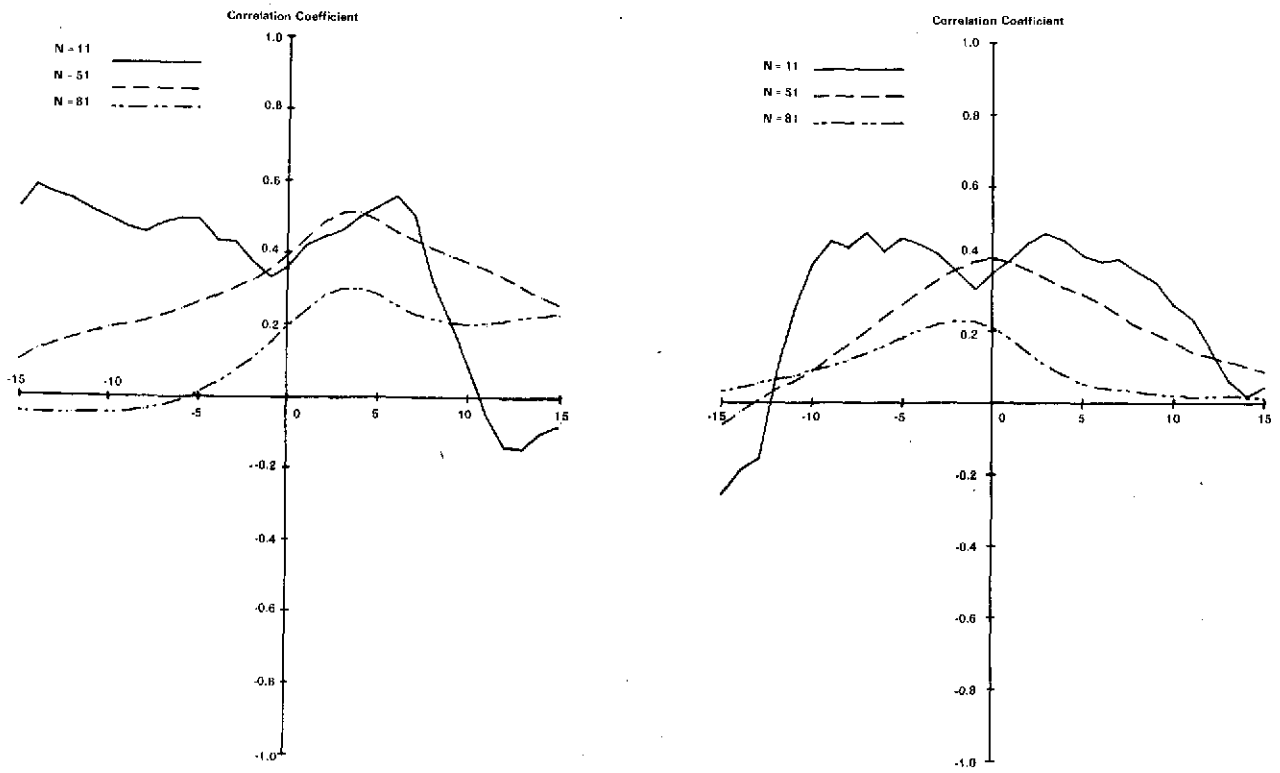

(a) East-West Shift

(b) North-South Shift

Figure 2.2-15. Cross Correlation, Control Point 13

because of the noise problem. This is illustrated by control points 13 and 16 which obviously have low contrast on the photomosaic reference (Figure 2.2-5). Cross sectional plots of the correlation surface for these control points are presented in Figures 2.2-15 and 2.2-16. Note that the peak values are relatively low.

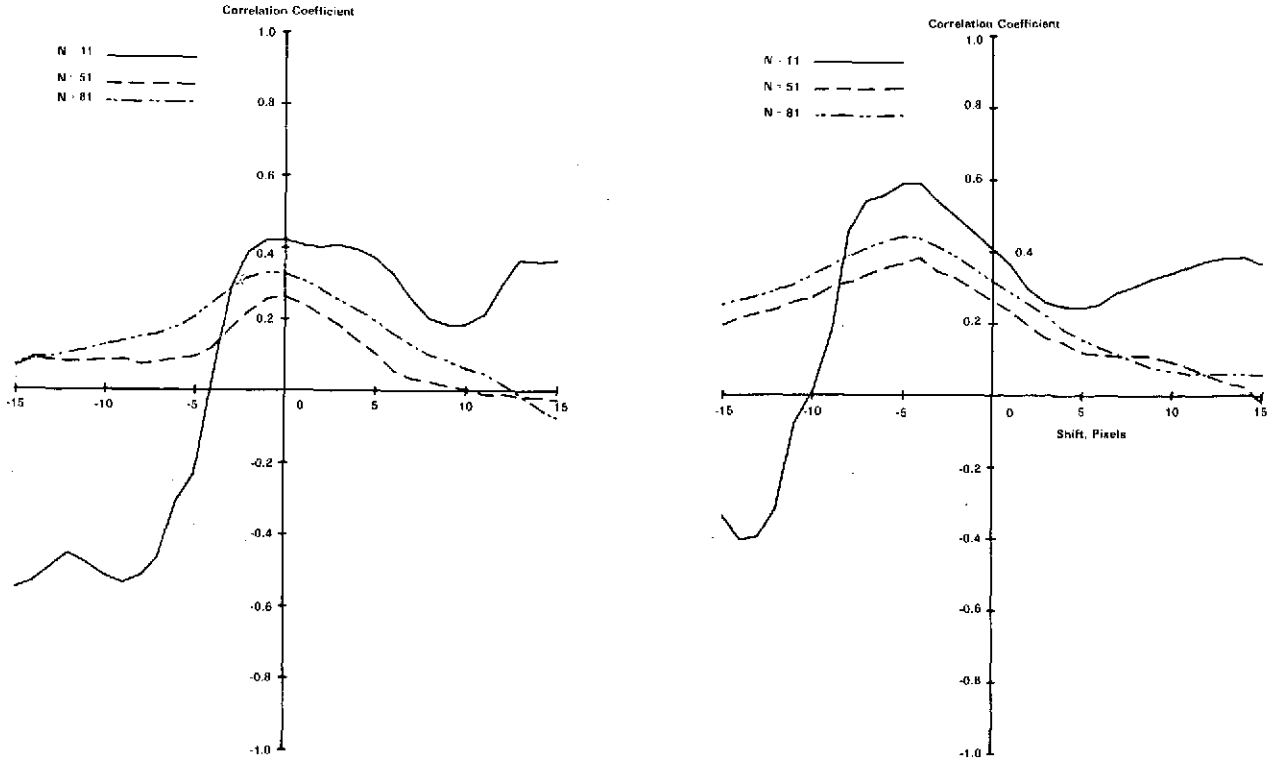

(a) East-West Shift

(b) North-South Shift

Figure 2.2-16. Cross Correlation, Control Point 16

On the average low contrast can be expected to lead to low correlations. This can lead to problems in automatic processing because low correlation peaks may be rejected as secondary maxima.

The reason for requiring variation in both x and y is to allow both the x and y coordinates of the control point to be accurately fixed. Hill County provides some good examples to illustrate this point, since most features (fields) run in a north-south direction. Consider, for example, control point 5. Features for this control points are mainly fields which

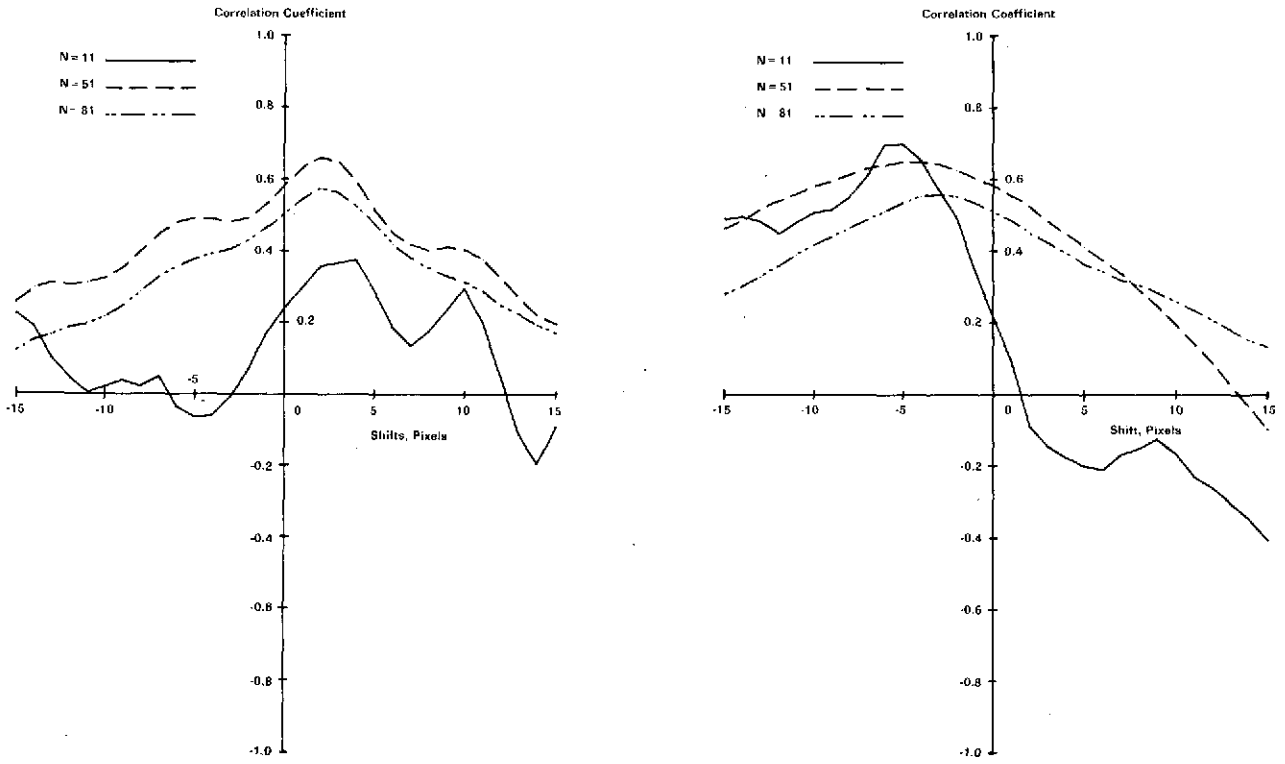

(a) East-West Shift

(b) North-South Shift

Figure 2.2-17. Cross Correlation, Control Point 5

are much longer in the north-south direction. This means that for east-west shifts there are distinct secondary maxima in the correlation surface (Figure 2.2-17(a)), corresponding to various parallel alignments of the fields. These secondary maxima are even in evidence for N = 51.

Aside from the secondary maxima, however, the correlation peak is fairly sharp. This means that the longitude for control point 5 can be fixed

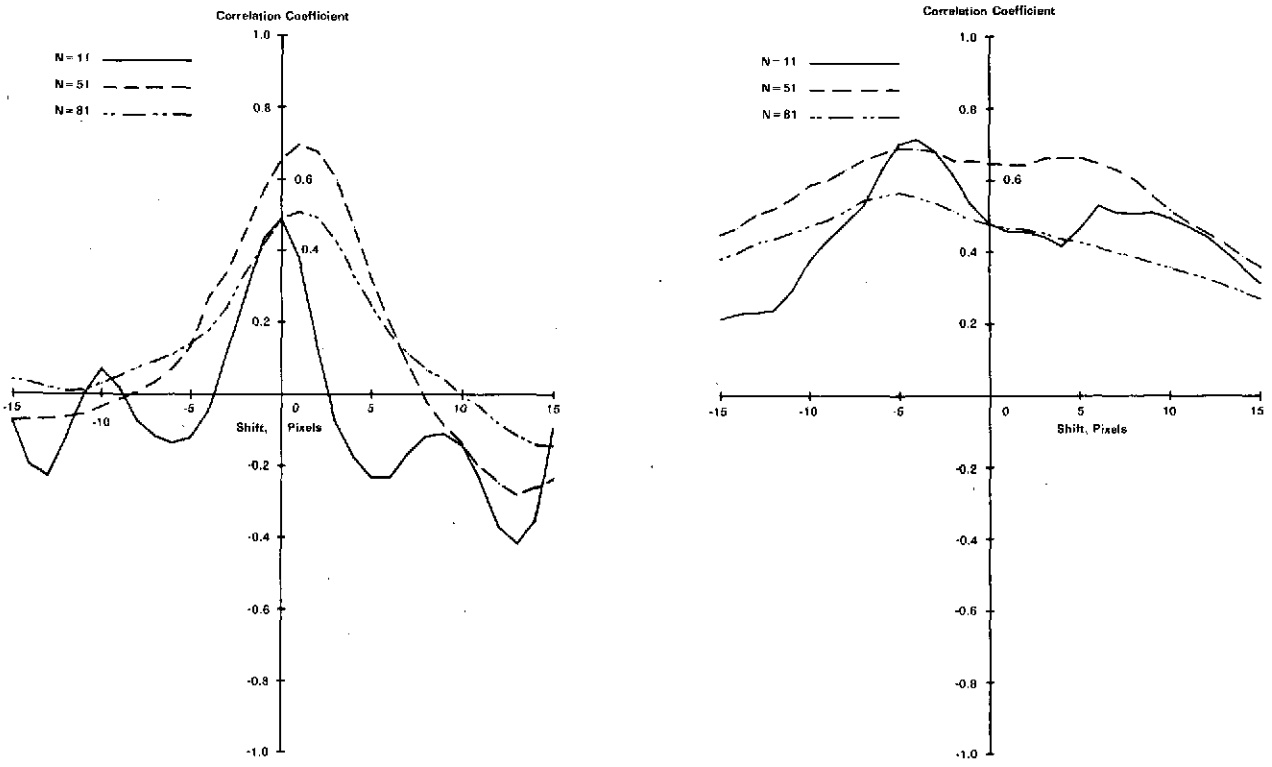

(a) East-West Shift

(b) North-South Shift

Figure 2.2-18. Cross Correlation, Control Point 19

accurately. On the other hand for north-south shifts (Figure 2.2-17 (b)) the correlation peak is broad. This is of course because there is very little variation in features in the north-south direction. It means that the latitude of control point 5 can not be fixed to the same accuracy as longitude.

A similar example is control point 19 where many sharp features run in a north-south direction. The correlation surface therefore has a relatively sharp peak for east-west shifts (Figure 2.2-18(a)). On the other hand, there

is very little variation in the north-south direction, and the correlation peak is quite broad in this direction (Figure 2.2-18(b)).

2.2.7 Enhancement and Resolution Differences

The foregoing results indicate that differences in resolution between the photomosaic reference and ERTS imagery are relatively unimportant, provided, of course, that features are selected large enough for ERTS resolution. A heuristic explanation for this result can be found from frequency considerations. The photomosaic and ERTS imagery (any band) can be represented by random processes $P_M(x,y)$ and $P_E(x,y)$, respectively. Obviously $P_E(x,y)$ is a band-limited signal because of the discrete sampling interval. The cutoff frequency is on the order of half the sampling frequency. For purposes of discussion we will assume cutoff frequencies to be w_x in the x-direction and w_y in the y-direction.

Then decompose $P_M(x,y)$ into $P_{M_1}(x,y)$, $P_{M_2}(x,y)$, i.e.

$$P_M(x,y) = P_{M_1}(x,y) + P_{M_2}(x,y) \qquad (2.2\text{-}5)$$

where $P_{M_1}(x,y)$ represents all components of P_M at frequencies within the band limited by (w_x,w_y), and $P_{M_2}(x,y)$ represents all higher frequency components.

Even if the resolution of the two images were the same differences are to be expected because of temporal variation, different spectral response, etc. Therefore assume

$$P_E(x,y) = K\, P_{M_1}(x,y) + C + n(x,y) \qquad (2.2\text{-}6)$$

where the constants K, C allow for difference in mean density and contrast. The term $n(x,y)$ represents "noise" in the form of non-repeatabilities between the ERTS image and the photomosaic reference. Effects of spatial distortion between ERTS and the photomosaic are neglected for this discussion.

The correlation coefficient, assuming the same resolution would then take the form

$$p^* = \frac{E\{[P_E(x,y) - \bar{P}_E][P_{M_1}(x,y) - \bar{P}_{M_1}]\}}{\sigma_E \sigma_{M_1}} \qquad (2\ 2\text{-}7)$$

where

$$\bar{P}_E = E[P_E(x,y)] = K\,\bar{P}_{M_1} + C + \bar{n}$$

$$\bar{P}_{M_1} = E[P_{M_1}(x,y)]$$

$$\bar{n} = E[n(x,y)]$$

$$\sigma_E^2 = E\{[P_E(x,y) - \bar{P}_E]^2\} = K^2\sigma_{M_1}^2 + \sigma_n^2 + 2K\,E\{[P_{M_1}(x,y) - \bar{P}_{M_1}][n(x,y) - \bar{n}]\}$$

$$\sigma_{M_1}^2 = E\{[P_{M_1}(x,y) - \bar{P}_{M_1}]^2\}$$

$$\sigma_n^2 = E\{[n(x,y) - \bar{n}]^2\} \qquad (2.2\text{-}8)$$

Assume that $P_{M_1}(x,y)$ and the noise term $n(x,y)$ are uncorrelated. Then

$$p^* = \frac{K\,\sigma_{M_1}^2}{\sigma_{M_1}\sqrt{K^2\sigma_{M_1}^2 + \sigma_n^2}} = \frac{\mathrm{sgn}(K)}{\sqrt{1 + \left(\frac{\sigma_n}{K\sigma_{M_1}}\right)^2}} \qquad (2.2\text{-}9)$$

As the "noise" level, i.e. dissimilarity between images is increased p* decreases from 1 to zero (assuming K>0). The same type of effect occurs for the case with different resolution. Basically the high frequency components for the higher resolution sensor look like "noise" to the correlation process and decrease the correlation coefficient somewhat. Assume that P_{M_1} and P_{M_2}

are uncorrelated and P_n is not correlated with the noise term n. Also define σ_{M_2} as the standard deviation of P_{M_2}. Then the correlation coefficient takes the form

$$\rho = \frac{E\{[P_E(x,y) - \bar{P}_E][P_n(x,y) - \bar{P}_n]\}}{\sigma_M \sigma_E} \qquad (2.2\text{-}10)$$

$$= \frac{K\,\sigma_{M_1}^2}{\sqrt{(\sigma_{M_1}^2 + \sigma_{M_2}^2)(K^2\,\sigma_{n_1}^2 + \sigma_n^2)}} = \frac{\mathrm{sgn}(K)}{\sqrt{1 + \left(\frac{\sigma_n}{K\sigma_{M_1}}\right)^2}\ \sqrt{1 + \left(\frac{\sigma_{M_2}}{\sigma_{M_1}}\right)^2}}$$

There will be a reduction in the correlation coefficient, but provided that low frequency features dominate the higher frequency features, i.e.

$$\sigma_{M_1} > \sigma_{M_2} \qquad (2.2\text{-}11)$$

this reduction will not be too great. Obviously any attempt to correlate on fine structure in the photomosaic reference will be doomed to failure.

What this means in terms of possible enhancement techniques is that there is no reason to equalize resolution before correlation by some sort of band-pass filtering on the higher resolution image. Another possible enhancement technique that is suggested from time to time is edge enhancement. Edges could be enhanced by some operator such as the (absolute) gradient prior to correlation.

It has been our experience from processing imagery of the Houston-Baytown area that enhancing edges does not necessarily buy anything from a correlation standpoint. There are some pathological cases in which edge correlation is better than correlation with no enhancement, but generally if imagery is dissimilar edge enhancement enhances the dissimilarities and correlation is less successful. This is even

more apparent in this case. Results shown in Figures 2.2-19 and 2.2-20 for control points 3 and 17 respectively, are typical. Boundaries have distinctly different shapes in the ERTS and photomosaic images, and applying the gradient only enhances these differences. Note from the joint distributions that there appears to be no relation at all between the two gradient images.

2.2.8 Automatic Multi-Sensor Registration

The results described above indicate that automatic correlation is indeed feasible for image-to-ground correlation. The successful application of a continuous automatic registration process to Hill County data is described in the following paragraphs.

Generally the computer can match control points as well as a human operator or better really, since the computer doesn't need any form of contrast enhancement. Further, successful correlation has been demonstrated between ERTS MSS imagery and a photomosaic with a correlation patch measuring only 16 by 19 pixels in terms of ERTS resolution. Finally enhancement of either or both images to match resolution or enhance edges is not necessary.

The one form of pre-processing that is necessary prior to correlation is "shaping" ERTS data to remove rotation and scaling effects. This can be done implicitely as data is loaded into memory and is done automatically in strip processing, assuming of course that the strip processor has been properly initialized. At this stage strip processing software (Program TRAK) is initialized by entering control points. In a production processing enviroment this initialization phase would have to be automated, probably based on ERTS satellite housekeeping data. An interesting example of automatic registration of ERTS MSS imagery to a photomosaic was prepared with the Hill County data (Figure 2.2-21). This was done with the TRAK process using the digital photomosaic data as the reference and the semi-automatically warped MSS data as the collateral image. In this manner MSS images for each of the four

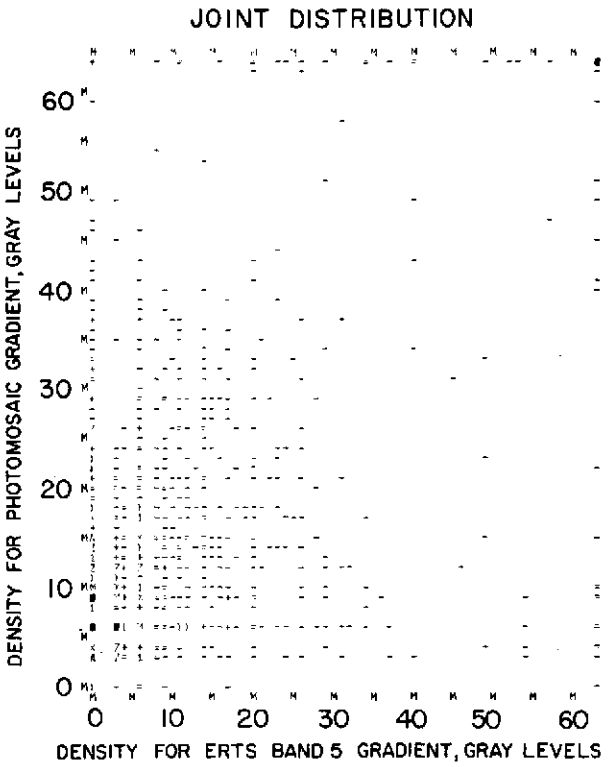

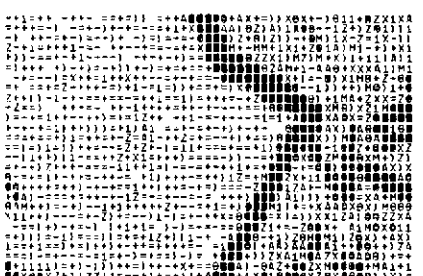
PHOTOMOSAIC

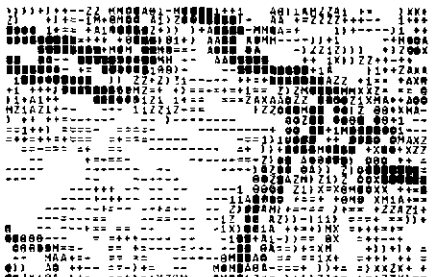
ERTS BAND 5

D1803

Figure 2.2-19. Automatic Correlation on Gradient Images for Hill County, Control Point 3.

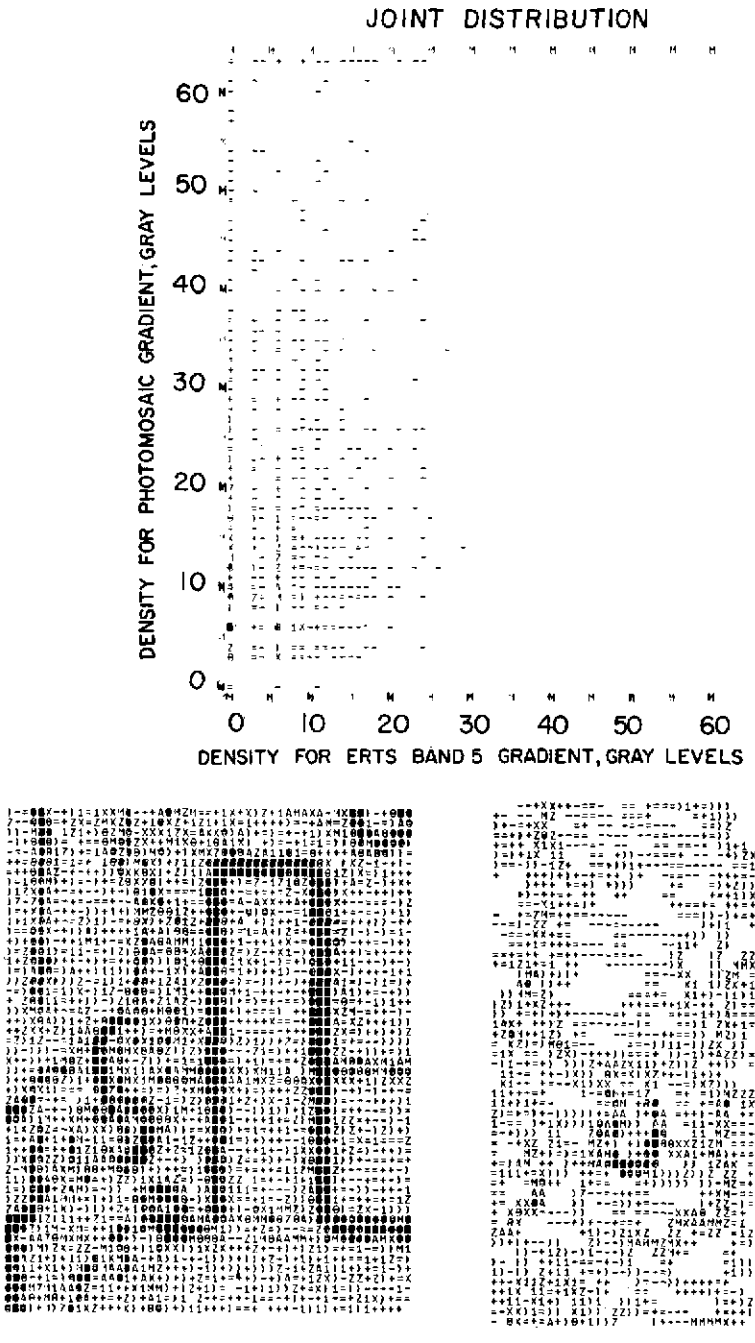

Figure 2.2-20. Automatic Correlation on Gradient Images for Hill County, Control Point 17

Figure 2.2-21. Automatic Registration of ERTS-MSS Image to Photomosaic Hill County, Montana

bands over the Hill County Area were prepared in registration with the photomosaic image.

In the previous discussion of semi-automatic processing the mean registration error was shown to be about 4 pixels in the digital photomosaic format or 1.4 pixels in the bulk MSS format. This is visually demonstrated by superimposing a gradient image of the photomosaic on the MSS image as shown for Band 5 in Figures 2.2-22 and 2.2-23 (selected portions of Hill County).

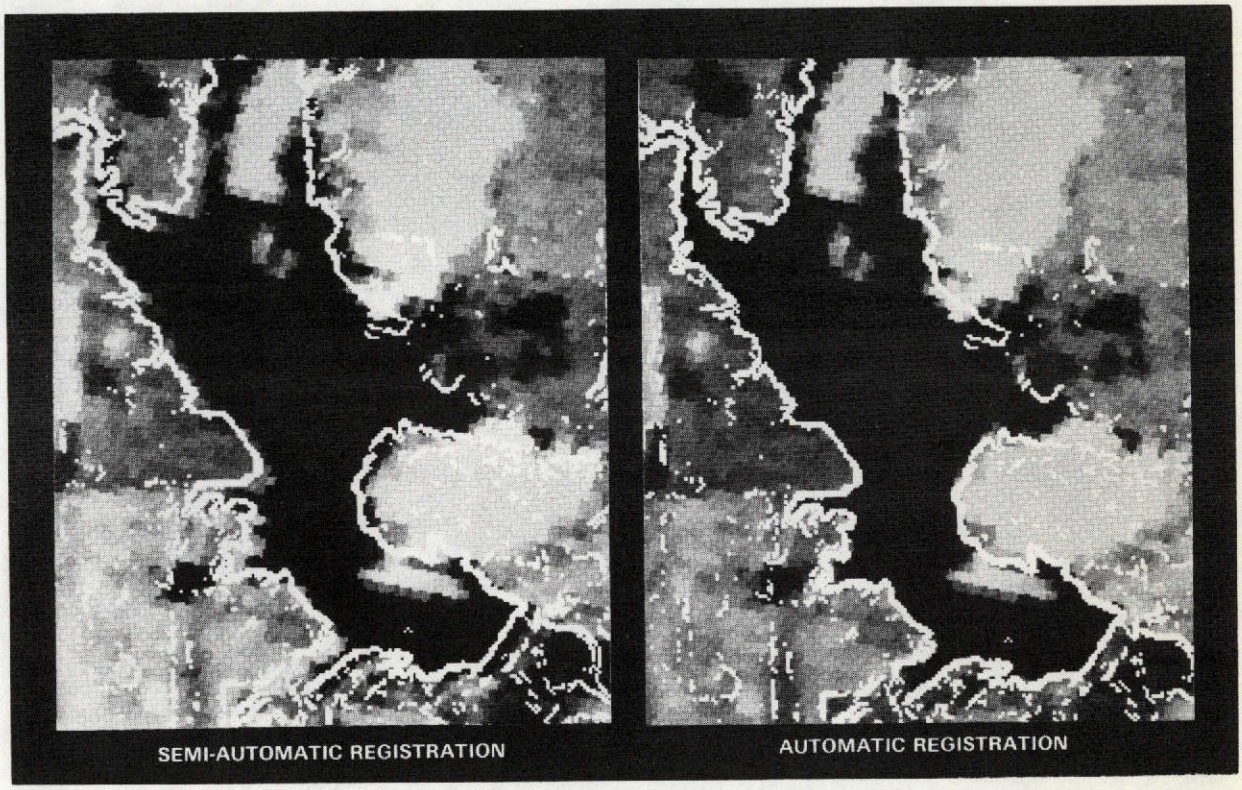

Figure 2.2-22. Automatic Registration of ERTS MSS Image to Photomosaic (Gradient Mosaic Superimposed on MSS Image - Hill County, Montana)

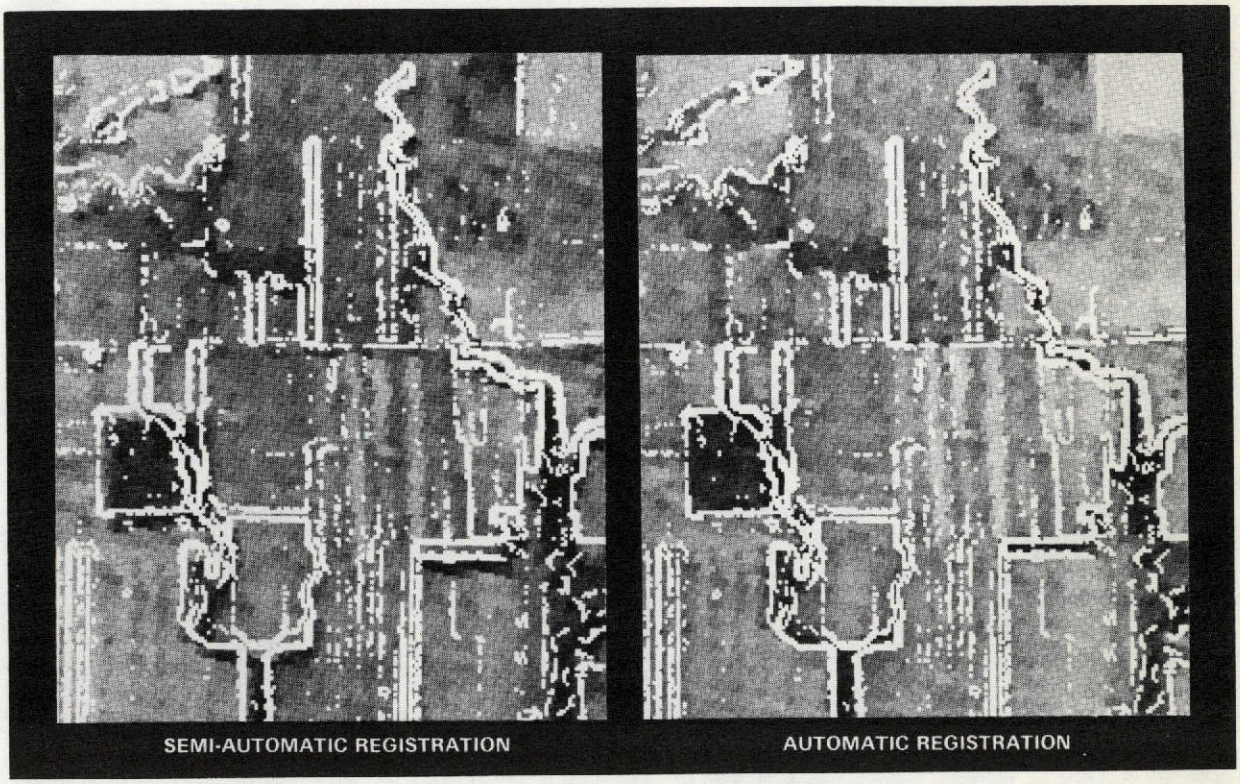

Figure 2.2-23. Automatic Registration of ERTS MSS Image to Photomosaic (Gradient Mosaic Superimposed on MSS Image - Hill County, Montana)

Automatic TRAK processing very effectively improved the overall registration to within 1 pixel error in the photomosaic or about 0.4 pixel in the bulk MSS format. This is visually demonstrated with two zoom views of the gradient photomosaic superimposed on the registered MSS image (Figures 2.2-22 and 2.2-23).

In conclusion, automatic ERTS image-to-ground registration is feasible and TRAK processing appears to be capable of meeting this registration requirement. Automatic registration is discussed further in subsequent sections

as it was applied to the registration of MSS data acquired on different passes of the satellite. These results also demonstrate that TRAK processing can yield accuracy superior to that obtainable by semi-automatic methods.

2.3 TRINITY BAY

The registration requirement imposed for ERTS-1 MSS imagery obtained over Trinity Bay, Texas, was simply temporal image-to-image registration. That is, images obtained on August 28, October 3, and November 26, 1972 were to be registered to one another without any correction to a ground coordinate system.

The August 28 image was chosen as the reference (Figure 2.3-1), and the October 3 and November 26 images (Figures 2.3-2 and 2.3-3, respectively) were registered to the reference. This small area of interest is dominated by the bay which contains non correlating detail. For this reason, and also because the relative distortions are not complex over such a small area, a semi-automatic warp process was chosen. Spatial transformation was effected with linear polynomials and was based upon 50 manually selected control points in each case.

Control points were measured much more accurately for this imagery than in the case of the image-to-ground registration for Hill County, Montana. Transparent images of Band 5 MSS data were first prepared upon photographic film with an Optronics P-1500 Photowrite System. Then matching coordinates were measured with a Bendix Datagrid digitizer to an accuracy of approximately 1 pixel.

Registration accuracy is demonstrated visually by superimposing a threshold gradient image of the reference image upon each of the other two registered images (Figures 2.3-4 and 2.3-5). In this way the outline of predominant features in the reference are shown in white upon the dependent registered images. These results, as well as color composite analysis performed at the

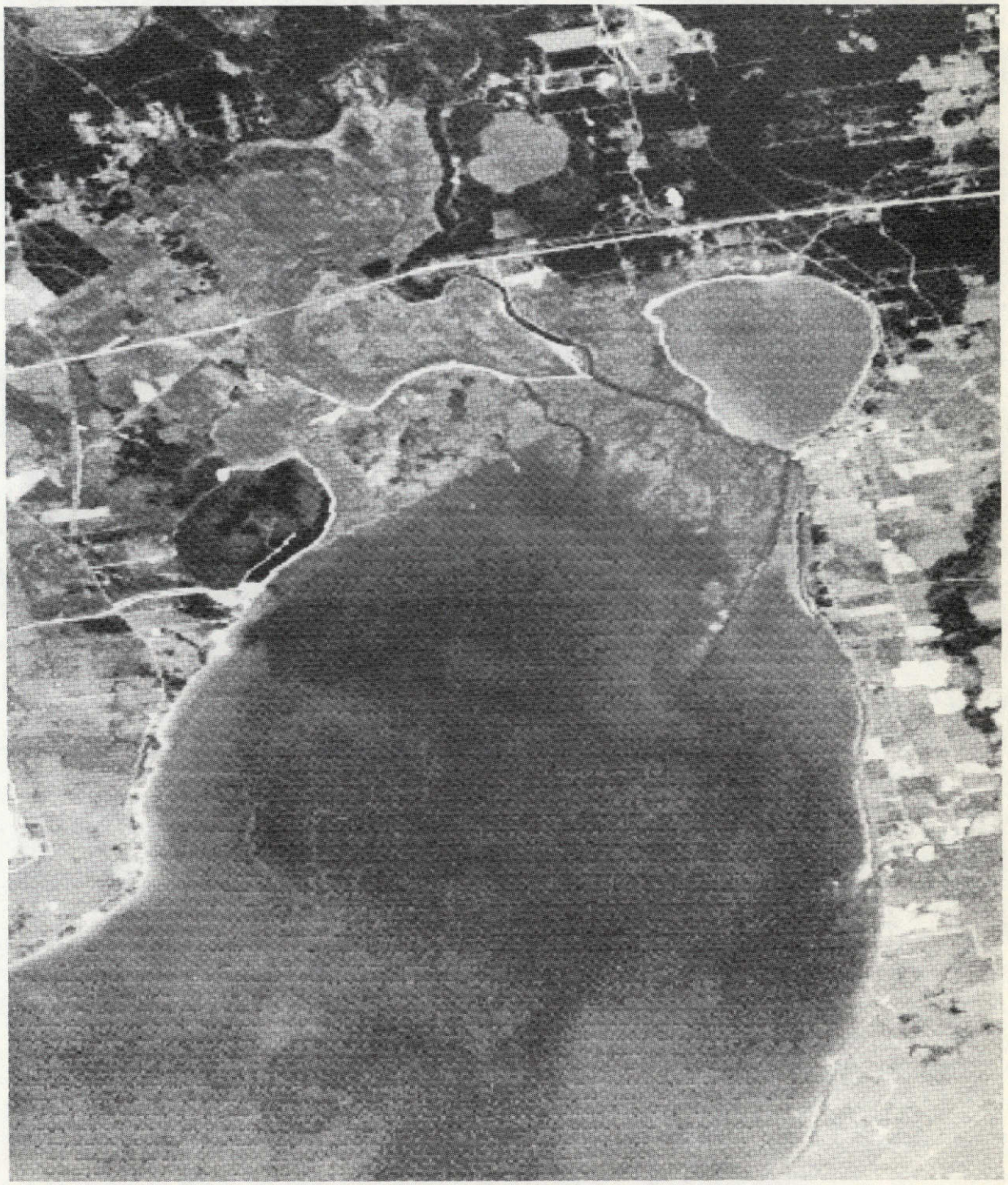

Figure 2.3-1. Reference Image for Trinity Bay Registration Processing, ERTS MSS Band 5, August 28, 1972

Figure 2.3-2. Trinity Bay ERTS MSS Band 5, October 3, 1972 after Registration to August 28, 1972.

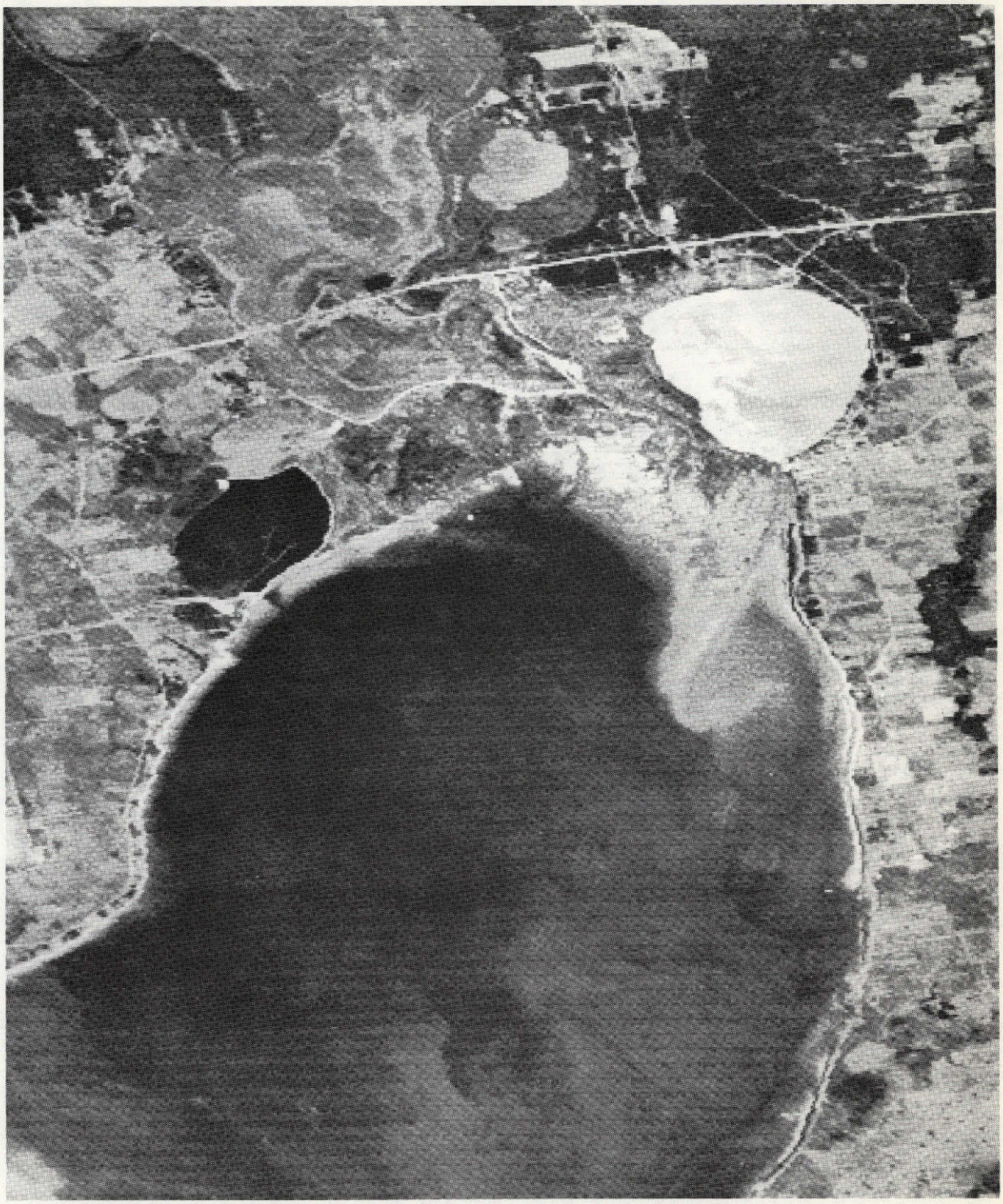

Figure 2.3-3. Trinity Bay ERTS MSS Band 5, November 26, 1972 after Registration to August 28, 1972.

Figure 2.3-4. Gradient of Reference Image Superimposed upon Registered Dependent Image Trinity Bay, ERTS-1 MSS, Band 5, October 3, 1972.

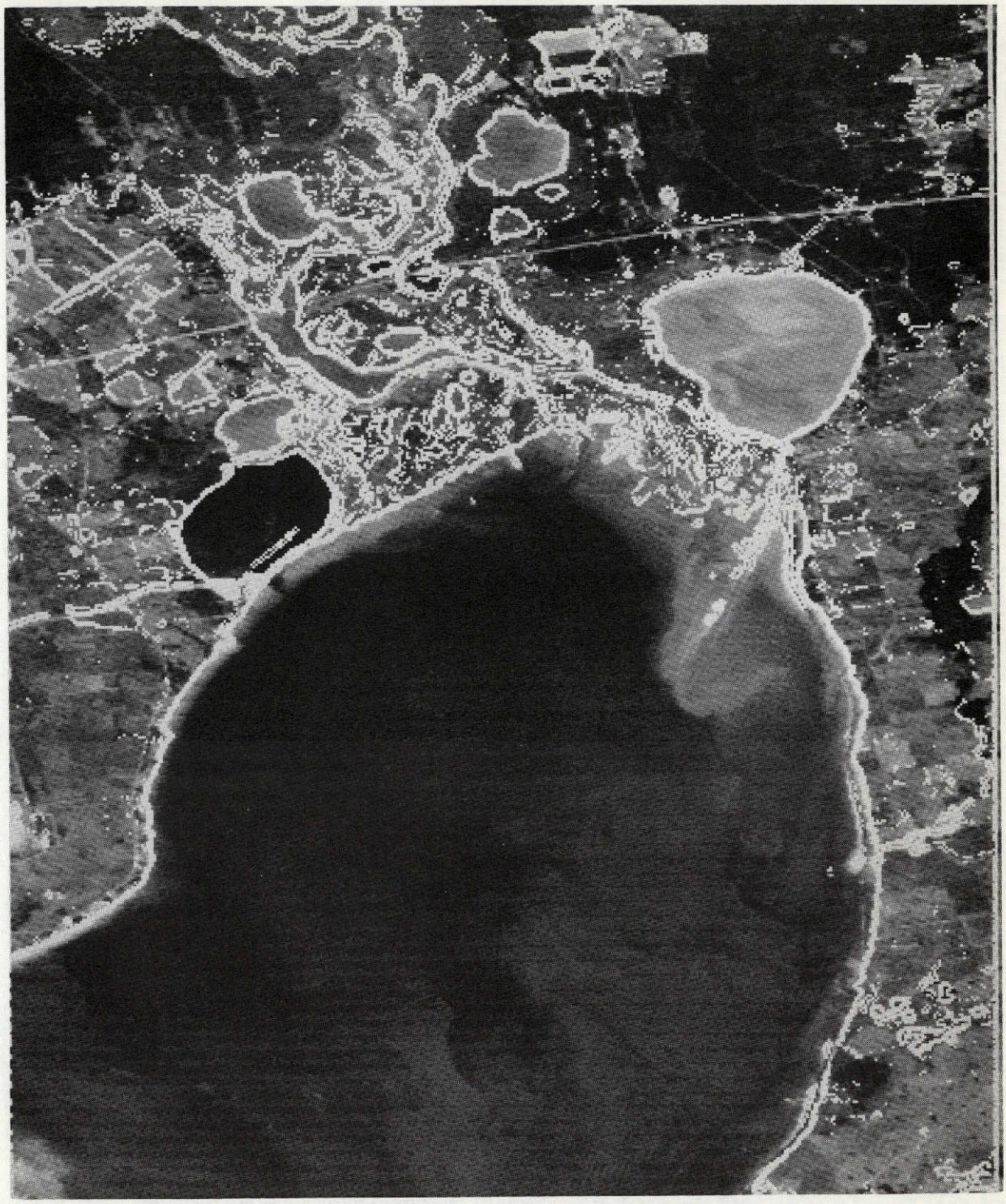

Figure 2.3-5. Gradient of Reference Image Superimposed upon Registered Dependent Image Trinity Bay, ERTS-1 MSS, Band 5, November 26, 1972.

Johnson Space Center, indicate accurate registration.

These visual tests however are not precise enough to provide a quantitative measure of registration accuracy. Therefore, the registered data was analyzed with the polynomial warp error analysis and automatic correlation (WECK) analysis procedures described in Section 2.1.2. Polynomial warp error analysis (Table 2.3-1) is based on the approximately 50 control points used for the semi-automatic warp. WECK error analysis (Table 2.3-2) is based upon automatic correlation at 33 locations in one pair and at 41 locations in the other.

Results of the two analyses are in close agreement with registration accuracies on the order of 0.7 to 0.8 pixel RMS for a linear warp. The spatial transformations consist predominantly of translation. Rotation is on the order of 0.1 degree or less, and scale differences between images are on the order of 1% or less. Registration accuracy for a three-degree-of-freedom spatial warp is one to two pixels mean radial error. By introducing more degrees of freedom registration error can be further reduced, but little is to be gained beyond the linear terms.

In Table 2.3-1 the three-degree-of-freedom spatial transformation (warp) consists of a translation plus rotation, i.e.

$$x' = a_0 + x \cos \theta + y \sin \theta$$

$$y' = b_0 + x \sin \theta + y \cos \theta \qquad (2.3\text{-}1)$$

where (x,y), (x',y') represent coordinates of a given point on the reference and collateral image, respectively. The x direction is taken parallel to the orbiting direction, and y is taken parallel to the scan line direction.

The four-degree-of-freedom warp consists of a translation, rotation and uniform scaling, i.e.

TABLE 2.3-1: POLYNOMIAL WARP ERROR ANALYSIS OF SEMI-AUTOMATIC REGISTRATION OF ERTS-1 MSS IMAGERY, TRINITY BAY

Registration of 10-3-72 to 8-28-72

No. of Fit Points = 50

Rotation between images = 0.08°

Scale Compression in x*= 0.44%

Scale Expansion in y**= 0.20%

DEGREES OF FREEDOM	FIT ERROR STATISTICS (PIXELS)			
	σ_x	σ_y	$\bar{r}$	σ_r
3	0.82	0.82	1.02	0.54
4	0.74	0.87	1.00	0.53
5	0.63	0.75	0.84	0.48
6 (linear)	0.49	0.62	0.70	0.36
12 (quadratic)	0.47	0.61	0.69	0.34

Registration of 11-26-72 to 8-28-72

No. of Fit Points = 47

Rotation between images = 0.15°

Scale Compression in x*= 1.16%

Scale Expansion in y**= 1.24%

DEGREES OF FREEDOM	FIT ERROR STATISTICS (PIXELS)			
	σ_x	σ_y	$\bar{r}$	σ_r
3	1.82	2.00	2.44	1.11
4	1.75	2.06	2.43	1.11
5	0.60	0.94	0.92	0.62
6 (linear)	0.53	0.90	0.85	0.59
12 (quadratic)	0.52	0.89	0.84	0.59

*X is taken parallel to the flight direction for the reference (August 28) image.

*Y is taken parallel to scan lines, i.e. perpendicular to the flight direction for the reference image.

TABLE 2.3-2. SUMMARY OF WECK ERROR ANALYSIS FOR TRINITY BAY FOR SEMI-AUTOMATIC REGISTRATION

Correlation Patch Size = 51 x 51

Correlation Rejection Threshold = 0.45

REGISTRATION CASE	NUMBER OF SAMPLES	FIT ERROR STATISTICS			
		σ_x	σ_y	$\bar{r}$	σ_r
10- 3-72 to 8-28-72	41	0.62	0.71	0.69	0.66
11-26-72 to 8-28-72	33	0.80	0.69	0.73	0.83

$$x' = a_0 + x(M \cos \theta) + y(M \sin \theta)$$

$$y' = b_0 - x(M \sin \theta) + y(M \cos \theta) \qquad (2.3\text{-}2)$$

and the five-degree-of-freedom warp consists of a translation, rotation and differential scaling in x and y, i.e.

$$x' = a_0 + x(M_x \cos \theta) + y(M_y \sin \theta)$$

$$y' = b_0 - x(M_x \cos \theta) + y(M_y \sin \theta) \qquad (2.3\text{-}3)$$

Statistical parameters in the two tables are defined as follows:

σ_x = standard deviation in the direction of flight.

σ_y = standard deviation along a scan line.

$\bar{r}$ = mean radial error.

σ_r = standard deviation in radial error. (2.3-4)

2.4 SNOOK SITE

An excellent example of automatic image-to-image registration is discussed in this section. Quarter frames of ERTS-1 MSS imagery containing significant temporal changes in the form of clouds and vegetation changes were automatically registered to a mean radial displacement error of 0.28 pixels (Figure 2.4-1). Each image represents an area measuring 25 by 100 nautical miles.

Snook Site is specifically a small area adjacent to the Somerville Reservoir north of Columbus, Texas. It can be found in the central part of each image in Figure 2.4-1. The specific requirement was to obtain image-to-image registration for this local test site. However, this was considered an ideal test case for automatic correlation techniques for three reasons:

- A complete 25 by 100 nautical mile strip of data was supplied for both images.
- There are significant temporal differences between the two images over the 90 days between ERTS passes.
- One of the images contains partial cloud cover.

In other words there is sufficient data on which to experiment, and the data represents "typical" ERTS imagery with typical problems such as changing vegetation and cloud cover.

2.4.1 Process Results

The computer program used to process this data is Program TRAK, also

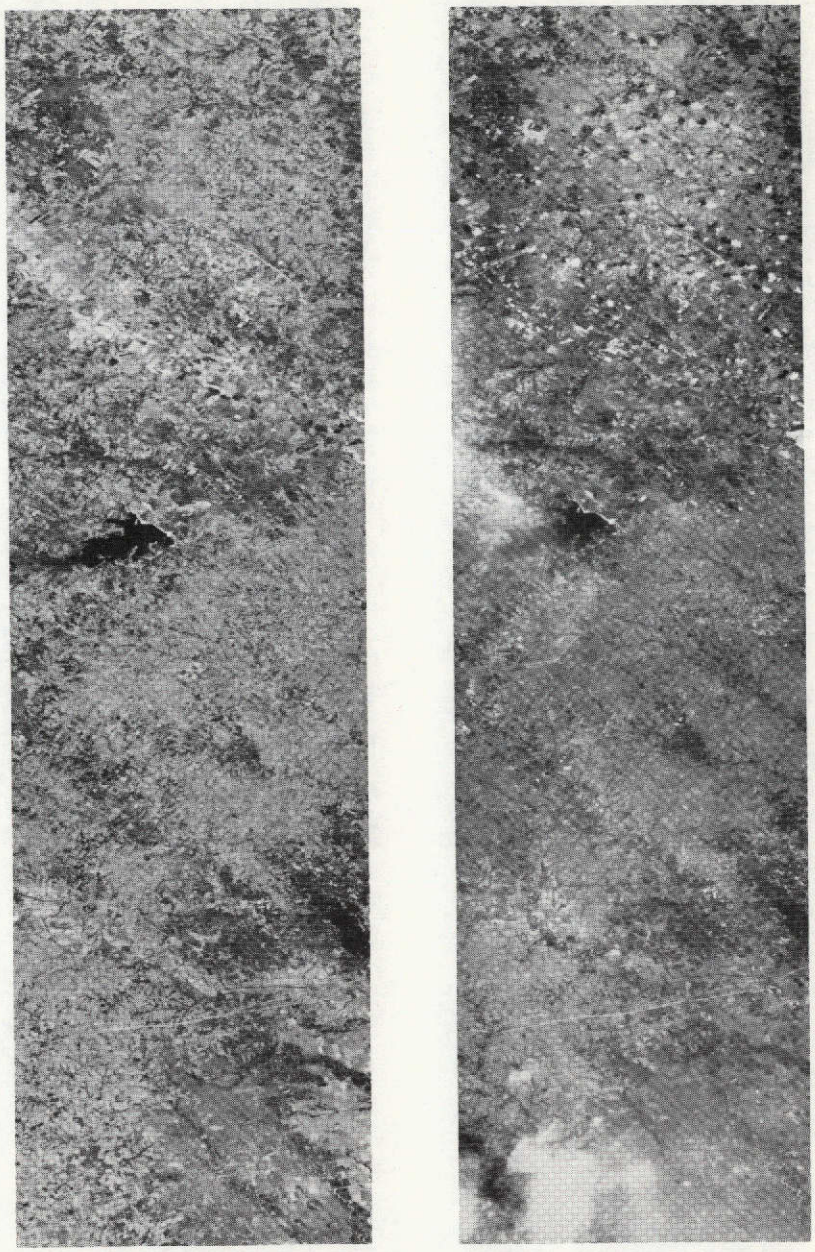

Reference
November 28, 1972

Registered Dependent
August 30, 1972

Figure 2.4-1. Automatic Registration, Snook Site, Texas
ERTS-1 MSS, Band 5

known as the "strip" or "pipeline" processor. This program is a simulator for the ARRES automatic change detection system built by Control Data for the U.S. Air Force [2]. The objective in processing ERTS data with this program is to demonstrate that high-speed high-accuracy fully automatic image registration is feasible for ERTS.

Program TRAK is not a production processing program. Moreover because it was designed for side-looking-radar imagery, many algorithms and processing parameters need modification for ERTS imagery. With such modifications Program TRAK can form the basis for production processing software. Moreover, because TRAK is a hardware simulator, continued development of this technique can ultimately lead to special-purpose production processing hardware.

The Band 5 data of November 28, 1972 is chosen as the reference because it is cloud free (Figure 2.4-1). A number of control points were measured at the north end (beginning of recorded data) to provide accurate initialization of the automatic process. Processing with the TRAK program then proceeded automatically and continuously without interruption from the north end to the south end of the image strip. A gray scale threshold was imposed upon the data used for correlation to minimize the effects of clouds upon the correlation and matching process. In this manner the Band 5 data of August 30, 1972 (dependent image) was accurately registered to the reference image (Figure 2.4-1).

A tonal difference image was generated by subtracting pixel gray-scale values in the dependent image from corresponding values in the reference (Figure 2.4-2). The difference image provides a means of assessing real changes and registration accuracy. Misregistration is detected by black and white pairing (ghosting) of given image features. Note that no such ghosting is apparent. It is also important to note the preponderance of temporal changes in the river bottom near the Somerville Reservoir.

In the manner discussed in Section 2.1.2 a composite gradient superposition image was generated by superimposing the gradient of the reference image

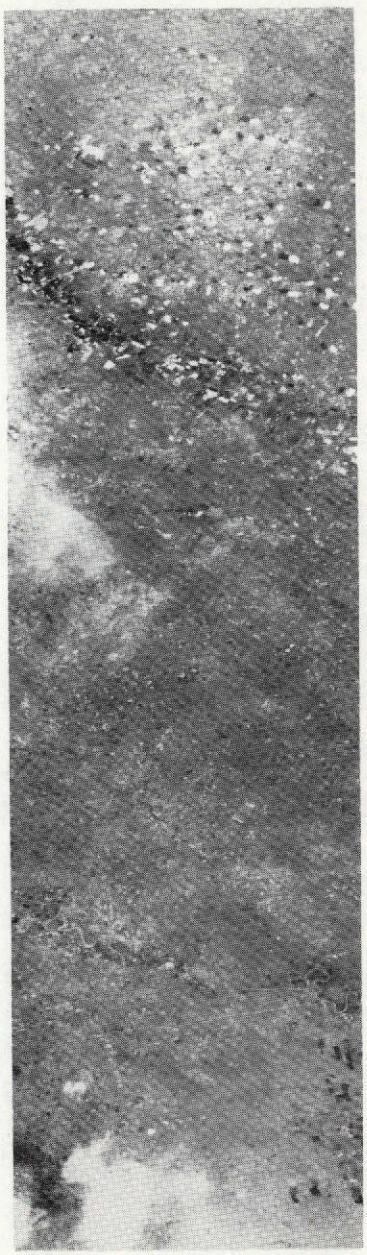

Emphasized Tonal
Difference Image

Gradient of Reference
Superimposed upon Registered
Dependent Image

Figure 2.4-2. Tonal Changes and Automatic Registration Accuracy, Snook Site, Texas
ERTS-1 MSS, Band 5, November 28, 1972 (Reference) and August 30, 1972 (Dependent)

(November 28, 1972) upon the registered dependent image data of August 30, 1972 (Figure 2.4-2). Registration accuracy can be assessed by comparing the white gradient boundaries from the reference image with feature detail in the background image.

Figure 2.4-2 certainly indicates good registration over the entire 25 by 100 nautical mile area. Yet, registration accuracy is somewhat difficult to assess because of the scale and of degeneration in the half-tone printing process for this report. For these reasons enlargements of two specific areas of interest are provided for analysis in greater detail. The two areas considered are Snook Site near the Somerville Reservoir and an area near Columbus, Texas. Reference, registered dependent, tonal difference, and gradient superposition images for Snook Site are shown in Figures 2.4-3 through 2.4-6, respectively. Some "popcorn" clouds and their shadows are present in the dependent image (Figure 2.4-4). Note also the differences in fields near the river running from the upper left to the right central area. These changes took place between August 30 and November 28, and not only are many of the fields different in density, but they also differ in shape. Furthermore, the average tone value is significantly darker on the August 30 image.

Differences in fields are readily apparent in the tonal difference image (Figure 2.4-5); clouds are also in evidence. From the standpoint of registration accuracy, it appears that there is possibly some ghosting near a landing strip on the left and along the river. Registration appears to be reasonably accurate, however.

From the gradient superposition image (Figure 2.4-6) it can be seen that many boundaries are not the same on the two images because of temporal change. Also there is a certain amount of noise amplification in the gradient process. Generally, though, wherever common, identical features can be identified on the two images, their boundaries appear to be in proper alignment. Along the river there appears to be some slight misregistration in places. Note in this

Figure 2.4-3. Reference Image, Snook Site
ERTS-1 MSS, Band 5, November 28, 1972

Figure 2.4-4. Automatic Registration of Dependent Image, Snook Site ERTS-1 MSS, Band 5, August 30, 1972

Figure 2.4-5. Emphasized Tonal Difference Image, Snook Site
ERTS-1 MSS, Band 5, November 28, 1972

Figure 2.4-6. Gradient of Reference Superimposed Upon Registered Dependent Image, Snook Site ERTS-1 MSS, Band 5, November 28, 1972 (Reference) and August 30, 1972 (Dependent)

connection that the threshold gradient image for a feature such as a river will consist of two lines, one on either side of the feature. In such a case the feature (river) should fall between the lines.

Compared with the entire 25 by 100 nautical mile area, Snook Site should demonstrate the poorest registration accuracy because it has the fewest common features to correlate on. There are two reasons for this: the preponderance of temporal change in this area and clouds and cloud shadows on the dependent image. In light of these considerations, registration accuracy in this area is quite good.

Similar results are presented for the Columbus area in Figures 2.4-7 through 2.4-10. Contrast is generally greater in the reference image (Figure 2.4-7) as compared with the registered dependent image (Figure 2.4-8). Note also that the Colorado River appears dark on the reference (November 28) image and light on the dependent (August 30) image. The river therefore gives rise to a relatively strong change event as can be seen in the tonal difference image (Figure 2.4-9).

Note that there is very little ghosting in the difference image, an indication of good registration accuracy. This is further substantiated by results displayed in the gradient superposition image of Figure 2.4-10. Again, features that can be identified appear to be in alignment. Note particularly highways, and again note the double line on the gradient image.

2.4.2 Registration Error Analysis

Inspection of the displacement vectors required to register the dependent image (August 30) upon the reference image (November 28) reveals variations of 2 pixels parallel to the orbital track and 2 to 21 pixels perpendicular to the track (Figure 2.4-11). Thus the raw data is misregistered in the direction perpendicular to the orbital track by amounts varying from about 0.1 to 1 nautical mile, which is significant in many earth resources measurements.

Figure 2.4-7. Reference Image, Columbus, Texas
ERTS-1 MSS, Band 5, November 28, 1972

Figure 2.4-8. Automatic Registration of Dependent Image, Columbus, Texas ERTS-1 MSS, Band 5, August 30, 1972

Figure 2.4-9. Emphasized Tonal Difference Image, Columbus, Texas
ERTS-1 MSS, Band 5, November 28, 1972
and August 30, 1972

Figure 2.4-10. Gradient of Reference Superimposed Upon Registered Dependent Image, Columbus, Texas ERTS-1 MSS, Band 5, November 28, 1972 (Reference) and August 30, 1972 (Dependent)

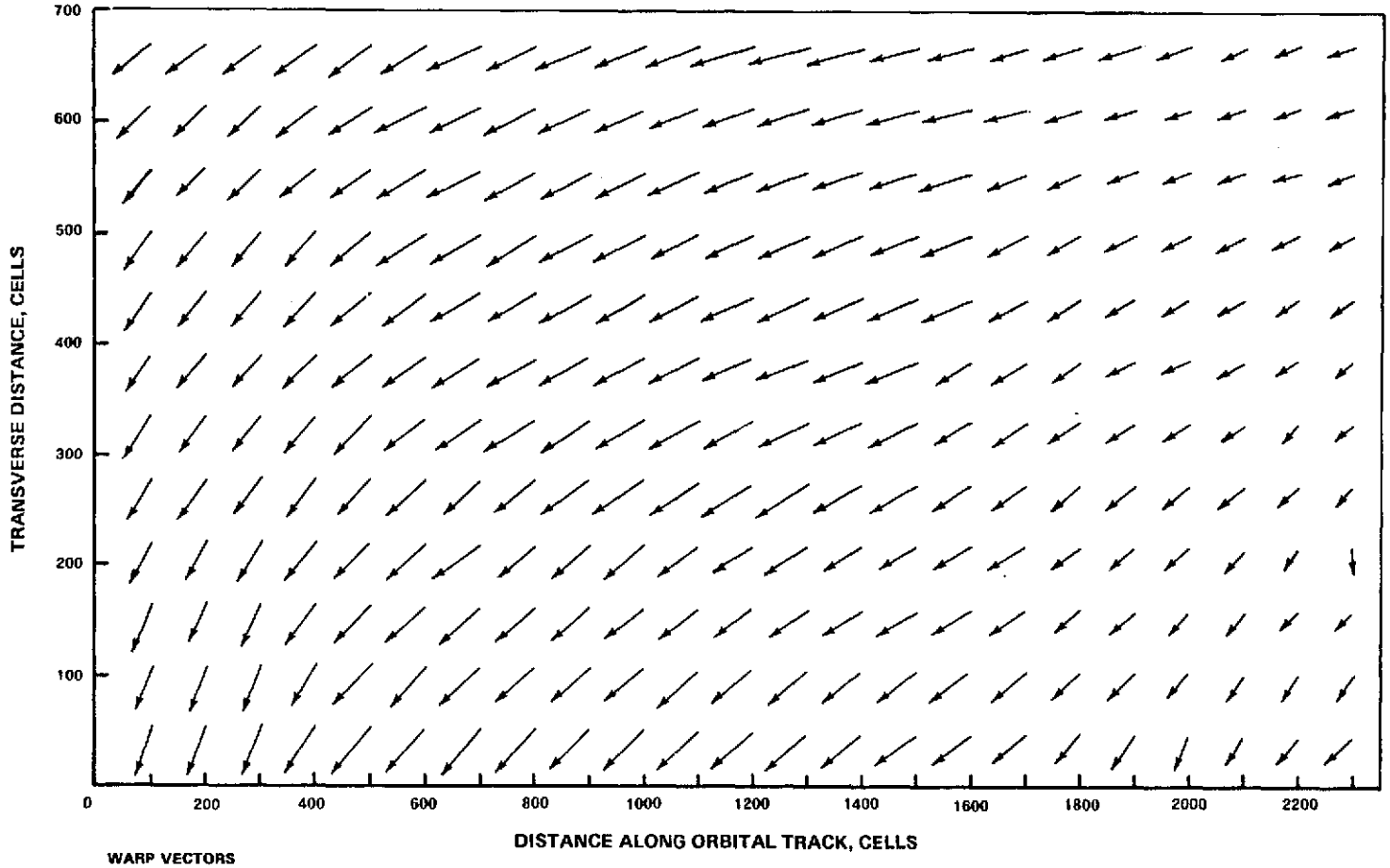

Figure 2.4-11. Vector Displacements Between ERTS-1 MSS Images at Snook Site, Texas, August 30 and November 28, 1972

In addition, there is an additional translation of the data files along the orbital track amounting to 25 pixels which was automatically compensated in the registration process. Registration accuracy over the entire 25 by 100 nautical mile strip (700 pixels by 2340 lines) was measured with the correlation error (WECK) analysis method following registration of Band 5 data in the TRAK process. The mean radial displacement error is 0.28 pixel (Table 2.4-1).

TABLE 2.4-1: SNOOK SITE: CORRELATION ERROR (WECK) ANALYSIS OF AUTOMATIC (TRAK) REGISTRATION PROCESS OVER 25 BY 100 NAUTICAL MILE AREA

ERTS-1 MSS, Band 5, Image Data
August 30 and November 28, 1972

Correlation Patch Size = 51 x 51 Pixels
Correlation Rejection Threshold = 0.45
Total Number of Samples = 315

DESCRIPTION	SYMBOL	PIXELS
Mean Registration error in direction of flight	$\bar{x}$	0.007
Standard Deviation in direction of flight	σ_x	0.19
Mean Registration error parallel to scan lines	$\bar{y}$	-0.05
Standard Deviation parallel to scan lines	σ_y	0.30
Mean radial error	$\bar{r}$	0.28
Standard Deviation in radial error	σ_r	0.21

An important question related to registration accuracy is warp complexity. Just how complex does the spatial warp have to be to yield an accuracy on the

order of ¼ pixel? It would appear from inspection of the vector displacement diagram that a linear warp may generally be sufficient over areas of about 400 x 400 pixels as in the Trinity Bay example. Over the complete frame, however, the warp is of higher order.

A quantitative evaluation of the warp complexity was made with a polynomial warp error analysis performed on control points matched by Program TRAK. The set of control points was divided into sets of "fit" and"check" points (Figure 2.1-1). Polynomial fits of order N, where N varies from one to four, were applied to the fit points, and residual error statistics were computed over both the fit points and interspersed check points (Table 2.4-2).

TABLE 2.4-2: SNOOK SITE: POLYNOMIAL ERROR ANALYSIS OF AUTOMATIC (TRAK) REGISTRATION PROCESS

Based upon control points matched by Program TRAK over a 25 by 100 nautical mile area.

Number of fit points = 88

Number of check points = 95

Total number of points = 183

ORDER OF FIT	ERROR STATISTICS (PIXELS)								
	FIT POINTS			CHECK POINTS			ALL POINTS		
	σ_x	σ_y	$\bar{r}$	σ_x	σ_y	$\bar{r}$	σ_x	σ_y	$\bar{r}$
1	1.00	0.75	1.16	0.96	1.25	1.20	0.98	1.04	1.18
2	0.37	0.71	0.70	0.47	1.30	0.89	0.43	1.06	0.80
3	0.35	0.66	0.66	0.46	1.35	0.94	0.41	1.07	0.80
4	0.29	0.60	0.58	0.51	1.31	0.88	0.42	1.03	0.74

σ_x = standard deviation in fit residual, direction of flight

σ_y = standard deviation in fit residual, parallel to scan lines

$\bar{r}$ = mean radial error

A test against the correlation coefficient for each control point was made to ensure that points employed in the error analysis represent good matches of corresponding features on the two images. The results are based on a total of 88 fit points and 95 check points distributed over the complete 25 by 100 nautical mile strip.

It is apparent that the spatial warp is globally second order (quadratic). That is, the best global fit is of the form

$$x' = a_0 + a_1x + a_2y + a_3xy + a_4x^2 + a_5y^2$$

$$y' = b_0 + b_1x + b_2y + b_3xy + b_4x^2 + b_5y^2 \qquad (2.4\text{-}1)$$

where (x,y), (x',y') represent coordinates of the reference and dependent images, respectively. As in the previous examples, x is measured parallel to the flight direction, and y is measured parallel to the scan lines. With 12 unknown coefficients equation 2.4-1 represents 12 degrees of freedom. These fit coefficients for the 25 by 100 nautical mile area are given in Table 2.4-3.

Clearly six degrees of freedom are not sufficient, since mean radial error over all fit points is decreased 32% by increasing the number of degrees of freedom from six to twleve, i.e. by increasing fit order from one to two. On the other hand, fits higher than second order lead to no significant further decrease in mean radial error.

It is interesting to compare these results with those for the WECK error analysis and also with results of error analysis for the Trinity Bay imagery. From the coefficients in Table 2.4-3 and the vector displacement diagram it can be seen that locally, i.e. over an area of 400 to 500 pixels on a side as for Trinity Bay, the spatial warp is predominantly linear. Note also that a quadratic warp over the 25 by 100 nautical mile strip (700 pixels by 2340

TABLE 2.4-3. QUADRATIC FIT COEFFICIENTS FOR SPATIAL TRANSFORMATION BETWEEN ERTS-1 MSS IMAGES AT SNOOK SITE (25 BY 100 NAUTICAL MILE STRIPS)

Reference: November 28, 1972

Dependent: August 30, 1972

POWER OF x	POWER OF y	COEFFICIENTS FOR DIRECTION OF FLIGHT	COEFFICIENTS FOR SCAN LINE DIRECTION
0	0	-25.32	-22.39
1	0	0.9945	0.0054
0	1	-0.0044	1.016
1	1	6.75×10^{-7}	-8.50×10^{-8}
2	0	2.48×10^{-6}	-7.50×10^{-6}
0	2	2.20×10^{-6}	1.16×10^{-7}

lines) at Snook Site and a linear warp over the smaller Trinity Bay area (400 pixels by 500 lines) yield similar mean radial errors of about 0.8 pixel.

A comparison of the polynomial error analysis and the WECK error analysis of Snook Site processing reveals a significantly lower mean radial error for the TRAK spatial warp. What this means is that the spatial warp between ERTS frames may deviate locally from a low-order global fit. Program TRAK, which updates the spatial warp on a line by line basis can respond to these local deviations to decrease the mean registration radial error from on the order of 3/4 pixel to on the order of 1/4 pixel.

2.5 IMPERIAL VALLEY

Two objectives for registration of ERTS-1 MSS imagery of Imperial Valley were:

- Automatic image-to-image registration (MSS imagery only).
- Semi-automatic registration to ground control points, simulating transformation to Universal Transverse Mercator (UTM) grid projection.

As the following discussion and examples will shown, these objectives were well attained.

2.5.1 Automatic Image-To-Image Registration (MSS)

The procedure used in processing this image pair was to first perform image-to-image registration with automatic techniques (Program TRAK), then to register both images to ground control semi-automatically (Program SAW). The images are compared with the preparation of difference images, and registration accuracy is evaluated with gradient superposition images and statistical error analysis.

Automatic registration processing was performed on MSS Band 5 data for a 25 by 100 nautical mile area in Imperial Valley. The image obtained on November 6, 1972 was chosen as the reference (Figure 2.5-1). The dependent image (November 24, 1972) after registration to the reference is also shown in Figure 2.4-1. Within the limits of scale factor and half-tone reproduction for this report a gradient superposition image shows good registration over the entire strip (Figure 2.5-2). The white boundaries are the threshold gradient of the reference image.

A tonal difference image was created without equalization of the gray-scale distributions in the reference and registered dependent image (Figure 2.5-2). This was done to preserve the radiometric integrity (within the limits of the interpolation process) for possible signature analysis. As might be

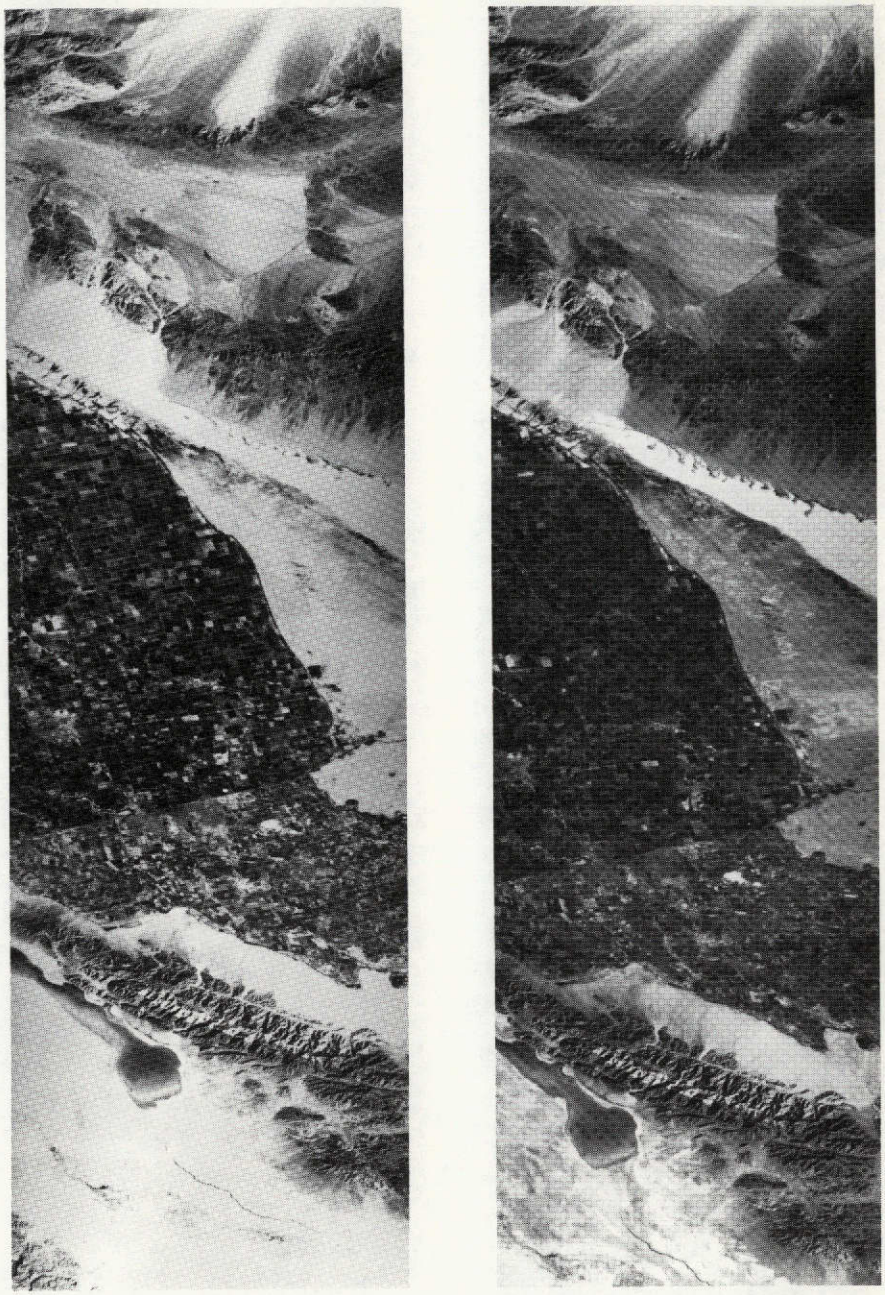

Reference
November 6, 1972

Registered Dependent
November 24, 1972

Figure 2.5-1. Automatic Registration, Imperial Valley, California
ERTS-1 MSS, Band 5

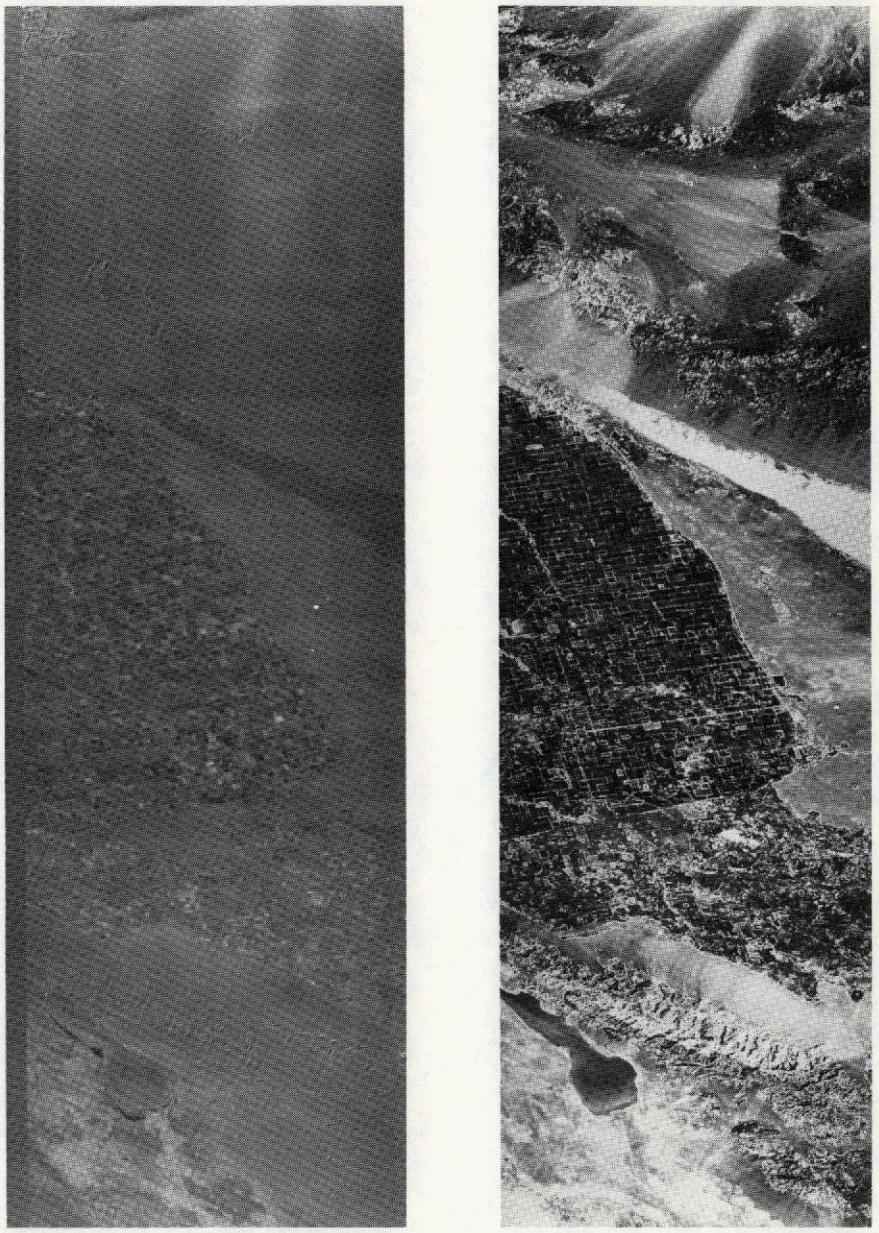

Emphasized Tonal Difference Image

Gradient of Reference Superimposed Upon Registered Dependent Image

Figure 2.5-2. Tonal Changes and Automatic Registration Accuracy, Imperial Valley
ERTS-1 MSS, Band 5, November 6, 1972 (Reference) and November 24, 1972 (Dependent)

expected by viewing the original images the differences are great, particularly in the fields of the central area and also in the southwest corner of the strip.

The extent of these tonal differences are further analyzed with the aid of enhanced three-level difference images. A simple nonlinear enhancement algorithm is employed in which all differences greater than twice the threshold setting are set to the maximum (63 on a six bit scale). All differences less than twice the negative of the threshold are set to the minimum (zero), and all in between values are set to an intermediate shade of gray (32). Thus as the threshold is raised only the strongest changes remain as black or white areas on a gray background. Thresholds of 8 and 10 are shown here (Figure 2.5-3).

It appears from the tonal difference image that there is a definite photo-equalization problem for these two images. There is little doubt in this case that density distributions are considerably different for the two dates, as is further demonstrated by histograms of gray-scale distributions for the two original images (Figure 2.5-4). Yet, feature detail is remarkably similar throughout the image, and dissimilarities are not as extensive as for the Snook Site imagery. This can be expected because of a shorter interval (18 days) between passes over Imperial Valley as opposed to 90 days for Snook Site. Furthermore, the Imperial Valley imagery has very well defined features of good contrast.

The foregoing observations are in complete agreement with the obtained result that correlations between the Imperial Valley images were significantly higher, typically in the range of 0.7 to 0.8, as opposed to 0.6 to 0.7 for Snook Site.

The scale factor of Figure 2.5-2 does not provide a good opportunity to accurately assess registration by visual inspection. Since the area of primary interest is Imperial County (Figure 2.5-5), a 500 by 500 pixel section of the MSS imagery including this area is digitally enlarged for closer in-

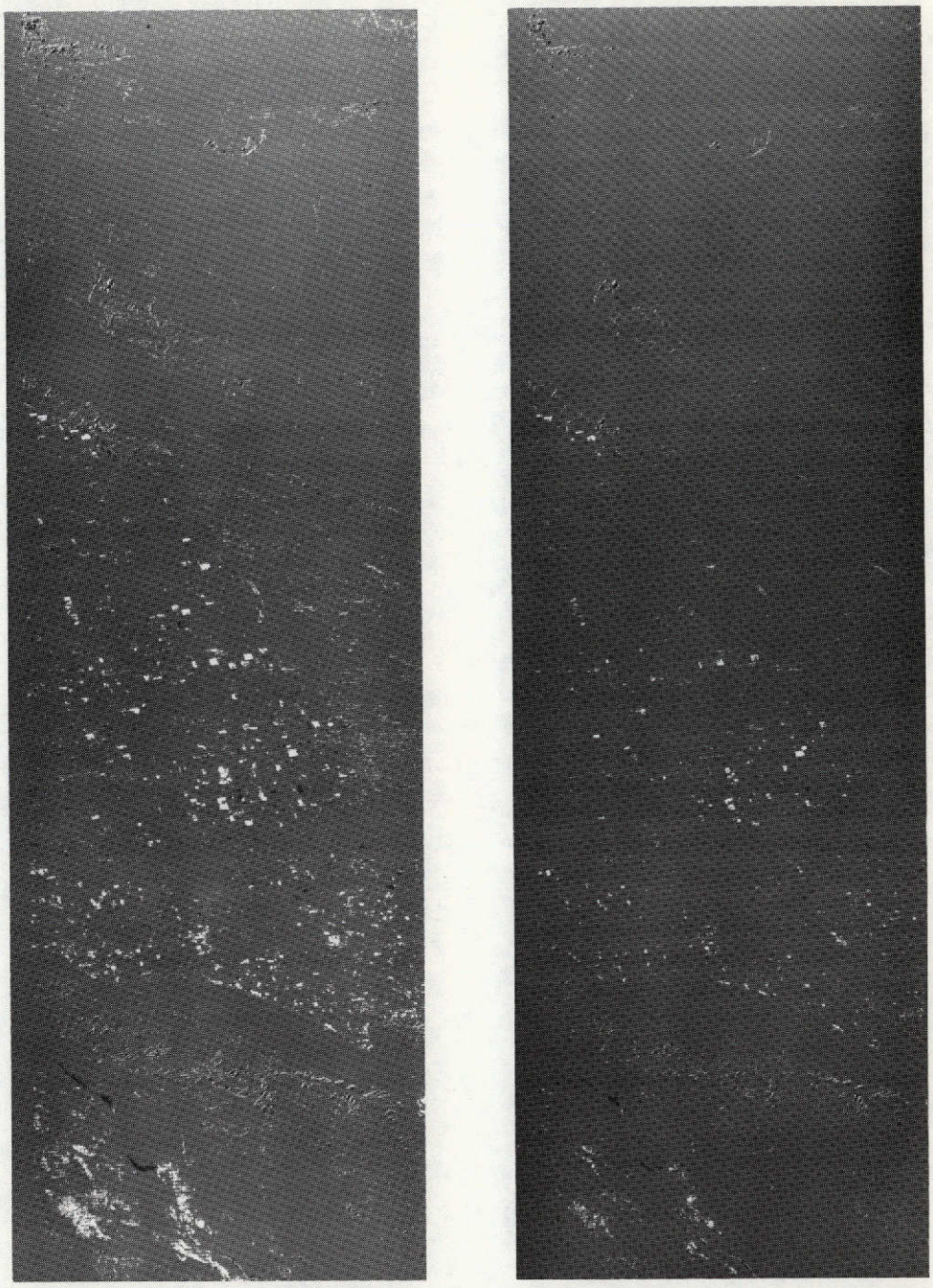

Threshold = ±8 Threshold = ±10

Figure 2.5-3. Three Level Difference Image, Imperial Valley ERTS-1 MSS, Band 5, November 6, 1972 (Reference) and November 24, 1972 (Dependent)

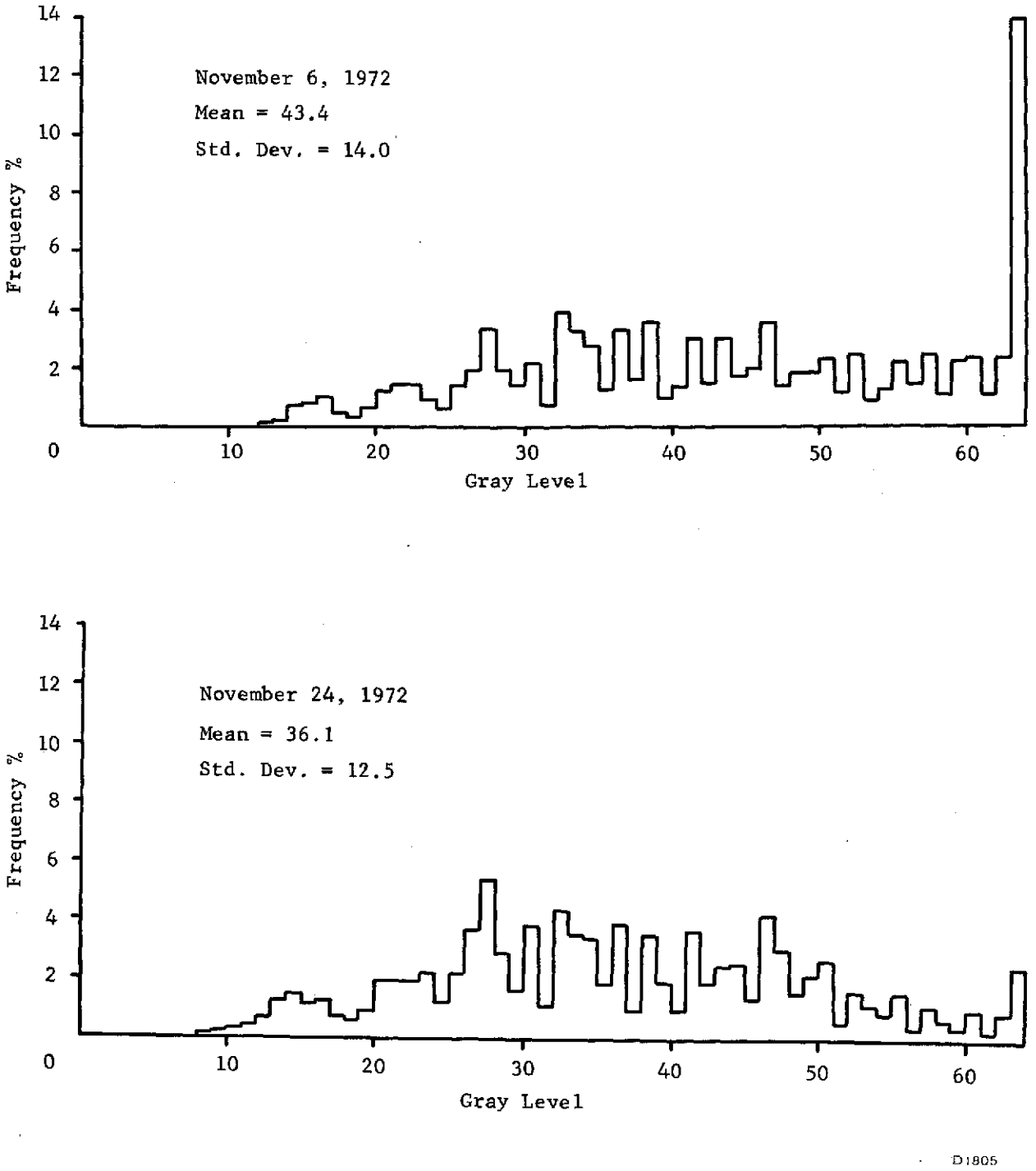

Figure 2.5-4. Gray Scale Distributions for Imperial Valley ERTS-1 MSS Imagery, Band 5

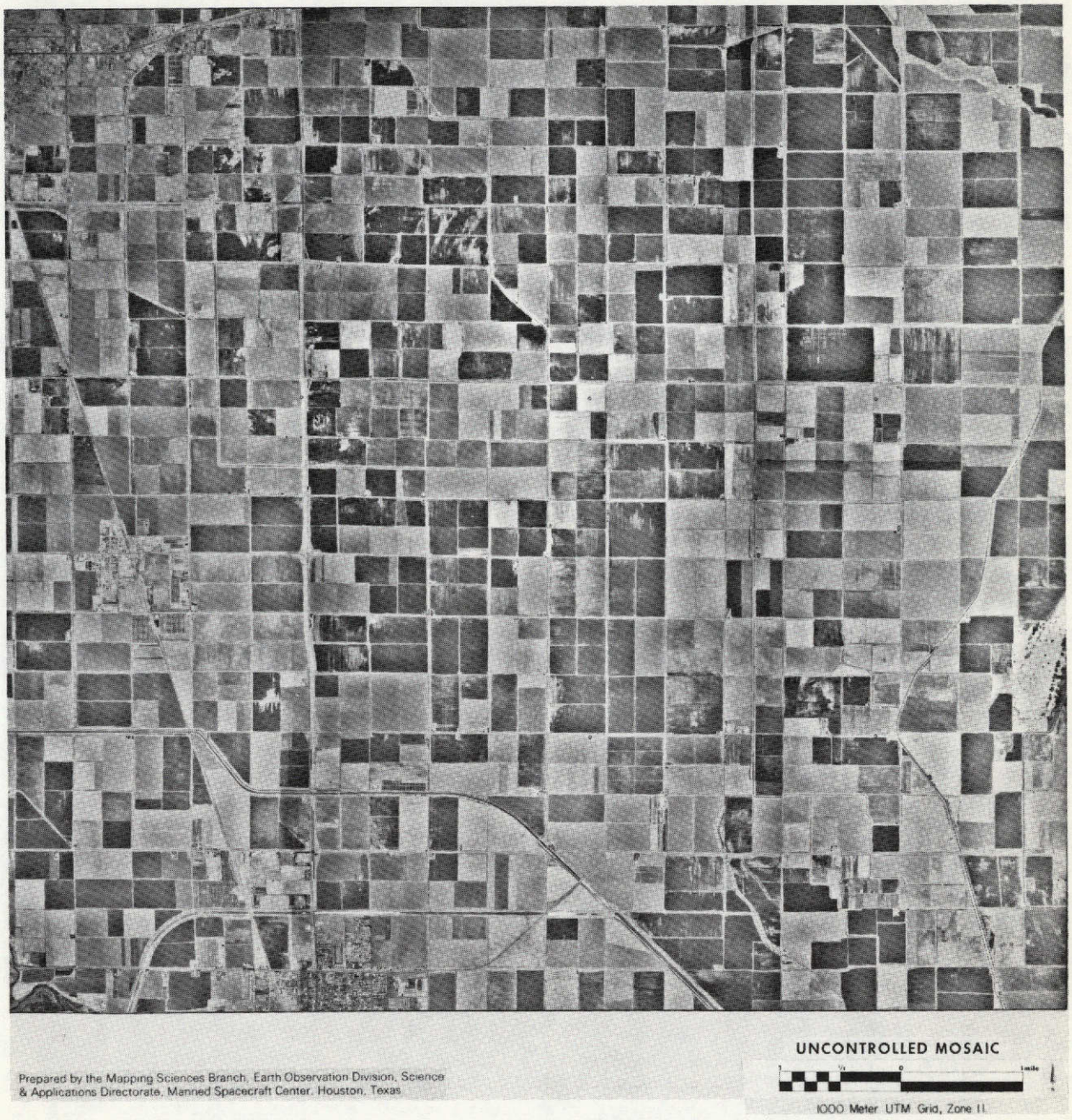

Figure 2.5-5. Uncontrolled Photomosaic
Imperial County, California

spection (Figures 2.5-6 and 2.5-7). Superposition of the gradient reference image upon the registered dependent image reveals that registration is generally within one pixel over this selected area (Figure 2.5-8). Note that this data is extracted from the entire 25 by 100 nautical mile strip which was previously registered with the automatic strip (TRAK) process.

The mean radial displacement error was found to be 0.58 pixel for TRAK processing of the quarter frame of MSS imagery in image-to-image registration (Table 2.5-1). This result is the accumulation of statistics over 373 locations at which independent correlations were made on the registered image data

TABLE 2.5-1: IMPERIAL VALLEY: CORRELATION ERROR (WECK) ANALYSIS OF AUTOMATIC (TRAK) REGISTRATION PROCESS OVER 25 BY 100 NAUTICAL MILE AREA

ERTS-1 MSS, Band 5, Image Data
November 6 and November 24, 1972

Correlation Patch Size = 51 x 51 Pixels

Correlation Rejection Threshold = 0.60

Total Number of Samples = 373

ERROR STATISTICS

DESCRIPTION	SYMBOL	PIXELS
Mean Registration error in direction of flight	$\bar{x}$	-0.04
Standard Deviation, direction of flight	σ_x	0.52
Mean Registration error parallel to scan lines	$\bar{y}$	-0.08
Standard Deviation parallel to scan lines	σ_y	0.75
Mean radial error	$\bar{r}$	0.58
Standard Deviation in radial error	σ_r	0.70

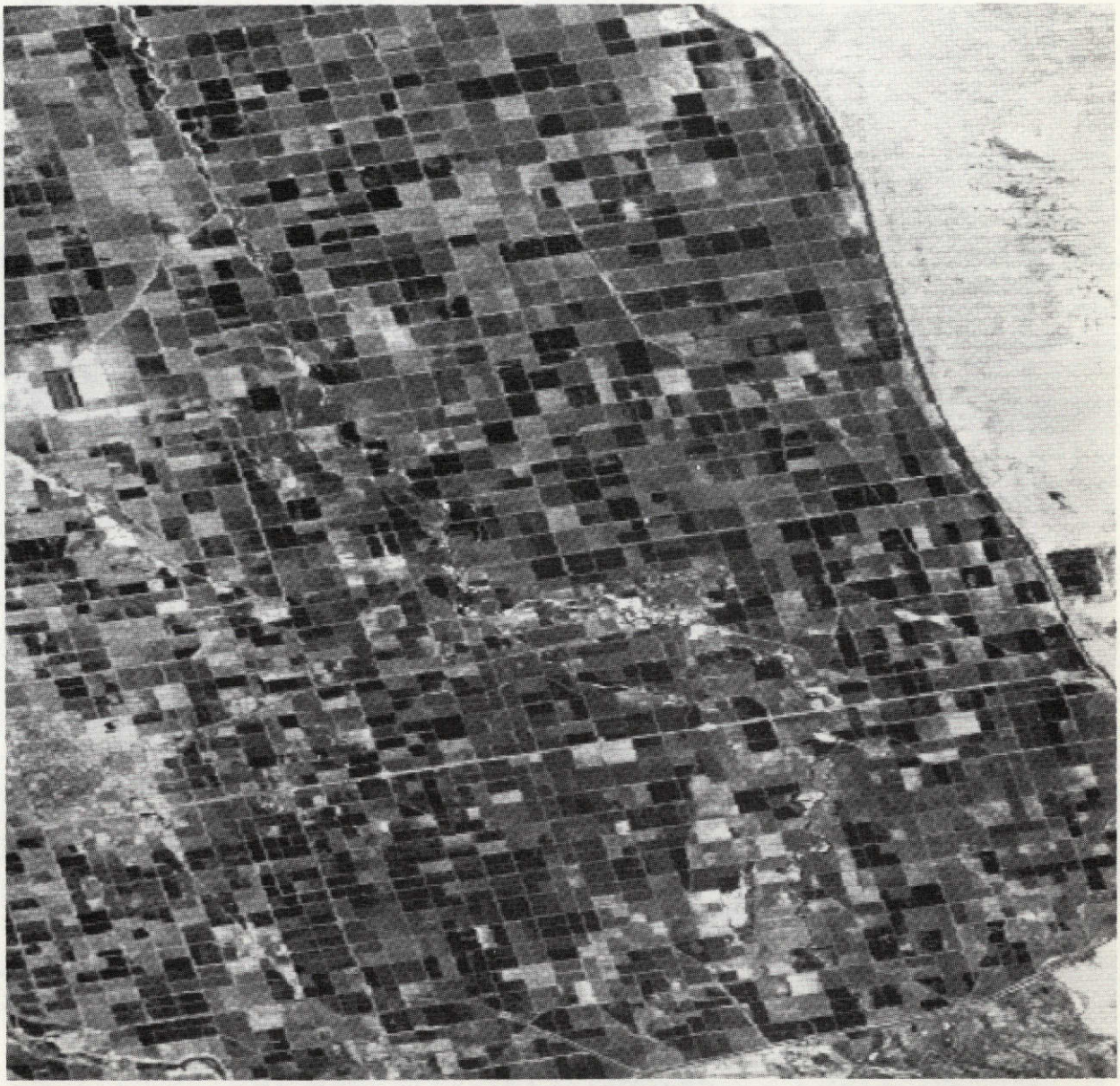

Figure 2.5-6. Reference Image, Imperial County
ERTS-1 MSS, Band 5, November 6, 1972

Figure 2.5-7. Registered Dependent Image, Imperial County
ERTS-1 MSS, Band 5, November 24, 1972

Figure 2.5-8. Superposition of Gradient Reference Upon Registered Dependent Image for Imperial County, California Area ERTS-1 MSS Band 5, November 6, 1972 (Reference) and November 24, 1972 (Dependent)

with a correlation patch size of 51 by 51 pixels.

Thus, the registration of Imperial Valley MSS data is not quite as good as that of Snook Site where the mean radial error was only 0.28 pixel. Furthermore the spatial warp between images appears to be somewhat more complex, as evidenced by the vector displacement diagram (Figure 2.5-9*) and a polynomial warp error analysis (Table 2.5-2). A third or fourth order fit is needed to reduce mean radial registration error to the same level as a second order fit provides for Snook Site (Table 2.4-2).

It is interesting to speculate why the Imperial Valley imagery should have a higher registration error, even though temporal change is less and correlations are higher. From the vector displacement diagram it appears that the process may have experienced occasional local difficulties in correlation, e.g. in the beginning (north end) and in the south west. Otherwise there were indeed complex local distortions between the two images.

Actual elevation induced distortions in the mountainous regions of either image may be in the range of 1 to 5 pixels. However, the apparent flight paths differ by about 0.6 degrees in heading and only about 2 nautical miles in translation perpendicular to the flight path. The heading deviation could account for a maximum of 0.1 pixel relative displacement perpendicular to the scan lines in the regions of the high mountain ridges. If the lateral translation is valid, this could account for a maximum of 0.2 pixel relative displacement in the scan line direction in the mountain peaks, also. Instability of the satellite orientation would add further to these local distortions. Thus, it is possible that the higher residual error encountered here did arise in part from terrain induced distortions which were not compensated by the strip correlation process.

---

*In the vector displacement diagram of Figure 2.5-9 each vector has been biased by (-215,-44) to remove the translational offset between images. Also the vectors have been enlarged by a factor of 10 in the horizontal (flight) direction and a factor of 5 in the vertical (scan line) direction.

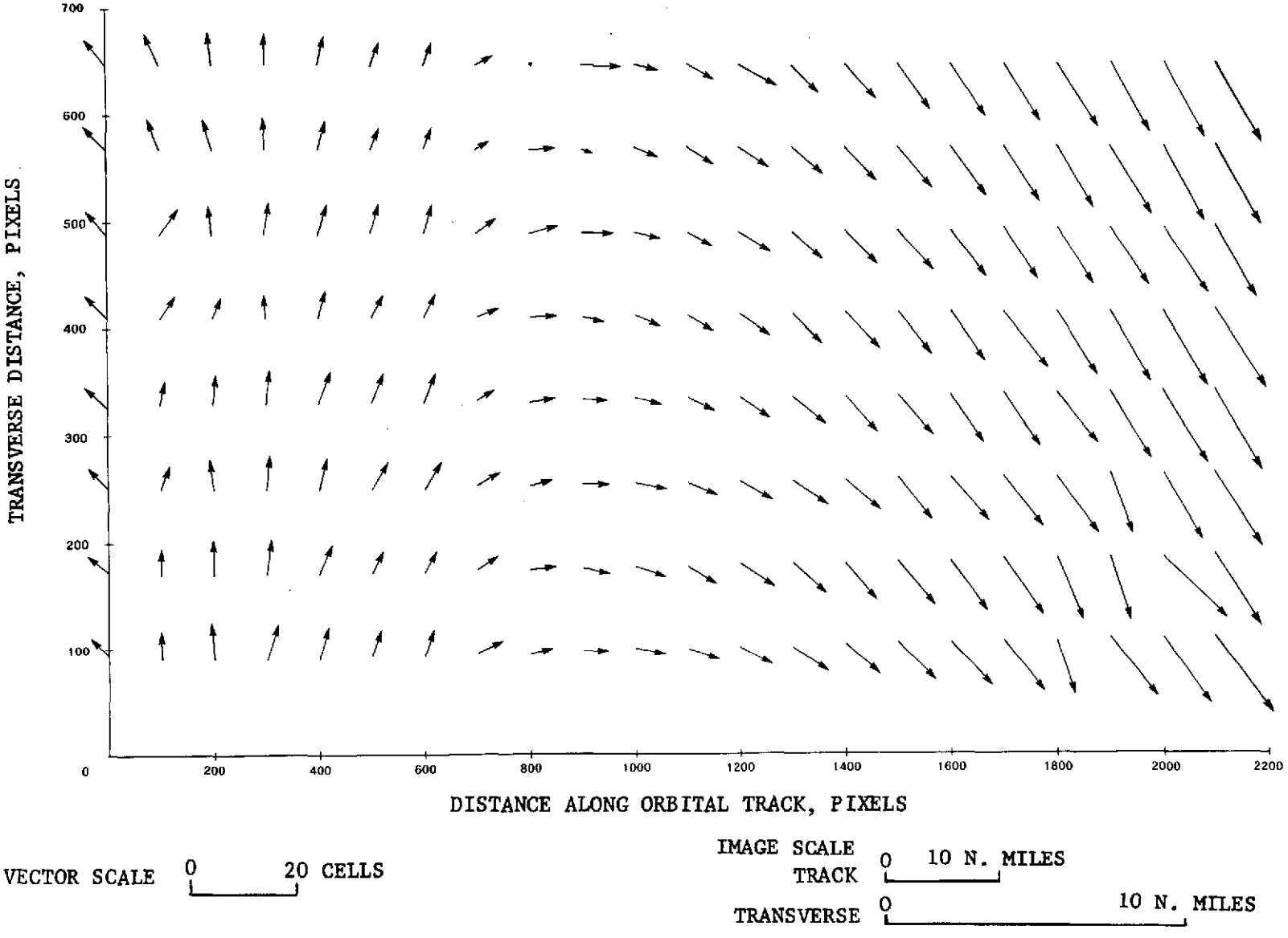

Figure 2.5-9. Vector Displacement Diagram for Spatial Distortions between ERTS Images for Imperial Valley, November 6 to 24, 1972

D1796 A

TABLE 2.5-2. IMPERIAL VALLEY: POLYNOMIAL ERROR ANALYSIS OF AUTOMATIC (TRAK) REGISTRATION PROCESS

Based upon control points matched by Program TRAK over a 25 by 100 nautical mile area.

Number of fit points = 74

Number of check points = 71

Total number of points = 145

ORDER OF FIT	ERROR STATISTICS (PIXELS)								
	FIT POINTS			CHECK POINTS			ALL POINTS		
	σ_x	σ_y	$\bar{r}$	σ_x	σ_y	$\bar{r}$	σ_x	σ_y	$\bar{r}$
1	0.96	1.04	1.10	1.07	1.22	1.18	1.01	1.13	1.14
2	0.80	0.87	0.91	0.93	0.98	1.00	0.86	0.92	0.96
3	0.75	0.68	0.78	0.94	0.67	0.88	0.84	0.67	0.83
4	0.66	0.61	0.72	0.94	0.54	0.86	0.81	0.57	0.79

In addition, local variations in features cannot be ignored as possible causes in higher residual error. This raises the question of accuracies relating to man-made features as opposed to natural features. Also the noise line problem every sixth line seems to be more severe for the Imperial Valley ERTS imagery. More discussion of warp complexity follows in the discussion of registration to ground control over the Imperial County area.

2.5.2 Semi-Automatic Registration to Ground Control

As stated at the outset, one of the objectives is to simulate spatial transformation of MSS imagery into registration with a standard grid projection, such as the UTM grid. This was done with a linear semi-automatic warp based upon 16 control points measured from an uncontrolled photomosaic (Figure 2.5-5) and Band 5 data of the reference MSS image (Figure 2.5-6). The resulting transformation was applied to all four spectral bands of imagery for November 6 and November 24, 1972. (Figures 2.5-10 and 2.5-11, respectively). Properties of this fit, including the fit coefficients, are described in Table 2.5-3. The mean radial error is 0.77 pixel.

TABLE 2.5-3: IMPERIAL COUNTY: LINEAR POLYNOMIAL FIT FOR SEMI-AUTOMATIC REGISTRATION OF ERTS-1 MSS IMAGERY TO GROUND CONTROL POINTS

Order of Fit: First (linear) - 6 Degrees of Freedom
Number of Control Points: 16
Mean Radial Error in Fit (Based on 16 Control Points) = 0.77 Pixel

POWER OF x	POWER OF y	FIT COEFFICIENTS *	
		x TERM	y TERM
0	0	222.6	68.1
1	0	0.974	0.330
0	1	-0.170	1.341

*Coordinate Convention

Photomosaic Reference: x = east-west direction
y = north-south direction

ERTS MSS Reference: x = flight direction
y = scan line direction

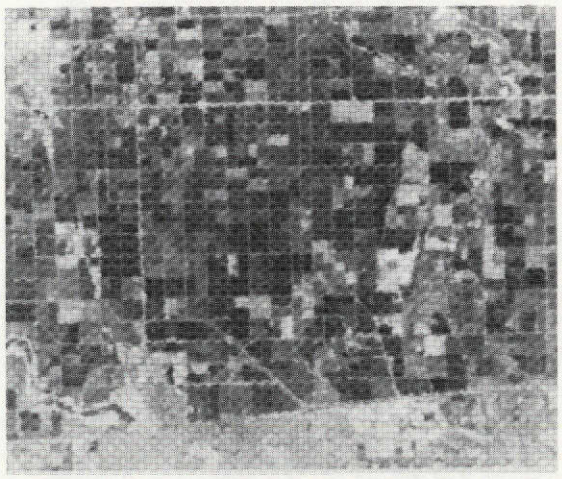

Band 4

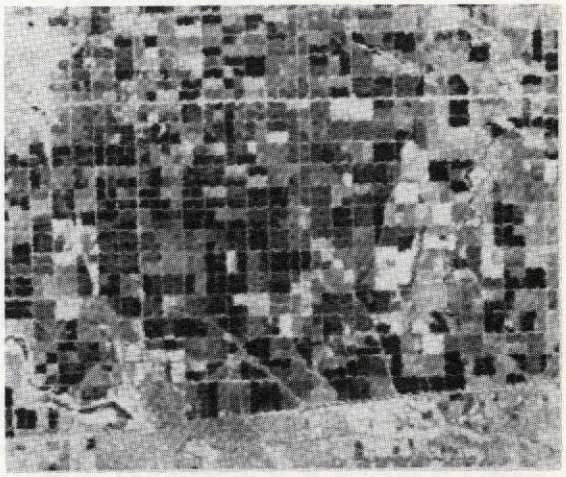

Band 5

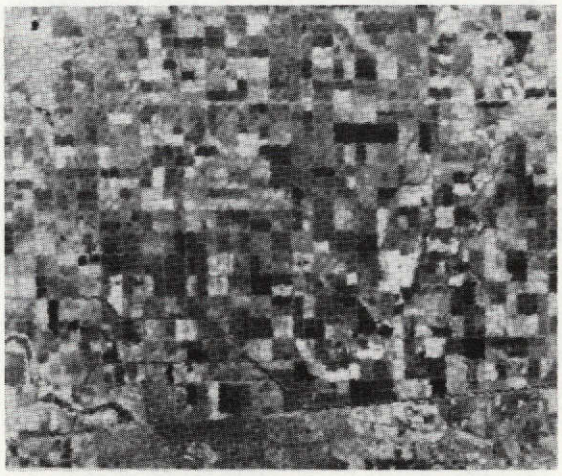

Band 6

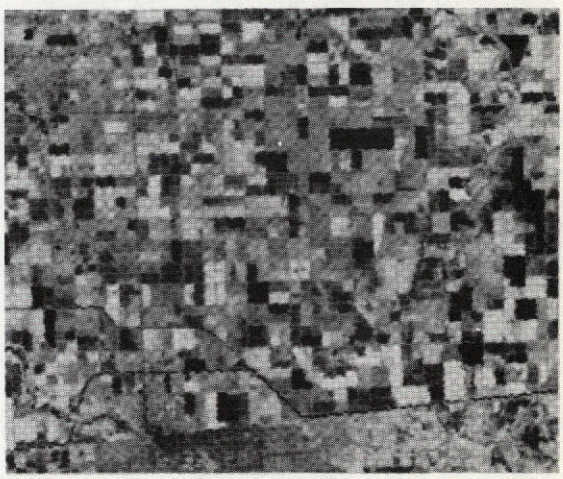

Band 7

Figure 2.5-10. Semi-Automatic Registration to Photomosaic, Imperial County ERTS-1 MSS, Band 5, November 6, 1972

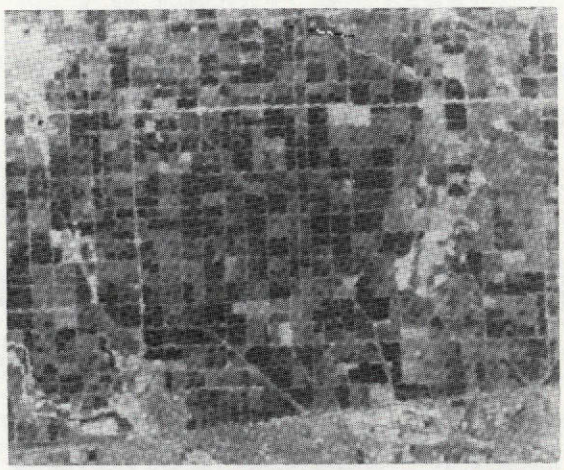

Band 4

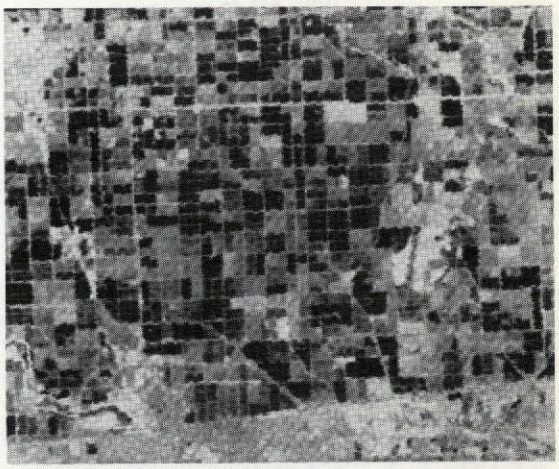

Band 5

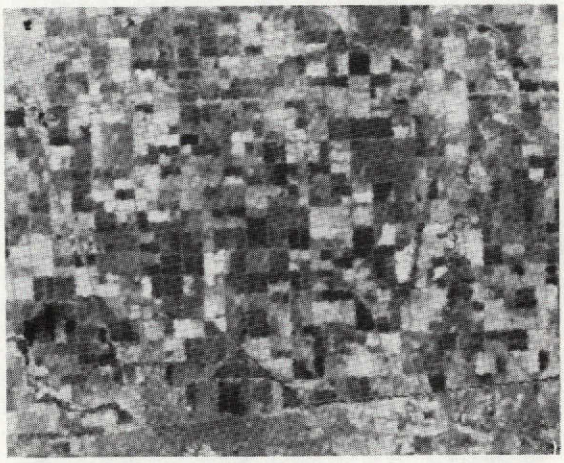

Band 6

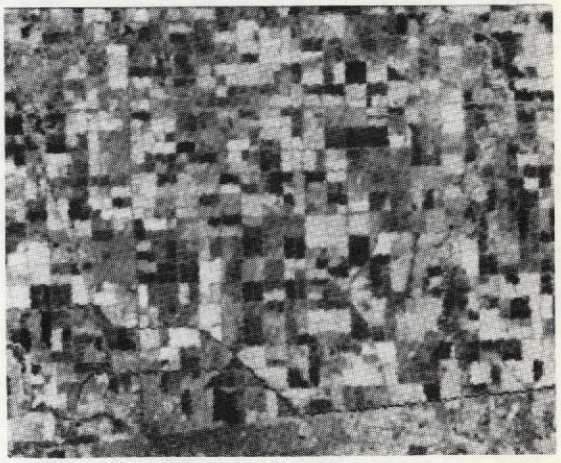

Band 7

Figure 2.5-11. Semi-Automatic Registration to Photomosaic, Imperial County ERTS-1 MSS, Band 5, November 24, 1972

The semi-automatic warp was scaled to provide a "one-to-one" digital transformation (same digital scale) in the flight direction. In the perpendicular direction (along a scan line) it was then necessary to compress the digital scale by approximately 31 percent.

Results of a polynomial registration error analysis based on the 16 control points are summarized in Table 2.5-4. Up to third order (cubic) polynomial fits are considered. Registration error drops dramatically as the number of

TABLE 2.5-4. IMPERIAL COUNTY: POLYNOMIAL ERROR ANALYSIS OF SEMI-AUTOMATIC REGISTRATION PROCESS

Based on 16 ground control points obtained from an uncontrolled photomosaic.

DEGREES OF FREEDOM	REGISTRATION ERROR STATISTICS (PIXELS)			
	σ_x	σ_y	$\bar{r}$	σ_r
4	9.12	12.19	13.93	4.74
5	5.50	7.10	8.26	2.80
6 (linear)	0.51	0.73	0.77	0.40
12 (quadratic)	0.36	0.55	0.58	0.26
20 (cubic)	0.34	0.41	0.45	0.25

σ_x = standard deviation in direction of flight

σ_y = standard deviation parallel to scan lines

$\bar{r}$ = mean radial error

σ_r = standard deviation in radial error

degrees of freedom is increased from three to six. Beyond this point registration error decreases much more slowly with increasing fit complexity. Registration error cannot be accurately assessed for higher order fits, say cubic and above, because of the limited number of control points available.

The data in Table 2.5-4 indicates that a linear fit over a 500 by 500 pixel area should be adequate (mean radial error = 0.77 pixel), and that some additional improvement is possible with a quadratic fit (mean radial error = 0.58 pixel). A linear warp of ERTS MSS imagery requires at least six degrees of freedom to account for differences in x and y scale factors, as well as a skew of about 12 degrees relative to a ground coordinate grid.

Though the four examples of MSS registration discussed in this work provide a limited sampling, it would appear that these examples provide a beginning point in requirements projections. The results indicate that it is perhaps not uncommon to find that about 12 degrees of freedom are required for MSS to ground registration over a 500 by 500 pixel area (380 square nautical miles) to reduce the mean radial registration error to 0.5 pixel or less. If so, a minimum of about 80 degrees of freedom are required for a quarter frame, and more than 300 are required for a full frame of standard ERTS imagery.

3. RECOMMENDATIONS FOR AUGMENTING THE GENERAL IMAGE PROCESSING CAPABILITY AT NASA JOHNSON SPACE CENTER

Image processing can be classed in two main categories: production processing and research processing. Computer requirements are quite different for these two categories, and an image processing computer facility must be capable of meeting requirements for both categories. The key concept in the design of an image processing facility is therefore versatility. Control Data feels that the most cost-effective means of attaining such versatility is to combine the computing power of a large scale general-purpose computer with an array of high-speed special-purpose image processing computers.

Consider computer requirements for research processing. Research processing is generally performed on a low-volume basis with a high degree of interaction required between researcher and computer. Each computer program must be tailored to a particular application, of which there are generally a wide variety at any image processing facility. Algorithms tend to be rather sophisticated and in a state of constant revision. In image research each researcher is attempting to extract information from ERTS data for his specialized application. This may require several iterations. First one technique is tried and results analyzed, then another, then perhaps some parameters are changed, etc.

Key computer requirements for research processing are therefore computer availability and computer flexibility. Each researcher must have ready access to the computer--either through an interactive display capability or through short turn-around time in a batch processing mode. Computer "flexibility" implies general-purpose processing capability. That is, the computer must be capable of sophisticated computations, it must be relatively fast, have large core and peripheral storage capability and it must be amenable to constant algorithm updates and programming changes. Also a multi-program environment is essential to allow ready access to a number of researchers simultaneously.

Computer requirements for special-purpose processing are best met by a large scale general-purpose computer such as the CDC 7600 or Cyber (6000) series with ample core and high-speed peripheral storage. This will generally assure any given researcher of the flexibility and computer power for his particular application.

The second requirement for special-purpose processing is computer availability, and again this will generally require a large scale general-purpose computer. The problem here is to ensure all researchers ready interaction with the computer. An interactive display system is essential for a facility such as NASA JSC, but it is not enough. Only a limited number of researchers can use the interactive display at any given time. The remainder must be ensured of ready access to the computer as well. Batch processing can ensure this provided that turn-around time is kept short. With short turn-around results of a given processing run can be analyzed from computer printout and at digital display stations. Modifications can then be made and the run resubmitted. Several iterations in this "semi-interactive" mode are possible per day.

In general, processing requirements tend to vary considerably among special-purpose runs, since each run is tailored to a particular application. Also, since special-purpose processing is research-oriented, algorithms are usually in a state of flux and many computer runs will tend to be "debugging" runs. Since runs can be profitably time-shared with interactive display runs to provide ready access and rapid turn-around.

Again, because each computer program is tailored to each individual application, program size varies widely for special-purpose runs but is typically on the order of $100{,}000_8$ (about $30{,}000_{10}$) storage locations or less. Thus a large scale computer with say $300{,}000_8$ locations of core storage should be capable of providing adequate turn-around in a multi-programming mode.

An image processing computer facility should have adequate digital storage facilities for several frames of ERTS imagery at any given time. This means a

reasonable amount of disc storage and medium speed extended core storage (ECS) or its equivalent. Also numerous magnetic tape units are required for input/output.

The current computer installation at NASA JSC meets all these requirements. Of course this installation is not dedicated to image processing users, but access seems to be reasonable. The one modification that we would recommend at this stage is a relatively minor one concerning the digital analysis stations (DAS). Our experience has been that programming of the DAS is too inflexible. More programming effort should be expended on the DAS so that a researcher can use the information he has available to best advantage. We are not suggesting that the DAS should perform the functions of the general-purpose computer, but it should be capable of simple tasks such as contrast enhancemsnt, digital enlargement, etc., and at the very least the operator should have the capability of changing constants such as those in the header record on MSDS format tapes.

In other words the current installation overall appears more than adequate to meet special purpose processing requirements. The problem arises in trying to meet both special-purpose processing and production processing requirements.

In many cases production processing represents pre-processing to prepare data for subsequent special-purpose runs. Thus it must be performed before various special-purpose runs. In any case there is a relatively high volume requirement so that production processing runs must be performed on a regular basis. Moreover production processing tends to involve larger images--usually complete frames or at least complete strips of imagery--requiring correspondingly larger amounts of storage and processing time than special-purpose processing.

In other words, production processing generally requires large amounts of digital storage (both core and peripheral) on a regular basis. On the other hand, by the time a computer program reaches the production phase, algorithms are more or less well-defined and a minimum of operator interaction is required. Also, because of data volume, algorithms tend to employ relatively simple operations.

What this means is that a large scale general-purpose computer does not provide the most cost-effective answer to the production processing problem. Production processing requires the speed and storage capabilities of a large scale general-purpose computer, but otherwise tends to under-utilize the computer's capabilities. Furthermore in a mixed processing environment production processing runs tend to monopolize the central processor, denying access to special-purpose users.

The problem in designing an image processing facility is to reconcile computer requirements for production and special-purpose processing. We at Control Data feel that this can best be done through combining the general capability of a large scale digital computer with high speed special-purpose image processing hardware. Basically the concept is to perform production processing in the high speed special purpose hardware under the control of the central processor, leaving the central processor free for special purpose applications. Thus both sets of requirements can be met simultaneously. Production runs can be processed regularly on a high-speed, high volume basis, while at the same time the general capability of the central processor is readily available for special-purpose processing.

Design of special purpose image processing hardware is very important. Through use of parallelism, special-purpose image processing computers can be designed for a given application which are one to two orders of magnitude faster than the most powerful general purpose computers. For example, a digital change detection system has been designed and built for the U.S. Air Force by Control Data Corporation [9] that has a processing rate of 250,000 pixels per second. The total time required to process a typical 1024 x 2048 frame of imagery on this equipment is therefore between 8 and 10 seconds. A simulator for this system on the CDC 6600 computer, on the other hand, requires on the order of 600 seconds of CP time to process the same frame of imagery. Thus the special purpose hardware is faster by about a factor of 70.

The price that must be paid in special-purpose design is flexibility. Special purpose computers are just that: computers designed specially for a

single application. However, a certain amount of flexibility can be built into a special-purpose image processing computer through use of microprogrammable, as opposed to hard-wired, components.

Control Data favors a modular approach in which the image processing computer is built from a series of micro-programmable mini-computers called Flexible Processors. The Flexible Processor (FP) is a specially designed image processing computer, which features are described in [14]. A special-purpose computer for a given application can be constructed from an array of FP's with the appropriate microprogramming. For a given application, the processing rate can be adjusted by changing the number of FP's. Since the FP's can operate in parallel, the number can be adjusted to meet any desired processing rate.

Furthermore, an array of FP's designed for a given application can be modified for a different application by simply changing the microprogramming. This is considerably simpler than modifying a hard-wired computer, but is, of course, more difficult than modifying a FORTRAN program on a general purpose computer.

Obviously, an array of flexible processors may not be the answer to the special-purpose programming problem. Algorithms tend to be too sophisitcated and too ill defined, i.e. subject to continual revision. Also various peripherals required in such applications are best interfaced with a general purpose computer.

Such a machine is, however, ideally suited to the production processing problem. In production processing applications numerical operations tend to be rather simple because of the volume of data to be processed. Further algorithms tend to be well-defined, i.e. they are more or less fixed. Thus an array of processors could be set up and microprogrammed for a given production processing problem, then applied to high speed processing on a production basis. The number of FP's could be chosen to yield the desired processing rate at the lowest cost. Then more processors can be added as needed to meet higher processing rates or as required for other applications.

REFERENCES

1. Lillestrand, R. L., "Techniques of Change Detection," IEEE Transactions on Computers, Vol. C-21, No. 7, July 1972.

2. Anuta, P. E., "Spatial Registration of Multispectral and Multitemporal Digital Imagery Using Fast Fourier Transform Techniques," IEEE Transactions on Geoscience Electronics, Vol. GE-8, No. 4, October 1970.

3. Will, P. M., R. Bakis and M. A. Wesley, "Digital Image Processing for the Earth Resources Technology Satellite Data," Information Processing 71, North-Holland Publishing Company, 1972.

4. Lam, Major C. F. and R. R. Hoyt, "High Speed Image Correlation for Change Detection," presented at the National Aeronautics and Electronics Conference (NAECON), Dayton, Ohio, May 1972.

5. Henrikson, P. J., J. P. Glish and R. R. Hoyt, "Investigation of the Effect of Operational Requirements on the Design of SLR Change Detection Systems (U)," RADC-TR-73-20, Rome Air Development Center, Air Force Systems Command, Griffiss Air Force Base, New York, February 1973 (Confidential).

6. Henrikson, P. J., "Investigation of the Effects of Flight Path Deviations on Digital Change Detection (U)," AFAL-TR-72-36, Air Force Avionics Laboratory, Air Force Systems Command, Wright-Patterson Air Force Base, Ohio, March 1972 (Confidential).

7. Bonrud, L. O., R. R. Hoyt and J. P. Glish, "Tactical Radar Target Analysis (TARTAN) (U)," AFAL-TR-71-308, Air Force Avionics Laboratory, Air Force Systems Command, Wright-Patterson Air Force Base, Ohio, December 1971 (Confidential).

8. Lillestrand, R. L., R. C. Sine et. al, "Tactical Radar Target Analysis Investigation (U)," Air Force Avionics Laboratory, Air Force Systems Command, Wright-Patterson Air Force Base, Ohio, June 1970 (Confidential).

9. Hoyt, R. R. et al, "Final Report on the Advanced On-Line SLR Exploitation Equipment (ARRES) (U)," RADC-TR-73-85, Rome Air Development Center, Air Force Systems Command, Griffiss Air Force Base, New York, April 1973 (Confidential).

10. Bonrud, L. O., et al, "Digital Change Detection Analysis, Volume III. AN/UPD-3 Radar Imagery (U)," AFAL-TR-72-244, Air Force Avionics Laboratory, Air Force Systems Command, Wright-Patterson Air Force Base, Ohio, November 1973 (Confidential).

11. Bonrud, L. O., et al, "Digital Change Detection Analysis, Volume IV. FOPEN 1A Radar Imagery (U)," AFAL-TR-72-244, Air Force Avionics Laboratory, Air Force Systems Command, Wright-Patterson Air Force Base, Ohio, March 1974 (Secret).

12. Bonrud, L. O., et al, "Digital Change Detection Analysis, Volume II. Aerial Photography," AFAL-TR-72-244, Air Force Avionics Laboratory, Air Force Systems Command, Wright-Patterson Air Force Base, Ohio, October, 1973.

13. Henrikson, P. J., "Automatic Correlation and Registration of Multispectral Imagery, Interim Report: Preliminary Processing Results for Hill County," CDC TM 9627-3, Control Data Corporation, March 1973.

14. Allen, G. R., L. O. Bonrud, J. J. Cosgrove, R. M. Stone, "The Design and Use of Special Purpose Processors for the Machine Processing of Remotely Sensed Data," LARS Conference on Machine Processing of Remotely Sensed Data, Purdue University, October 1973.